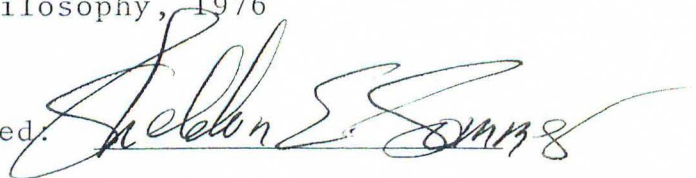


APPROVAL SHEET

Title of Dissertation: The Kinetics and Mechanism of  
Sedimentary Iron Sulfide Formation

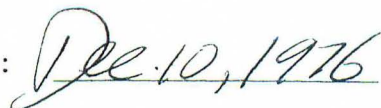
Name of Candidate: Albert John Pyzik  
Doctor of Philosophy, 1976

Dissertation and Abstract Approved.

A handwritten signature in dark ink, appearing to read 'Sheldon E. Sommer', is written over a horizontal line.

Dr. Sheldon E. Sommer  
Associate Professor  
Department of Geology

Date Approved:

A handwritten date 'Dec. 10, 1976' is written in dark ink, with the text 'Date Approved:' printed to its left.

THE KINETICS AND MECHANISM  
OF  
SEDIMENTARY IRON SULFIDE FORMATION

by

Albert John Pyzik  
"

Dissertation submitted to the Faculty of the Graduate School  
of the University of Maryland in partial fulfillment  
of the requirements for the degree of  
Doctor of Philosophy  
1976



## ABSTRACT

Title of Dissertation: The Kinetics and Mechanism of  
Sedimentary Iron Sulfide Formation

Albert John Pyzik, Doctor of Philosophy, 1976

Dissertation directed by: Dr. Sheldon E. Sommer  
Associate Professor  
Department of Geology

The reaction between goethite,  $\alpha\text{-FeOOH}$ , and aqueous bisulfide ion,  $\text{HS}^-$ , was studied under conditions representative of estuarine sediments. The concentration-time curves of the following species were determined by spectrophotometric methods: total sulfide, dissolved sulfide, precipitated sulfide, thiosulfate ion, sulfite ion, elemental sulfur, and dissolved ( $<0.1\mu$ ) iron. Polysulfides ( $\text{S}_4^{=}$  and  $\text{S}_5^{=}$ ) were monitored by ultraviolet absorbance measurements, while the hydrogen ion concentration was determined with a pH electrode. Elemental sulfur, both as free and polysulfide sulfur was found to be the major sulfide oxidation product. Thiosulfate ion comprised about  $14\pm 8\%$  (electron balance-wise) of the oxidation products.

Concentration-time curves of precipitated sulfide sulfur were analyzed by the initial rate method to determine the rate expression. The rate expression for the reaction

between  $\alpha$ -FeOOH and  $\text{HS}^-$  is

$$d[\text{FeS}]/dt = k [\text{HS}^-]_i^{0.97} (\text{H}^+)_i^{0.82} A_{\text{FeOOH}_i}^{1.1}$$

where  $d[\text{FeS}]/dt$  is the rate of precipitated iron sulfide formation,  $[\text{HS}^-]_i$  is the initial total sulfide concentration,  $(\text{H}^+)_i$  is the initial hydrogen ion activity,  $A_{\text{FeOOH}_i}$  is the initial goethite surface area in  $\text{m}^2/\text{l}$ , and  $k$  is the rate constant with the value  $31 \pm 10 \text{ M}^{-1} \text{ l}^{-1} \text{ m}^{-2} \text{ min}^{-1}$ . 0.97, 0.82, and 1.1 are the reaction orders for the species bisulfide ion, hydrogen ion, and goethite surface area respectively.

A combination of hydrogen balance and electron transfer balance and stoichiometric reactions were studied in view of the rate expression to yield a mechanism.

The multistep mechanism consisted of several parallel and consecutive reactions: (1) the protonation reaction of the goethite surface, (2) the parallel reduction reactions of ferric iron to yield elemental sulfur and thiosulfate as oxidation products, (3) the dissolution of the ferrous hydroxide, and (4) the precipitation reaction of dissolved ferrous species and aqueous bisulfide ion. The rate determining step in the reaction sequence was the dissolution step.

Results of this study indicate that the oxidation of sulfide species by ferric iron may be a significant source of elemental sulfur in the sediment. Elemental sulfur is necessary for the formation of pyrite ( $\text{FeS}_2$ ), the thermodynamically stable iron sulfide.

In addition, the previous studies of the interstitial waters of anoxic sediments showed an excess of "dissolved" iron which was greater than calculated from equilibrium solubility products. It is suggested from particle size studies of the precipitated iron sulfide that these high concentrations are a result of the submicron particles of ferrous sulfide ( $<0.1\mu$ ). These particles would obviously pass through the  $0.45\mu$  filters which are traditionally used as the dividing line for dissolved and particulate species.

## FOREWORD

Any man's finest hour -- his greatest fulfillment to all that he holds dear -- is that moment when he has worked his heart out in a good cause and lies exhausted on the field of battle -- victorious.

V.L.

DEDICATION

To my wife and my parents:

Without them, none of this would have been possible.



## ACKNOWLEDGMENTS

Many people and institutions have aided me in my work. Their assistance and efforts are greatly appreciated. Yet, there are several persons who require a special note of thanks.

The financial support of the Natural Resources Institute and the Office of Water Research and Technology, through the Water Resources Research Center of the University of Maryland (Project A026-Md) is greatly appreciated.

The Center for Materials Research (Electron Microscope Central Facility) is hereby thanked for instrument time on the transmission electron microscope. The assistance and instruction of Mr. Gene Taylor is gratefully appreciated.

Sr. M. Regina Alma and Dr. Harry O. Warren deserve my appreciation for their guidance in my chemical education.

The faculty of the Division of Geochemistry deserve my thanks for their friendship and intellectual support.

Special thanks are extended to my research advisor, Dr. Sheldon Sommer, for the guidance, moral support, and financial support with which he has provided me. I particularly want to thank him for the intellectual freedom that he allowed me in the pursuit of my research interests.

A special note of gratitude is extended to my parents, Mr. and Mrs. Albert Pyzik, for the many years of love, guid-

ance, and sacrifice which were necessary to give me this opportunity. This little note cannot truly express my appreciation for their effort.

To my wife, Iris, I want to extend my sincere appreciation for her love, understanding and support during my research, but particularly for the final few months of the laborious task. Also for her meritorious service above and beyond the call of duty in the typing of this manuscript. Finally, as a fellow scientist who served as a sounding board for my many ideas, she deserves my thanks.

## TABLE OF CONTENTS

FOREWORD	ii
DEDICATION	iii
ACKNOWLEDGMENTS	iv
TABLE OF CONTENTS	vi
LIST OF TABLES	vii
LIST OF FIGURES	viii
INTRODUCTION	1
REVIEW OF THE LITERATURE	9
EXPERIMENTAL	30
RESULTS AND DISCUSSION	60
CONCLUSIONS	107
APPENDIX A: DATA TABLES FOR REACTION RUNS	115
APPENDIX B: INITIAL RATE METHOD	135
BIBLIOGRAPHY	138



## LIST OF TABLES

1.	List of d-spacings (in Å) for Smythite and Siderite	17
2.	Summary of Reported Sulfide Products	29
3.	Palitzsch Borax-Borate Buffer	36
4.	Variation of % Thiosulfate with Initial Reaction Conditions	63
5.	Rate of Reduction During Phase II (Rate of Dissolution)	79
6.	Hydrogen Balance	92
7.	Rate of FeS Formation	99
8.	Particle Size Study	103
9.	"Dissolved Iron" Concentration	104

## LIST OF FIGURES

1. Stability Fields of Iron Minerals at 25°C and 1 Atm Total Pressure, pH 7.5, $p_{CO_2}$ $10^{-2.5}$ atm.	11
2. Schematic Diagram of Reaction Vessel	34
3. Flow Chart of Analytical Procedures	38
4. Sample Sulfide Calibration Curve	42
5. Sample $S^0$ Calibration Curve	44
6. Sample Thiosulfate Calibration Curve	46
7. Sample $SO_3^{=}$ Calibration Curve	47
8. Sample Fe Calibration Curve	49
9. Titration Curve for Borax-Borate Buffer	51
10. Equilibrium Distribution of Polysulfide Ion $S_nS^{=}$	54
11. Real and Synthesized Polysulfide Spectra	56
12. Change of pH Upon Dilution of Reaction Solution Due to Addition of Water	58
13. Concentration-Time Curves for Reactants and Products (Run 31)	61
14. Plot of Acid Extractable Sulfide Concentration vs. Reduced Iron Concentration	72
15. Plot of Reduced Iron and Acid Extractable Sulfide, $S_P^{=}$ , vs. Time (Run 6)	74
16. Plot of Reduced Iron and Acid Extractable Sulfide, $S_P^{=}$ , vs. Time (Run 24)	75
17. Plot of Rate of Fe Reduction vs. $S_{T_i}^{=}$	76
18. Plot of Rate of Fe Reduction vs. Initial Hydrogen Ion Concentration	77
19. Plot of Rate of Fe Reduction vs. Initial Goethite Surface Area	78

20.	Plot of Reduced Iron and Acid Extractable Sulfide, $S_p^=$ , vs. Time (Run 31)	81
21.	Idealized Reduction-Dissolution Curve	82
22.	Plot of Rate of Iron Sulfide Formation vs. Initial Bisulfide Ion Concentration	96
23.	Plot of Rate of Iron Sulfide Formation vs. Initial Hydrogen Ion Concentration	97
24.	Plot of Rate of Iron Sulfide Formation vs. Initial Goethite Surface Area	98
25.	Detailed Reaction Mechanism	108

## INTRODUCTION

The formation of sedimentary iron sulfide occurs as a result of a series of complex geochemical reactions and microbial processes in anoxic sediments. Mackinawite ( $\text{FeS}$ ), greigite ( $\text{Fe}_3\text{S}_4$ ) and pyrite ( $\text{FeS}_2$ ) are the most common iron sulfides found in anoxic sediments. These minerals form by the reaction of detrital iron minerals, particularly fine grained iron oxyhydroxides, and bacteriogenic hydrogen sulfide (Berner, 1970). Iron sulfides form in benthic environments which are characterized by low wave and current energy, high biological productivity, restricted bottom circulation and high depositional rates. These conditions restrict the horizontal and vertical transport of oxygen rich waters and permit the accumulation of organic matter (Richards, 1965). Aerobic oxidation of the organic matter reduces the dissolved oxygen concentration and results in the formation of anoxic conditions. Typical anoxic basins are the Black Sea (Caspers, 1957), Cariaco Trench (Richards and Vaccaro, 1956), Santa Barbara Basin (Kaplan et al., 1963) and Saanich Inlet (Nissenbaum et al., 1972). High biological productivity and high sedimentation rates in tidal flats and salt water marshes also result in dissolved oxygen depletion.

In both situations, the deposited organic matter is utilized by a series of microorganisms in a sequence of



respiratory and fermentation processes as follows:

- (1) Aerobic respiration  

$$\text{CH}_2\text{O} + \text{O}_2 \rightarrow \text{CO}_2 + \text{H}_2\text{O}$$
- (2) Nitrate reduction  

$$5 \text{CH}_2\text{O} + 4 \text{NO}_3^- + 4 \text{H}^+ \rightarrow 2 \text{N}_2 + 5 \text{CO}_2 + 7 \text{H}_2\text{O}$$
- (3) Sulfate reduction  

$$2 \text{CH}_2\text{O} + \text{SO}_4^{2-} \rightarrow \text{HS}^- + \text{HCO}_3^- + \text{H}^+$$
- (4) Methane production  

$$\text{CO}_2 + 4 \text{H}_2 \rightarrow \text{CH}_4 + 2 \text{H}_2\text{O}$$

(In the above reactions,  $\text{CH}_2\text{O}$  represents generalized organic matter in the form of carbohydrate.) Reaction two is not quantitatively significant due to the low concentration of nitrate in the sediment (Richards, 1965).

Several important effects of the sequence are (1) the removal of dissolved oxygen, (2) reduction of the redox potential (Eh), and (3) the formation of reduced sulfur species. The first two effects are interrelated and result in the formation of aerobic and anaerobic zones in the sediment and water columns. The boundary between these biological regions usually occurs at or below the sediment-water interface. Several multioxidation state elements (Fe, Mn, S, C, and N) are present in the sediment. The redox boundary for each element is a function of the redox species, concentration, and usually pH (Garrels and Christ, 1965).

Sulfate reduction is a microbial process that does not occur inorganically (Hem, 1960; Berner, 1970). The important sulfate reducing bacteria belong to the genera Desulfovibrio, Desulfotomaculum and Clostridium (Trudinger,

et al., 1972; Zajic, 1969). These obligate anaerobes are dissimulatory sulfate reducers, that is, they reduce sulfate in excess of that needed for cellular growth. Sulfate is the terminal electron acceptor in the respiratory process. In addition, it is a necessary source of oxygen and energy for the microbes. Hydrogen sulfide is a respiratory by-product which reacts with available chalcophile elements to form metallic sulfides (Zajic, 1969).

A few ppm of hydrogen sulfide imparts an unpleasant taste and odor to air and water. More important, it is extremely toxic to most microorganisms and higher organisms; the ceiling value for humans is 20 ppm (Christensen and Luginbyhl, 1974). It was responsible for massive fish kills in Norway and Canada when meteorological and hydrographic conditions resulted in the upwelling of sulfide-rich bottom waters (Ozretich, 1975; Brongersma-Sanders, 1957). Dissolved sulfide should diffuse out of the sediment as a result of the concentration gradient that exists between the anoxic sediment and the overlying water column. Fortunately, there are several processes which can remove or bind hydrogen sulfide in the environment: biological oxidation, chemical oxidation and metal sulfide precipitation. The last two mechanisms are of particular interest in this study. Iron sulfide precipitation would bind the hydrogen sulfide or the bisulfide ion in the sediment since the metal sulfides are extremely insoluble. The process would only be effective if the rate of reactive metal addition to the sediment exceeds



the rate of sulfate reduction. In addition, the concentration of hydrogen sulfide can be controlled by the coupling of the oxidation of hydrogen sulfide with the reduction of ferric iron. This is extremely likely since hydrogen sulfide is a strong reducing agent. This redox process would convert toxic hydrogen sulfide into several sulfur oxyanions such as sulfite, thiosulfate, and sulfate. However, some of these oxidation products (e.g. thiosulfate) can be utilized by Desulfovibrio and hence would be recycled by the bacteria. Both chemical oxidation and metal precipitation could reduce the concentration, the concentration gradient, and ultimately the diffusion of  $H_2S$  out of the sediment.

Dissolved sulfate is the principal source of sulfur for iron sulfide formation. Marine organic matter contains approximately 1% organic sulfur, and thus represents less than 1-2% of the sulfur budget for iron sulfide formation (Kaplan, Emery, and Rittenberg, 1963). Dissolved sulfate is trapped with organic and inorganic detritus upon deposition and is reduced by bacterial processes. Additional sulfate diffuses into the sediment from the overlying water in response to the concentration gradient that develops because of the sulfate reduction. The diffusion of sulfate is substantiated by sulfur isotope ratios which show a progressive enrichment of  $^{32}S$  in the reduced sulfur species. This enrichment can only be explained by assuming access by the sediment to the unlimited sulfate reservoir in the overlying waters (Thode and Kemp, 1968).

Two processes are important in the removal of sulfate from seawater: calcium sulfate formation and sulfate reduction-pyrite formation (Berner, 1972). At present, there are no quantitatively significant evaporite basins for calcium sulfate formation, hence pyrite formation must be the major control of oceanic sulfate concentration. Calculations by Berner (1972) for sulfur uptake due to pyrite formation in pelagic and semi-euxinic basins can only account for 5% of sulfate delivered by river water. Berner thus proposed that either metal sulfide formation is much higher in shallow water environments or the seawater sulfate concentration is increasing. Therefore an increased understanding of the formation of iron sulfides in nearshore and estuarine environments may allow explanation of the discrepancies in the sulfur budget.

Several possible sources of iron are present in a reducing sediment: dissolved iron, organic iron, detrital iron minerals, iron oxide and oxyhydroxide coatings on mineral grains, and structural iron in clay minerals. Previous work (Gibbs, 1973; Carroll, 1958; Drever, 1971) has shown that only the last two sources are quantitatively significant. Iron oxide coatings are formed as a result of weathering and soil forming processes. These oxides are goethite, lepidocrocite, haematite, and iron oxides of indefinite structure (Carroll, 1958). Although they are found on all detrital particles, they are mainly associated with the clay sized fraction (Berner, 1964a). Von Straaten (1954) showed



that the principal source of iron sulfide formation is adsorbed iron in the clay fraction. Precipitated and coprecipitated iron oxide coatings comprise 40-47% of the river load of iron (Gibbs, 1973).

These iron coatings are stable in an oxidizing environment but are removed by reducing conditions. Ferric hydroxide ( $\text{Fe}(\text{OH})_3$ ) is the thermodynamically stable phase in oxidizing environments. However, the lowering of Eh below +350 mv at pH 8 and 0 mv at pH 6 (Hem and Cropper, 1959) results in the reduction of ferric iron to ferrous iron. The latter is more soluble and more mobile. The particular ferrous species which predominates is a function of the salinity and the pH. At pH 7 and in fresh water,  $\text{Fe}^{+2}$  is the most stable species, while at pH 8,  $\text{FeOH}^+$  and  $\text{Fe}^{+2}$  are equally important. In saline waters at pH 7,  $\text{FeCl}^+$ ,  $\text{Fe}^{+2}$ , and  $\text{FeOH}^+$  are important, while  $\text{FeOH}^+$  predominates at pH 8 (Kester et al., 1975).

Structural iron (i.e. that within the crystal structure) comprises 45-48% of the total river load of iron (Gibbs, 1973). This iron species was assumed to be unavailable for reaction. However structural iron may be important where other iron sources are not present. Drever (1971) determined from studies of nonexchangeable magnesium in clay minerals that structural iron in clay minerals can be an additional source of iron for  $\text{FeS}$  formation. Higher values of nonexchangeable magnesium were determined in reducing sediments than in mineralogically similar oxidizing

sediments. This was attributed to replacement of ferrous iron in the octahedral layer by magnesium. This would be significant in sediments which contain clay minerals rich in iron, e.g. nontronite, glauconite, and chamosite.

Iron sulfide formation affects the distribution of trace metals in reducing sediments. Reactant iron oxides and oxyhydroxides adsorb trace metals (Co, Ni, Cu and Zn) in oxidizing environments (Jenne, 1968). During iron sulfide formation, the adsorbed trace and heavy metals would be released upon dissolution of the iron oxyhydroxides. Krauskopf (1956) indicated that the concentrations of Cu, Zn, and Cd in marine sediments could be explained by precipitation as the metal sulfides. On short time scales, the concentration of Mo in anoxic sediments was shown to be controlled by coprecipitation with the iron sulfides (Bertine, 1972). Thus in theory, the concentrations of chalcophile elements are controlled by the formation of metal sulfides. Studies of trace metal concentrations in interstitial waters of reducing sediments (Brooks et al., 1968; Preseley et al., 1972) have shown that the concentrations of several chalcophile elements (Cd, Co, Cu, Fe, Ni, and Zn) exceeded the equilibrium concentrations by several orders of magnitude. Polysulfide and bisulfide complexes were proposed to explain the greater solubility of the metals (Barnes and Czamanski, 1967; Krauskopf, 1956).

A better understanding of the formation of sedimentary iron sulfides is needed because of their importance in



several environmental and geological processes. The distribution of toxic  $H_2S$  in the sediment water column is affected by the precipitation of iron sulfides. The rate of this process is important. The precipitation rate must equal or exceed the rate of sulfate reduction to prevent the accumulation of sulfide and eventual diffusion of  $H_2S$  into the overlying waters where it could adversely affect aerobic organisms.

The concentration, distribution, and mobility of chalcophile elements is theoretically controlled by the solubility of metal sulfides. Recent data (Brooks, Preseley, and Kaplan, 1968; Preseley, et al., 1972) indicate trace metal concentrations in interstitial waters greater than predicted by solubility calculations. Possible intermediate species in the mechanism of iron sulfide formation, such as polysulfides, could explain the high solubility. Unfortunately, no data exist for intermediate species.

Geologically, the oceanic sulfur budget appears to be out of balance. There exists no quantitatively significant sink for dissolved sulfate; however, the rates for near-shore formation of iron sulfides are not known.

Thus additional data on the rates, kinetics, and mechanisms for the formation of the various iron sulfides are needed before their impact on these other processes can be adequately assessed.

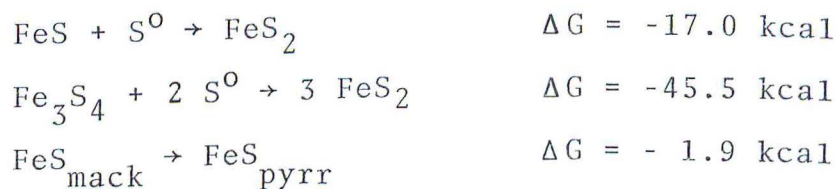
## REVIEW OF THE LITERATURE

"Iron sulfide" is used as a generic term to describe the several known minerals of iron and sulfur that form at low temperature in nature. Mackinawite, pyrite, greigite, smythite, marcasite and pyrrhotite have been identified in nature, although only mackinawite, greigite, and pyrite have been found in recent sediments. Mackinawite ( $\text{FeS}$ ) is the most common iron sulfide found in anoxic sediments and produced in laboratory studies. In the past it has been described by several names: troilite, hydrotroilite, kansite, tetragonal  $\text{FeS}$ , precipitated  $\text{FeS}$  and amorphous  $\text{FeS}$ . Berner (1964a) and Rickard (1969a) agreed that all of these materials were probably mackinawite.

Greigite ( $\text{Fe}_3\text{S}_4$ ) is a cubic magnetic iron sulfide (Skinner et al., 1964). It does not form directly from solution, but by the reaction of mackinawite with either adsorbed, coprecipitated, or solution sulfide. Greigite is believed to be identical with reported cases of melnikovite (Berner, 1964). Both mackinawite and greigite are thermodynamically unstable relative to stoichiometric pyrrhotite and pyrite (Berner, 1967). The sedimentary record contains no occurrences of either mineral in sediments older than the Tertiary.

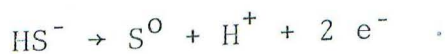
Although pyrite is the thermodynamically stable phase, pyrrhotite may form if there is insufficient elemental

sulfur present.



However, there is no evidence for authigenic pyrrhotite formation in recent sediments. Metastability of mackinawite and greigite is a problem (Berner, 1967).

Stability field diagrams of iron minerals in anoxic sediments are difficult to represent on the traditional Eh-pH diagrams because the variables  $P_{\text{CO}_2}$  and  $p\text{S}^=$  are also involved. Fortunately, the pH varies only from 6.9 to 8.3 (Ben Yaakov, 1973) while the  $P_{\text{CO}_2}$  ranges from  $10^{-3.5}$  to  $10^{-1}$ . Thus Eh- $p\text{S}^=$  diagrams at constant pH and  $P_{\text{CO}_2}$  yield the stability field diagram in Figure 1. This figure represents the average situation of anoxic marine sediments ( $\text{pH} = 7.5$  and  $P_{\text{CO}_2} = 10^{-2.5}$ ). The broken line in the pyrite field represents the Eh- $p\text{S}^=$  values recorded for anoxic marine sediments by Berner (1964b). These values indicate that the Eh of reducing sulfide sediments is controlled by the sulfur-sulfide half cell



The Eh- $p\text{S}^=$  values indicate that thermodynamic equilibrium is being established and metastable FeS is being altered to stable pyrite.



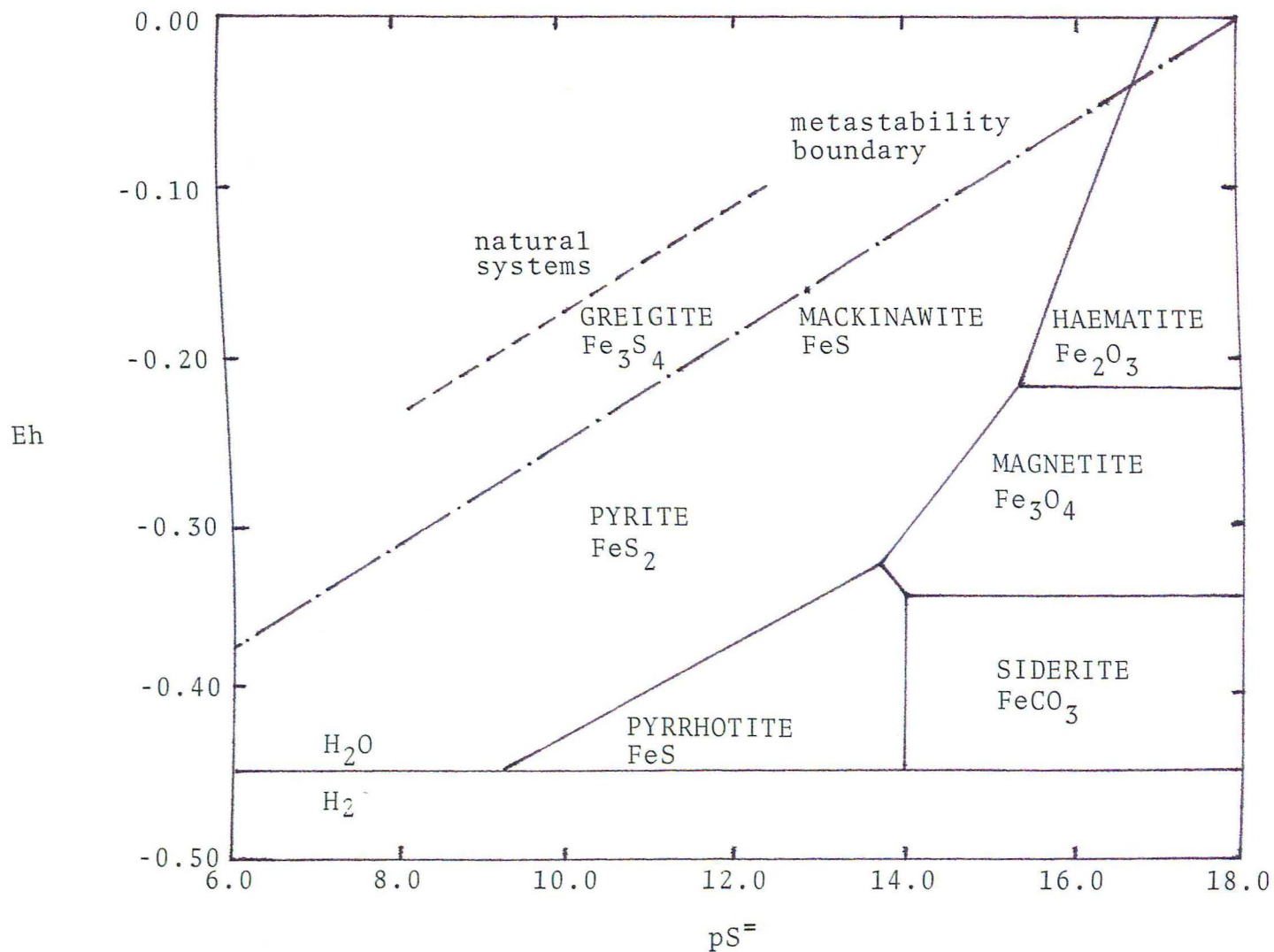


Figure 1. Stability Fields of Iron Minerals at 25°C and 1 Atm Total Pressure, pH 7.5,  $pCO_2$   $10^{-2.5}$  atm. This diagram represents the "average situation" expected for many anaerobic sediments (Berner, 1964).

Previous studies of the sedimentary occurrences of iron sulfides have been limited by the physical and chemical characteristics of these minerals. Tetragonal and amorphous FeS, and pyrite, (1) occur in low concentrations, (2) are poorly crystalline, (3) are extremely fine grained and (4) are susceptible to air oxidation. The low concentration and poor crystallinity hinder the identification of these minerals by x-ray diffraction because they produce broad peaks or no peaks at all. Identification by microscopic analysis is limited by the fine grain size, while extreme care is needed in handling to prevent air oxidation. Thus initial studies have been directed to the characterization of these minerals and the physico-chemical conditions that are necessary for their formation. Several modern laboratory studies have been directed to this end.

Berner (1964a) synthesized several iron sulfides from aqueous solutions at atmospheric pressure, temperatures from 20° to 90°C and pH conditions from 3 to 9. The purpose was to identify the iron sulfides that were prepared under simulated conditions by x-ray diffraction in light of the aforementioned difficulties. The results showed that the nature of the iron sulfide products was affected by the pH, temperature, presence of oxidizing agent, and type of iron source.

Tetragonal FeS was the most commonly produced iron sulfide. It was produced at pH 7-8 when reagent grade iron metal, ferrous sulfate solution and synthetic goethite were the reactants. Synthetic goethite of different crystallinities

was used to approximate natural limonite. Again goethite produced a more crystalline FeS.

Pyrite, marcasite and elemental sulfur were found only when an oxidizing agent such as air or ferric iron was present. This should not be unexpected, since an oxidizing agent would be needed to oxidize sulfide sulfur to elemental sulfur. Elemental sulfur reacted rapidly with dissolved sulfide to form polysulfides (Teder, 1971). The sulfur in pyrite and marcasite is in a mixed oxidation state; both the zero and the plus two states are present.  $S_2^{=}$  is a polysulfide and hence would require the presence of elemental sulfur to form.

Results (Berner, 1964a) also indicate that the type of iron source material is important in controlling the nature of the product sulfide. The use of dissolved ferrous iron promoted rapid reaction and the formation of an amorphous precipitate. The use of iron metal resulted in a slower reaction and a more crystalline product.

Unfortunately, there are several experimental factors which make the results of questionable applicability to sedimentary environments. In many runs, the temperature exceeded  $35^{\circ}\text{C}$  and the pH was either 4 or 9. These conditions lie outside the limits of temperature ( $<30^{\circ}\text{C}$ ) and pH values (6.9 to 8.3) of reducing marine and estuarine sediments. Also, most reactions were conducted in unbuffered solutions; the recorded pH values were the final pH values. There was no indication of the range of pH values over which the



solutions might have varied. In some experimental runs, a small air space was left in the reaction vessel which would have allowed volatilization of hydrogen sulfide from the solution phase into the gas phase. This would have been particularly important in reactions below pH 7 where molecular hydrogen sulfide is the stable species. More importantly, the presence of air resulted in the oxidation of sulfide to elemental sulfur and the subsequent formation of polysulfides. Air would not be present in reducing sediments since oxygen is a poison to sulfate reducing bacteria. The goal of this study was to determine the important conditions in the formation of iron sulfides and the identification of those products. No attempts were made to determine the kinetics and the mechanisms of the reaction.

Roberts et al. (1969) also stressed the importance of elemental sulfur in their study of pyrite formation. Sulfur was produced in situ by the oxidation of hydrogen sulfide by ferric iron. Pyrite was synthesized by the reaction of goethite and molecular hydrogen sulfide at 25°C. The results indicated two mechanisms for the formation of pyrite: (1) the reaction of ferrous iron with the disulfide ion ( $S_2^{=}$ ) and (2) the sulfidization of FeS with elemental sulfur. The latter reaction was much slower than the former. Several factors cast doubt upon their conclusions and the applicability to sedimentary environments. The presence of oxygen could have changed the reaction mechanisms. This is exemplified by the difference in the reaction products

that were observed in the reactions where all conditions except the addition or exclusion were the same. Little control was exercised over the pH of the reactions. Only a few pH values were listed. A great deal of emphasis was placed on the existence and importance of the disulfide ion. Studies of the equilibrium distribution of polysulfides (Schwarzenbach and Fischer, 1960; Teder, 1971; Giggenbach, 1972) showed that the disulfide ion would be stable only at extremely high pH levels.

Rickard (1969a) used a "qualitative semi-kinetic approach" to determine the mechanism of formation of the various iron sulfides from aqueous solutions at low temperature and pressure. This information was then used to define the physico-chemical conditions necessary for the formation of each iron sulfide. Results indicated that the minerals may be used as indicators of the conditions in the environment. However, this is subject to limitations since several conditions may permit the formation of a few iron sulfides.

The following iron phases were used as reactants: ferrous carbonate, ferrous sulfate and synthetic goethite. Reactant sulfide phases were sodium sulfide, sodium polysulfide, and sodium thiosulfate. The solutions were not buffered and the pH values given were those measured at the end of the experiment. Previous work by Berner (1964a) showed that the pH of the solution affects the product iron sulfides.



Reactions of ferrous carbonate with sodium sulfide solutions at pH 6-10 produced smythite, with minor amounts of mackinawite. This was the only circumstance in which the rhombohedral  $\text{Fe}_3\text{S}_4$  was produced. At lower pH values, the ferrous carbonate dissolved and mackinawite was formed. Rickard thus concluded that the preexistence of siderite ( $\text{FeCO}_3$ ) was necessary for the formation of smythite. A comparison of the diffraction patterns of smythite and siderite (Table 1) revealed a close similarity of the interplanar distances of the two minerals. This similarity could have caused the epitaxial growth of smythite on the surface of siderite particles. Natural occurrences of smythite do not indicate a siderite precursor.

Mackinawite was produced by the reaction of ferrous sulfate and sodium sulfide at pH 6.5 to 11.7 and also synthetic goethite and sodium sulfide at pH 7.0 to 9.0. This mackinawite contained adsorbed or coprecipitated sulfide as shown by chemical analysis. The Fe:S ratio was 1:1.1. When this material was dried and heated at  $70^\circ\text{C}$ , greigite was formed. At lower pH values, the reaction of ferrous sulfate and sodium sulfide produced greigite. This indicated to the author that there was a mackinawite to greigite transformation which was pH dependent. pH values of anoxic sediments are such that greigite should not form. The use of lower pH values for the goethite reaction resulted in the formation of sulfur, marcasite and pyrite. A check of the Eh-pH diagram for the five species indicated that elemental

Table 1

List of d-spacings (in Å) for Smythite and Siderite

<u>Siderite</u>	<u>Smythite</u>
	11.6
	5.75
3.59	3.82
	3.00, 2.96
2.79	2.86, 2.83, 2.75
2.56	2.56
2.35	2.45, 2.29, 2.26
2.13	2.16
1.96	1.979
	1.897
1.795	
1.734	1.732
	1.687, 1.672
1.527	1.577, 1.546
1.426	1.435, 1.427
1.395	
1.354	1.351
	1.306
1.281	1.28
1.258	1.25
1.229	
	1.15, 1.10
	1.06

Siderite: Data from ASTM Powder Diffraction File Card  
8-133.  $a_0 = 5.796 \text{ Å}$

Smythite: Data from Erd, Evans, and Richter (1957)  
 $a_0 = 3.465 \text{ Å}$ ,  $c = 34.34 \text{ Å}$

sulfur is a stable species at lower pH values.

Pyrite, marcasite and sulfur were produced by the reaction of sodium polysulfide with ferrous sulfate, synthetic goethite and mackinawite at sedimentary pH values. This supported Rickard's major conclusion that the sulfur bearing phase was important in controlling the nature of the iron sulfide product. This was concluded because only ferrous iron was used as a reactant. This contention was made in spite of the fact that goethite was one of the reactants. Ferric iron is present in goethite.

The pyrite:marcasite product ratio was found to be a function of pH. At pH 4.4, marcasite was a major product, but the ratio decreased as the pH increased, until at pH 9.5 no marcasite was observed. The variation in the product ratio was ascribed to the different mechanisms of formation for the two minerals. Pyrite was believed to form by the direct precipitation reaction between (1) dissolved ferrous iron and polysulfide ions or (2) mackinawite and polysulfide. The formation of marcasite involved a solid state oxidation reaction between sulfur and a preexisting iron sulfide. This last reaction was slow at low temperature and hence marcasite would not be found in recent anoxic sediments.

Pyrrhotite was not observed in any of these experiments.

These reactions were conducted with rigorous exclusion of air to prevent errors in interpretation due to unknown side effects from air oxidation. However, no such



precautions were taken with respect to the pH of the solutions. In anoxic sediments, the pH of the interstitial water ranges from 6.9 to 8.3 (Ben Yaakov, 1973) due to the buffering systems in the water. These experiments by Rickard were conducted in unbuffered solutions to prevent the possibility of reactions between the precipitates and the buffer components. Thus the pH of the solutions might have changed considerably, particularly in those experiments in which goethite was used as a reactant. The ferric iron in goethite would have oxidized the hydrogen sulfide to either elemental sulfur or sulfur oxyanions. This would have produced considerable hydroxide ions as in the following reaction



which would have changed the pH of the solution considerably. This would have been important since high concentrations of iron (0.9M) and sulfur (1.85M) would have produced considerable amounts of hydroxyl ions. In his discussion, Rickard also noted that the high concentrations of iron and sulfur resulted in a higher rate of precipitation for mackinawite and pyrite than the rate of crystallization. The resulting fine grained sulfides could have affected the rates of transformation of mackinawite to greigite and the mackinawite to pyrite transformation. It was suggested that inconsistencies in the results could have been caused by the importance of grain size on the reaction rates.

Thus concentrations that are more realistic should be used in order to make comparisons between laboratory experiments and authigenic iron sulfide formation.

The formation of iron sulfides is a biologically mediated process insofar as the reactant hydrogen sulfide molecule or ion is produced by bacteria. Thus Rickard (1969b) conducted a series of experiments to determine if the microbial formation of iron sulfides differed from the abiogenic reactions. Ferrous salts and synthetic goethite were biogenically sulfidized by the metabolic processes of Desulfovibrio desulfuricans at pH 6-8. Mackinawite was the initial iron sulfide produced from both iron reactants. After three months greigite was observed at pH values of 6 and 7 in the experiments with ferrous salts. This was in agreement with the earlier observed mackinawite to greigite transformation that was observed in the abiogenic study. Mackinawite was the predominant phase present at pH 8 after nine months.

Marcasite and pyrite were observed at pH values 6 and 7 after three months, in the reactions where goethite was the reactant iron phase. Mackinawite persisted at pH 8 for three months. After six months, pyrite and marcasite were found at all pH values from 6 to 8; marcasite was the predominant phase at pH levels 6 and 7. This latter result was in agreement with Rickard's earlier abiogenic result that showed that marcasite was formed at acid pH values.

No crystallographic differences were detected between



the iron sulfides produced in the inorganic study and the microbial study. Pyrite framboids were not found in this study. This added credence to Berners (1969) statement that biological control was unnecessary for framboid formation.

Rickard therefore concluded that there was no difference between the mechanisms of formation of biogenic and abiogenic iron sulfides. One important difference was the absence of rhombic sulfur as a product of the sulfidization of goethite in all but the initial products. The rapid disappearance of the sulfur was attributed to the formation of polysulfides initially, which then reacted with organic compounds to form organic sulfur complexes.

Although this study delineated the reactions and conditions necessary for the formation of iron sulfides, rate expressions and mechanisms for the reactions were not developed.

Sweeney and Kaplan (1973) studied the formation of pyrite framboids, both in the laboratory and in nature. Freshly precipitated iron sulfides were reacted with excess elemental sulfur in aqueous and anhydrous conditions at 60°-80°C. X-ray diffraction and scanning electron microscopy were used to determine the mineralogy and the texture of the products. Framboids were produced only in the reactions with water. The mechanism for framboid formation suggested was: (1) precipitation of the iron monosulfide mackinawite, (2) reaction with elemental sulfur to form greigite, and (3) transformation of greigite spheres to pyrite framboids. The mackinawite to pyrite transformation was consistent with



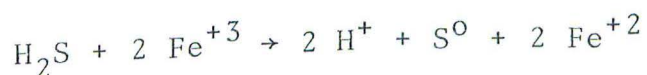
Rickard's (1969a) work. However, no pH data was given so that direct comparison between the studies was not possible. The texture of sedimentary pyrite was both framboidal and non-framboidal, which indicated to the authors that two mechanisms for pyrite formation were involved.

Berner (1970) also studied the formation of pyrite in the laboratory and in nature. Framboidal pyrite was synthesized from 0.1 and 1 M solutions of sodium bisulfide, ferrous sulfate, and elemental sulfur at 65°C, and pH conditions of 6.9 and 7.9. After two weeks, pyrite was formed in the experiments where excess sulfur was used. No pyrite was formed in those runs in which barely sufficient sulfur was added to form polysulfides. Pyrite framboids were found on the surface of sulfur particles. Thus it was concluded that sulfur served as a nucleation surface for the formation of pyrite.

Field studies by Berner (1970) of Connecticut coastal sediments showed that pyrite was forming at the expense of the iron monosulfides. The source of the elemental sulfur which was necessary for this reaction was not identified. In sediments overlain by aerobic bottom waters, sulfur can be formed in the aerobic zone by either the chemical or biological oxidation of the hydrogen sulfide which diffuses into the aerobic zone. However, in sediments overlain by anaerobic waters such as the Black Sea, the process for the formation of elemental sulfur is not known. Yet, the formation of pyrite has been observed in these environments.

This transformation reaction of FeS to FeS<sub>2</sub> was predicted to be completed within several years at the concentration and temperature of the sediments (Berner, 1970).

The first kinetic study of the ferric iron-sulfide system was conducted by Cheng (1972). The object of this study was to determine the affects of ferric ions on the oxygenation kinetics of reduced sulfur species in simulated natural water environments at pH values of 4, 7, and 10. Results showed that the reaction rate was directly proportional to the iron concentration. In the presence and absence of air at pH 4, the ferric ion was reduced to the ferrous species.



However, at higher pH values and in the presence of oxygen, the ferrous ion was not detected. This was probably due to the rapid oxidation of ferrous to ferric ion at neutral and alkaline pH values (Stumm and Lee, 1961). One interesting result showed that the rate of the reaction increased directly with the ageing of the ferric solutions. This was attributed to the increased coordination of the ferric iron to hydroxyls during the longer ageing periods.

No analysis of solids was reported in this study.

The kinetics and mechanism of the sulfidation of goethite was studied by Rickard (1974). pH measurements were combined with mass balance and equilibrium relationships to determine the rate of the reaction. A proposed

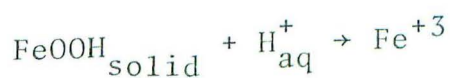
mechanism consisted of a simple initial stage and a complex secondary stage. The rate expression for the initial stage was shown to be

$$d(\text{FeS})/dt = k (\text{H}^+)^2 [\text{S}^=]^{3/2} (\text{A})$$

where  $d(\text{FeS})/dt$  was the rate of production of FeS in  $\text{M}^{-1} \text{sec}^{-1}$ ,  $(\text{H}^+)$  was the hydrogen ion activity,  $[\text{S}^=]$  was the total sulfide ion concentration in  $\text{M}^{-1}$  and (A) was the goethite surface area in  $\text{cm}^2$ . The rate constant  $k$  was  $1.5 \times 10^7 \text{ M}^{-1/2} \text{ l}^{-1/2} \text{ cm}^{-2} \text{ sec}^{-1}$ .

The black product was shown to be identical with a mixture of x-ray amorphous ferrous sulfide and poorly crystallized mackinawite. No pyrite or elemental sulfur was observed in the x-ray diffraction scans. The proposed mechanism included a dissolution reaction in the first stage. The second order rate dependance in the rate expression on the hydrogen ion activity was interpreted as an indicator of a dissolution process. This was concluded from a comparison with a study of the opposing oxidation reaction of aqueous ferrous iron (Stumm and Lee, 1961) in which a second order rate dependance was observed for hydroxyl ions. Line broadening in the x-ray scans indicated to the author a fine grained iron sulfide product. This was interpreted as additional evidence for a dissolution reaction.

A dissolution step was proposed to produce ferric ions in solution.





The stability field of ferric ion,  $\text{Fe}^{+3}$ , ( $>750$  mv,  $<\text{pH } 2$ ; Hem, 1960) is incompatible with the reaction conditions used by Rickard (1974;  $\text{pH } 7-9$  and  $\text{Eh } <-100$  mv). Conditions in anoxic sediments,  $\text{pH } 6.9-8.3$  and  $\text{Eh } <-100$  mv are also incompatible with the existence of dissolved ferric iron. Thus the dissolution step is more likely to be preceded by the reduction of iron. Thermodynamically, ferrous ions are more stable than ferric ions at the pH and Eh conditions found in anoxic sediments.

However, Rickard proposed that the second step in the mechanism of iron sulfide formation involved the reduction of ferric iron by sulfide ion which was then followed by the precipitation of the iron monosulfide.



This work (Rickard, 1974) resulted in a rate expression and rate constant. The proposed mechanism had insufficient verification since the dissolved products, intermediates, and elementary step were not identified. The solid products were studied and characterized, but the solution products were not identified. Yet a study of the dissolved reaction products could give more detailed information about the mechanism and the rate of the reaction. This is true because the sulfide oxidation products are easier to identify than are the solid products. Dissolved species are not affected by the problem of small grain size or that of poor crystallinity. In addition, the concentrations of the



dissolved species are easier to measure.

Studies of the oxidation of sulfide solutions by oxygen (Chen and Morris, 1972; Cline and Richards, 1969; O'Brien, 1974) have shown that several sulfur species were produced by the sulfide-oxygen reaction. Sulfate was the thermodynamically stable sulfur oxidation product, but elemental sulfur, polysulfides, thiosulfate and sulfite were also produced and persisted at sedimentary conditions for varying periods of time. Similar studies of the ferric iron-sulfide system are not available.

The reaction order for each species in the rate expression was determined by maintaining the concentrations of all other species in the reaction constant except the one to be studied. The rate of the reaction was followed by the change in the pH. pH changes of 0.1 to 0.4 pH units were observed. Yet hydrogen ion was one of the species in the rate expression and as such should have been kept constant. This variation in the pH might have affected the reaction order of the other species. More likely, the rate constant would have been altered. In addition, the experiments were conducted at relatively high total sulfide concentrations (0.05-0.5 M). This is 10 to 100 times the maximum concentration of total sulfide that could be expected in nature. This could conceivably have altered the rate of the reaction by changing the texture of the product. Rickard noted this in an earlier study (1969a). Future studies should be conducted at more realistic or natural sulfide values ( $<0.005$  M).

The complex secondary stage of the sulfidation of goethite, the formation of pyrite, was studied by Rickard (1975). Iron monosulfides were reacted with elemental sulfur in aqueous sulfide solutions to determine the kinetics of pyrite formation. The rate expression for this reaction was determined to be

$$d(\text{FeS}_2)/dt = k (\text{FeS})^2 (\text{S}) (\Sigma \text{S}^{=}) (\text{H}^+)$$

where  $d(\text{FeS}_2)/dt$  was the rate of pyrite formation in  $\text{M}^{-1} \text{l}^{-1} \text{sec}^{-1}$ ,  $k$  was the rate constant,  $(\text{FeS})$  was the surface area of FeS in  $\text{cm}^2$ ,  $(\text{S})$  was the surface area of elemental sulfur in  $\text{cm}^2$ ,  $(\Sigma \text{S}^{=})$  was the sum of activities of the dissolved sulfide species, and  $(\text{H}^+)$  was the hydrogen ion activity. The rate constant varied from  $1 \times 10^{-12}$  ( $40^\circ\text{C}$ ) to  $3 \times 10^{-14}$  ( $5^\circ\text{C}$ )  $\text{cm}^6 \text{mole}^{-1} \text{l}^{-1} \text{sec}^{-1}$ .

A proposed mechanism included (1) dissolution of both sulfur and ferrous sulfide, (2) formation of polysulfide ions, and (3) precipitation reaction between aqueous ferrous ions and polysulfide ions. The pyrite produced was non-framboidal although the reactant sulfur was classified as framboidal by the author. The reactant iron sulfide particles were spherical with a mean diameter of  $0.02\mu$ .

These studies have contributed greatly to the understanding of the formation of iron sulfides. However, it is difficult to correlate the results because of the wide range of experimental conditions that were used by the various researchers. Different temperatures, pH values, reactant

concentrations, iron phases and sulfide reactants were used. Yet by limiting the range of some of the conditions (temperature to 20°-25°C, and pH to 6-8) some agreement can be achieved. Results from similar experimental conditions are listed in Table 2.

Several general statements can be made about these results:

- (1) mackinawite was the initial iron sulfide formed
- (2) greigite formed at acid pH values only
- (3) mackinawite transformed to greigite in acid pH conditions
- (4) marcasite and pyrite needed elemental sulfur to form
- (5) mackinawite altered to pyrite when elemental sulfur was present.

Other results not listed in the table showed that greigite transformed to pyrite. The texture of the pyrite was affected by the presence of greigite as an intermediate. No adequate explanations have been advanced to consistently explain the nature of the products.

The product distribution can only be explained by determining the elemental chemical steps of each reaction. In order to accomplish this, the dissolved products, intermediates, and time-concentration curves of each species must be determined, in addition to characterizing the mineralogy of the solid iron sulfides.



Table 2  
Summary of Reported Sulfide Products

Iron and sulfur reactant species	pH				
	<6	6.5	7	8	>8
Fe <sup>+2</sup> , S <sup>=</sup>					
initial	G	M	M	M	M
3 months	G	G	G,M	M	M
6 months	G	G	G	M	M
Goethite, S <sup>=</sup>					
initial	S,MS,P	M	M	M	M
3 months	MS,P	MS,P,M	MS,P,M	M	
6 months	MS,P	MS,P	MS,P	P,MS	
Fe <sup>+2</sup> , S <sub>X</sub> <sup>=</sup>	P,MS,S	P,MS,S	P,MS,S	P,MS,S	
Goethite, S <sub>X</sub> <sup>=</sup>	S	S	S	S	S
M, S <sub>X</sub> <sup>=</sup>			P,MS		

Fe concentration: 0.05-1 M

S<sup>=</sup> concentration range: 0.05-1.8 M

G = greigite

MS = marcasite

M = mackinawite

S = sulfur

P = pyrite

S<sub>X</sub><sup>=</sup> = polysulfides

## EXPERIMENTAL

A mechanism of iron sulfide formation requires the identification of the solid and dissolved products of the reaction between ferric oxyhydroxides and aqueous bisulfide ion. In order to accomplish this, several series of experiments were conducted. Goethite and poorly crystalline goethite were reacted with aqueous bisulfide ion (0.002-0.09 M) to determine the kinetics of the initial sulfide oxidation products under the following conditions: pH 7.0-8.0,  $\text{Fe}_{\text{total}} = 0.8\text{-}5.6 \times 10^{-3}$ ,  $\mu = 0.295$  (salinity 24-25 ‰), temperature =  $25.0 \pm 0.2^\circ\text{C}$ . These values are representative of typical estuarine conditions.

### A. Preparation of Reactant Iron Minerals

#### 1. Goethite

Synthetic goethite ( $\alpha\text{-FeOOH}$ ) was prepared by the alkaline hydrolysis of ferric nitrate solutions (Atkinson et al., 1968). Ferric nitrate nonohydrate was dissolved in distilled water followed by the addition of 2.5 M NaOH to give a hydroxide:iron ratio between zero and two. The solution was next hydrolyzed at room temperature for 50 hours. Concentrated NaOH was added until the pH was greater than 10.6. The red brown suspension was aged in polyethylene bottles for 80 hours at  $60^\circ\text{C}$ . After ageing, the samples were centrifuged at 2100 RPM for 52 minutes and washed with

distilled water until a negative reaction with  $\text{AgNO}_3$  was obtained. Samples were suspended in distilled water and stored in polyethylene bottles.

The size of the particles was determined by transmission electron microscopy. High initial hydroxide:iron ratios produced small lath-like particles ( $630 \times 160 \text{ \AA}$ ) while larger particles ( $5100 \times 840 \text{ \AA}$ ) were produced by low hydroxide:iron ratios. The surface areas of these particles were found to be 66 and  $12 \text{ m}^2/\text{g}$ , respectively. Both samples gave electron and x-ray diffraction patterns corresponding to goethite, although not all reflections were observed for both samples. The amount of  $\text{FeOOH}$  in suspension was determined by drying aliquots of the suspension at  $90^\circ\text{-}100^\circ\text{C}$  for 24 hours.

## 2. Amorphous $\text{Fe}(\text{OH})_3$

Poorly crystalline  $\text{Fe}(\text{OH})_3$  was prepared by dropwise addition of 2 M KOH to 2M  $\text{FeCl}_3$  with constant stirring, until pH 7 was reached (Landa and Gast, 1973). The pH was monitored by a glass electrode referred against a single junction reference electrode. The brown-red precipitate was centrifuged and washed with distilled water until a negative chloride test was achieved. X-ray diffraction patterns ( $\text{Cr K}_\alpha$  radiation) showed no peaks. Electron diffraction patterns showed two broad, weak lines which were attributed to (021) and (002) reflections of goethite. The particle size was  $150 \text{ \AA}$ , and the surface area  $133 \text{ m}^2/\text{g}$ .



## B. Electrode Measurements

All pH measurements were made with a Ag-AgCl low sodium error glass electrode. This was referenced against a double junction reference electrode with a 10%  $\text{KNO}_3$  outer filling solution, or a single junction reference electrode with a saturated KCl-agar salt bridge. The glass electrode was calibrated and the slope was checked prior to each measurement with pH 7 and pH 10 buffers. The experimental slopes ranged from 95% to 100% of the theoretical slope of 59.16 mv (at 25°C). The Eh was measured with a platinum billet electrode referenced against a double junction reference electrode. The Pt electrode was calibrated with fresh Zobell solution at +0.430 mv (Parks, 1968).

The pS was measured with an Orion Ag-AgS electrode. All measurements were made with an Orion #701 digital pH meter and a #605 electrode switching box.

## C. Reagents

All solutions were prepared from reagent grade chemicals. The solutions were prepared with distilled water except the sulfide stock solutions. These were prepared with distilled water which was deoxygenated by bubbling with nitrogen gas for 8-12 hours. Stock sulfide solutions were prepared by flushing a glass stoppered flask with  $\text{N}_2$  for several minutes. The crystalline sodium sulfide monohydrate was rinsed with distilled deoxygenated water, to remove oxide coatings, and wiped dry with Kimwipes. The necessary weight

was dissolved in distilled, deoxygenated water, made to volume, and used within one hour of preparation. Tests for polysulfides, thiosulfate, and sulfite of the stock sulfide solution were negative.

#### D. Dissolved Reaction Products

##### 1. Reaction vessel

The studies of the oxidation products were conducted in a 0.5 liter plexiglas cylinder (Figure 2). (The interior surface area with the piston in, is 426 cm<sup>2</sup>.) The cylinder was sealed at top and bottom with plexiglas sheeting. The top had holes for a thermometer, gas bubbling tube, two sampling ports, and a glass piston. The piston permitted the removal of a sample without the introduction of a gas phase to the chamber.

The plexiglas bubbling and sampling tubes were sealed to the top lid with methylene chloride. The glass thermometer and piston barrel were sealed to the lid with General Electric silicone cement. A gastight seal was made between the piston and the barrel with silicone stopcock grease.

The reaction vessel was maintained at  $25.0 \pm 0.2^\circ\text{C}$  by means of a thermostated water jacket. All solutions were stirred with a glass stirring bar at constant rate for the duration of the run. (Private communication with R. Berner indicated that sulfide could diffuse through Teflon and react with the magnet of a Teflon coated stirring bar.) The top of the reaction vessel was covered with plastic

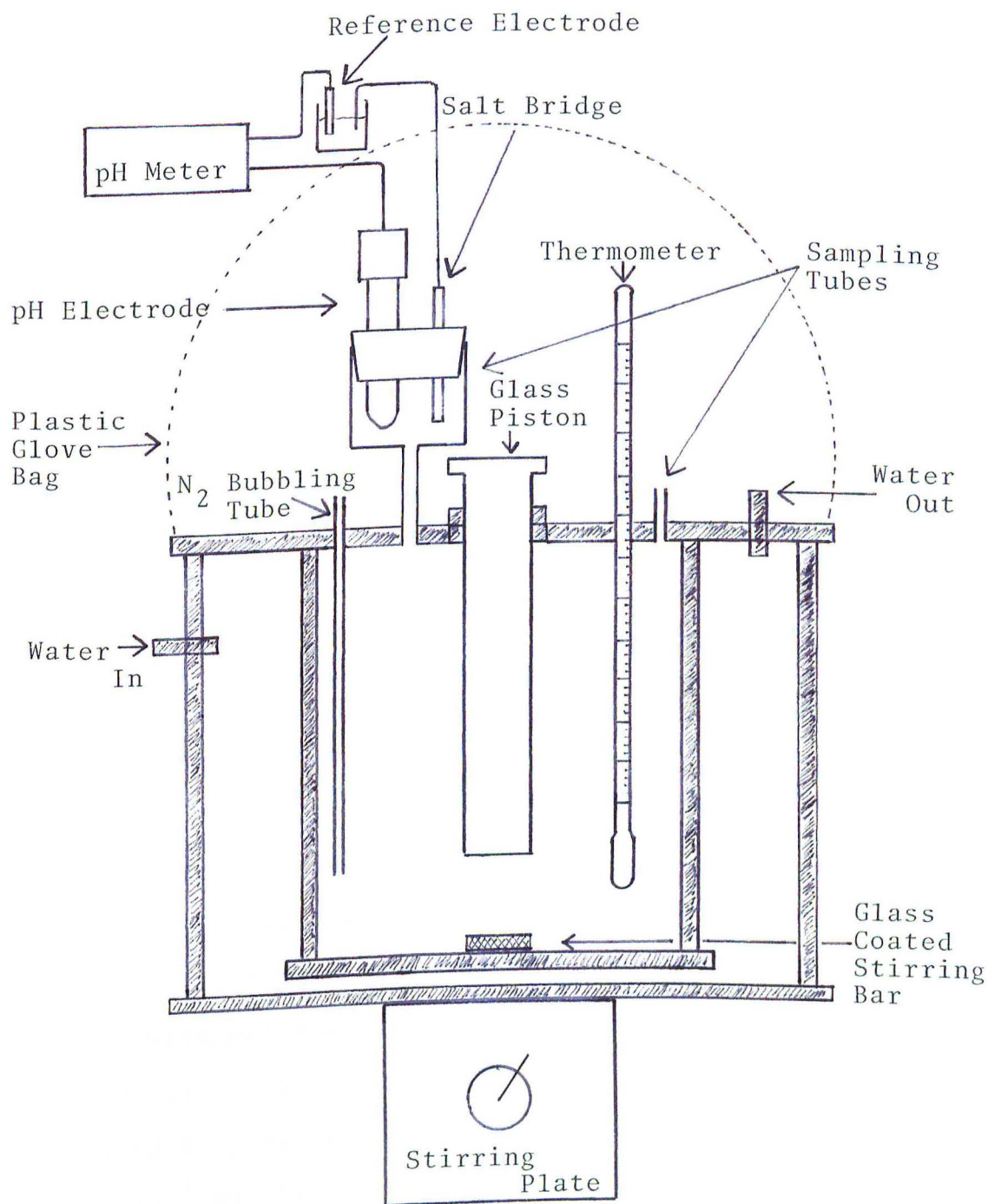


Figure 2: Schematic Diagram of Reaction Vessel



glove bags and flushed with nitrogen. This provided an inert atmosphere for sampling.

## 2. Reaction medium

The reaction was conducted in a buffered saline solution with an ionic strength of  $0.295 \pm 0.005$ . Sodium chloride was used to adjust the ionic strength. (The salinity varied from  $23.8 \text{ }^{\circ}/_{\text{oo}}$  at pH 7.45 to  $24.9 \text{ }^{\circ}/_{\text{oo}}$  at pH 8.55.) Palitzsch borax-borate buffer (Harvey, 1955) was used to maintain essentially constant pH from 7.45-8.55. The buffer capacity of the medium was determined experimentally, and found to range from 1.50 mM/0.1 pH units at pH 7.60 to 4.08 mM/0.1 pH units at pH 8.50. More extensive data on the medium is listed in Table 3.

## 3. Procedures

The reaction vessel was washed with dilute nitric acid, rinsed with distilled water and dried. Appropriate volumes of buffer, sodium chloride solution, distilled water, and acetic acid were pipetted into the reaction vessel and bubbled with purified nitrogen for 8-12 hours prior to addition of stock sulfide solution. Next, sulfide solution was added to give the desired total sulfide concentration ( $1-5 \times 10^{-3} \text{ M}$ ). The  $\text{S}^=$ , polysulfide, thiosulfate and sulfite concentrations and pH were determined. (The sulfite test was later discontinued due to early negative results.) After 30-60 minutes, an aqueous suspension of a reactant iron species was added and mixed for 5-10 minutes. The

Table 3

## Palitzsch Borax - Borate Buffers

Borax solution = 19.108 g  $\text{Na}_2\text{B}_4\text{O}_7 \cdot 10 \text{H}_2\text{O}$  / 1

Boric acid solution = 12.404 g  $\text{H}_3\text{BO}_3$  + 2.925 g  $\text{NaCl}$  / 1

Borax solution	ml	Boric acid solution	ml	pH @ 25°C	ionic strength $\mu$
	50		50	8.48	0.075
	45		55	8.38	0.072
	40		60	8.28	0.070
	35		65	8.17	0.067
	30		70	8.05	0.065
	25		75	7.92	0.063
	20		80	7.76	0.060
	15		85	7.58	0.057
	10		90	7.34	0.055

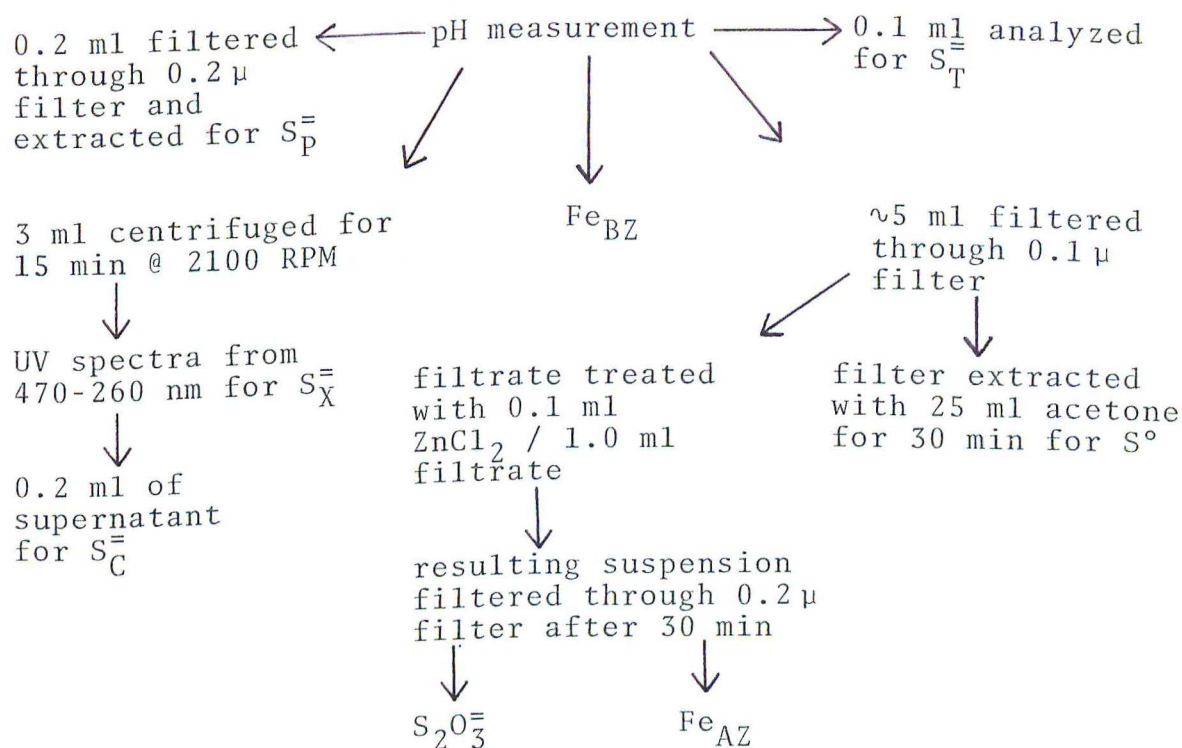
first sample was taken after 15-30 minutes and at regular intervals for generally 24 hours.

The sample was extruded into a syringe barrel. The pH was measured and total sulfide was determined. Next, 0.2 ml was filtered through a 0.2 $\mu$  Nuclepore filter, and the solid was analyzed for precipitated sulfide. (Precipitated sulfide refers to adsorbed or reactant sulfide.) Approximately 3 ml was removed, placed in UV cuvettes and centrifuged at 2100 RPM for 15 minutes. This procedure removed particles larger than 1000 Å. The UV spectra of the centrifuged solutions were recorded from 470-230 nm. In several runs, the UV spectrum was recorded after filtering through the 0.1 $\mu$  filter, but it was found that the filtering process resulted in loss of solution sulfide. Solution sulfide refers to dissolved sulfide and sulfide from particles smaller than 1000 Å. The supernatant liquid was sampled for solution sulfide. Approximately 3-6 ml of suspension was filtered through a 0.1 $\mu$  filter. 0.1 M ZnCl<sub>2</sub> was added to the filtrate to precipitate S<sup>=</sup> as ZnS (0.1 ml ZnCl<sub>2</sub> / ml sample). The filtered solid was refluxed for 30 minutes with 25 ml of acetone to extract elemental sulfur. This suspension was set aside, shaken after 30 minutes and filtered through a 0.2 $\mu$  filter. The filtrate was analyzed for thiosulfate, sulfite, and dissolved iron. A flow chart of the analytical procedure is shown in Figure 3.



Figure 3

## Flow Chart of Analytical Procedures



$S_T$  = total sulfide = solution and acid extractable solid sulfide

$S_C^=$  = solution sulfide

$S_P^=$  = acid extractable solid sulfide

$S^°$  = acetone extractable elemental sulfur

$S_2O_3^=$  = thiosulfate ion

$Fe_{BZ}$  = dissolved iron (<0.1μ) before addition of  $ZnCl_2$

$Fe_{AZ}$  = dissolved iron (<0.1μ) after addition of  $ZnCl_2$

$S_X^=$  = polysulfide,  $S_4^=$  and  $S_5^=$

#### 4. Electron microscopy and electron spectroscopy

In several runs the solids were studied by transmission electron microscopy (200 KV Hitachi) to note changes in morphology and mineralogy. Here, the reaction suspension was centrifuged at 2100 RPM for 15 minutes. The supernatant liquid was decanted and the solid was resuspended in distilled deoxygenated water. This suspension was spotted on copper electron microscope grids, with a collodion substrate. After drying in a nitrogen atmosphere, the sample was analyzed by transmission electron microscopy. Both micrographs and diffraction patterns were recorded. The diffraction patterns were calibrated with thallium chloride or aluminum.

Several samples were also analyzed by ESCA (Electron Spectroscopy for Chemical Analysis). Electron spectroscopy (Siegbahn, 1967) is a technique for measuring the binding energy of ejected electrons after interaction of the sample with high energy photons or x-rays. The values of the binding energy can be calculated from the following equation:

$$E_b = E_i - \phi_{sp} - T_{sp} - E_r$$

where  $E_b$  is the electron binding energy,  $E_i$  is the energy of the exciting source,  $\phi_{sp}$  is the work function in the vicinity of the spectrometer, and  $E_r$  is the recoil energy. The work function and the recoil energy are generally neglected for light elements, and the binding energy can be calculated from the knowledge of the exciting source and kinetic energy. The binding energy is a function of the atomic number of the

element, and the chemical environment. Thus information about the structure of the molecule and the oxidation state of the element can be determined. ESCA measures these properties of the top 100 Å only, and therefore the surface must be representative of the bulk of the sample.

The suspensions were filtered through a 0.2 $\mu$  filter under a nitrogen atmosphere. After drying, the sample was transferred with double sided scotch tape to an aluminum sample holder. The Fe 3p and S 2p spectra were measured on a Varian induced electron emission electron spectrometer. The spectra were calibrated with a Au standard at 83.4 eV and smoothed by a standard computer program using five points.

## 5. Analytical procedures

Concentrations of dissolved species were determined colorimetrically. All measurements were made on a Cary 15 UV-visible spectrophotometer with a 1 cm quartz cell. Distilled water was used in the reference beam.

All methods were checked to insure that there were no interferences from reactant, buffer, or other product. Procedures were modified when necessary, due to small sample volume. Otherwise, all methods were used as stated in the referenced works in the sections that follow. Necessary modifications, detailed procedures, and calibration curves for the different species follow.



a. Sulfide sulfur

Total, solution and precipitated sulfide were determined by reaction with N,N-dimethyl-p-phenylenediamine sulfate (Budd and Bewick, 1952). 0.1 ml of total or solution sample was fixed in 5 ml of 2% zinc acetate. Precipitated sulfide was measured after filtration of 0.2 ml of sample through a 0.2 $\mu$  Nuclepore filter. The filter and precipitate were transferred to zinc acetate solution. 0.5 ml of dilute amine solution and 0.1 ml of saturated ferric chloride were added, mixed and made up to 25 ml. Absorbance was measured at 670 nm. The mean relative standard deviation of the method was 4.5% for triplicate analyses, while the detection limit was  $1 \times 10^{-5}$  M. A representative calibration curve is shown in Figure 4.

b. Elemental sulfur ( $S^0$ )

A known volume of reaction suspension was filtered through a 0.1 $\mu$  Nuclepore filter. The precipitate was extracted with 25 ml of acetone by refluxing for 30 minutes (Bartlett and Skoog, 1954). Tests showed that this volume of acetone and refluxing time was effective in dissolving over 95% of the sulfur present. Pyrite was not extracted under these conditions.

After cooling to room temperature, 2 ml of sample were added to 5 ml of 0.1% sodium cyanide solution in acetone solvent (5% water) and set aside for two minutes. This acetone solvent was added to make 10 ml and mixed. 5 ml of the resulting solution was added to an equal volume of

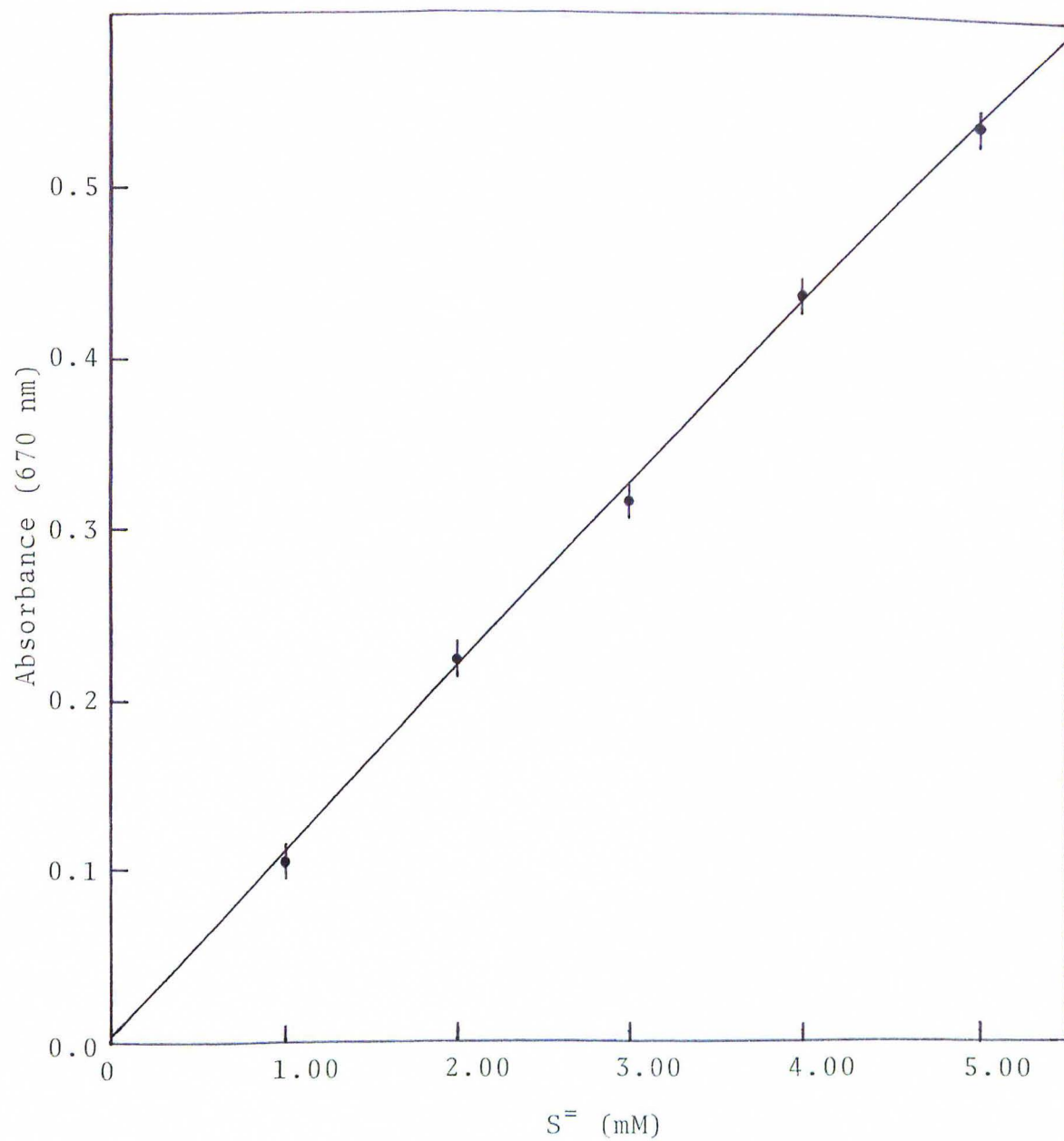


Figure 4: Sample Sulfide Calibration Curve

of saturated ferric chloride solution (acetone solvent) in opaque bottles. The absorbance was measured at 465 nm. The detection limit was 1 ppm  $S^{\circ}$  or  $1.5 \times 10^{-4}$  M  $S^{\circ}$ . The mean relative standard deviation for duplicate analyses was 2.7%. The calibration curves were prepared from weighed amounts of reagent grade elemental sulfur and were linear over the range 1-50 ppm (Figure 5). This volume was related to the original volume through the following equation:

$$M_S = \frac{\text{ppm } S^{\circ} \times 25 \text{ ml} \times 1 \times 10^{-3}}{\text{ml sample} \times 32 \text{ g mole}^{-1}}$$

c. Thiosulfate ion ( $S_2O_3^{--}$ )

1.0 ml of sample was mixed with 1.5 ml of deoxygenated distilled water and 0.5 ml of 1% sodium cyanide solution in as opaque bottle (Urban, 1961). 0.3 ml of 0.1 M cupric chloride solution was added with constant swirling to prevent formation of an insoluble precipitate. 0.5 ml of ferric nitrate-nitric acid reagent was also added with constant swirling. 1.0 ml of deoxygenated distilled water was added and mixed. The absorbance of the solution was measured within one hour at 460 nm.

Tests showed that sulfide gave a positive interference test and had to be removed prior to the thiosulfate test. Two methods were tested to remove aqueous sulfide from the filtered samples. The sample was acidified with 0.5 ml of 1 M acetic acid per 5 ml of sample and then bubbled with nitrogen gas for thirty minutes. A second method required



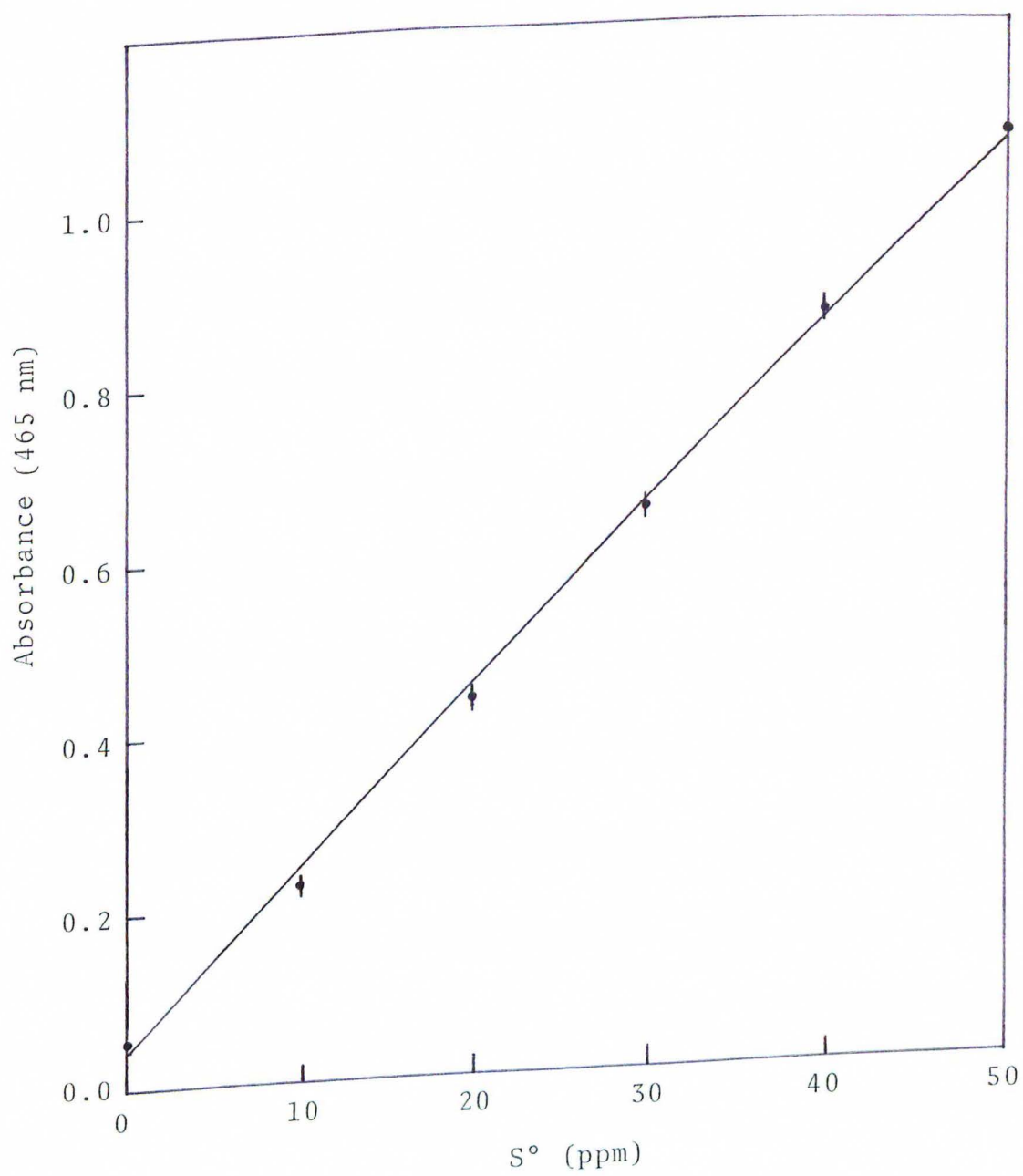


Figure 5 : Sample  $S^\circ$  Calibration Curve

the addition of 0.5 ml of saturated zinc chloride solution per 5 ml of sample, followed by filtration of the precipitate through a 0.2 $\mu$  filter after 30 minutes. Both gave similar results, but the latter was chosen for simplicity.

The samples were calibrated against sodium thiosulfate solution (Figure 6). The detection limit was  $1 \times 10^{-5}$  M  $S_2O_3^{=}$ , and the mean relative standard deviation was 3.3%.

d. Sulfite ion ( $SO_3^{=}$ )

Sulfite ion concentration was measured after treatment with zinc chloride (West and Gacke, 1956). One ml of sample was added to 5 ml of 0.1 M sodium tetrachloromercurate. 0.5 ml of 0.04% hydrochloric acid-bleached p-rosaniline was added and followed by 0.5 ml of 0.2% formaldehyde solution. The absorbance was measured at 565 nm between 15 and 35 minutes after addition of the formaldehyde solution. The absorbance was found to increase up to 15 to 20 minutes, and slowly decrease after that time.

The concentration was determined from a calibration curve (Figure 7) which was prepared from sodium sulfite solutions. The detection limit was  $1 \times 10^{-5}$  M  $SO_3^{=}$ .

e. Iron

Dissolved iron (<0.1 $\mu$  particles) was determined for the filtered sample (Charlot, 1964). 0.5 ml of sample was mixed with 0.2 ml of 0.1 M acetic acid, 0.5 ml of 10% hydroxylamine hydrochloride solution and 0.5 ml of 0.5% 1,10-phenanthroline hydrochloride. The solution was mixed and set aside

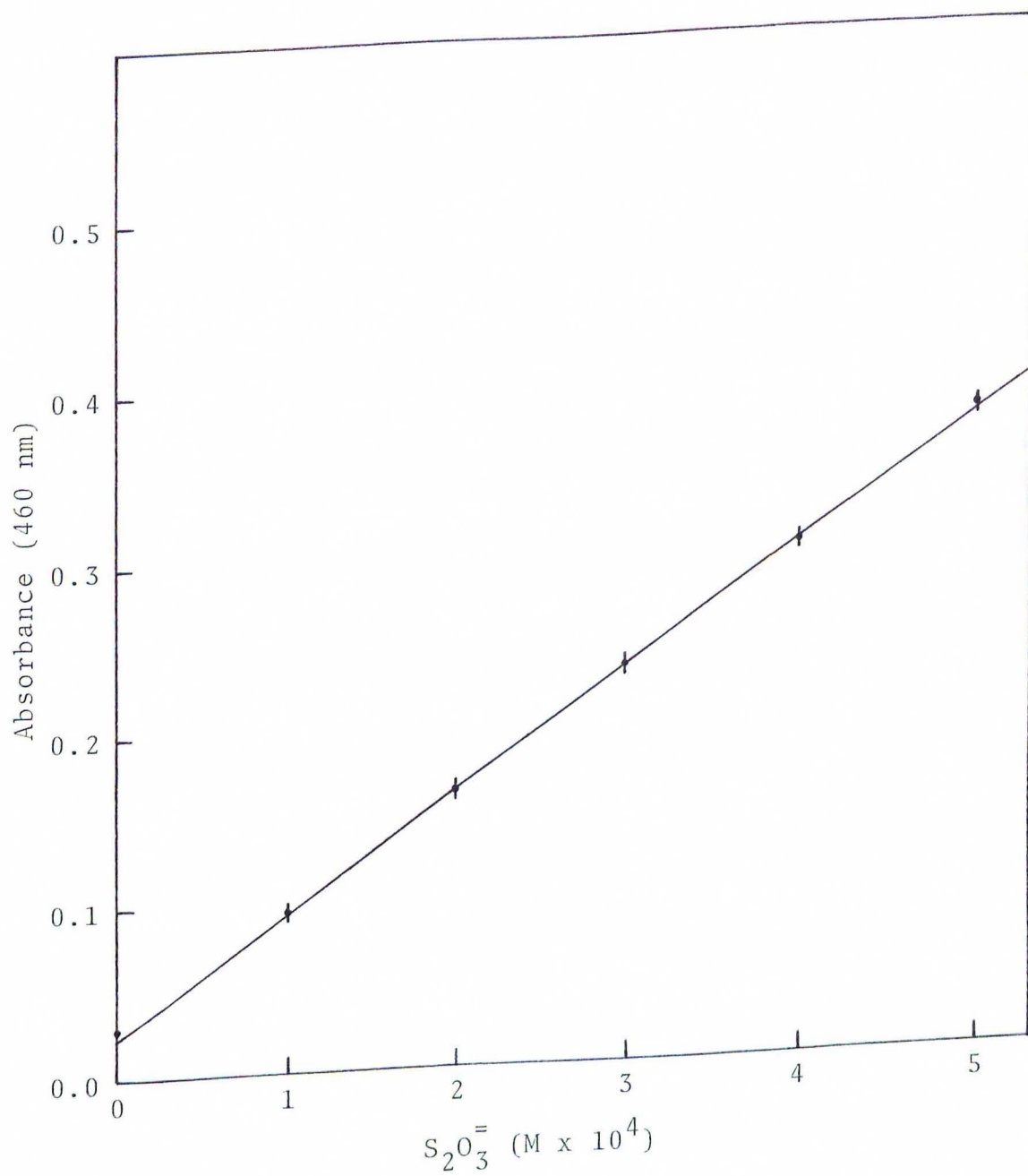


Figure 6 : Sample Thiosulfate Calibration Curve



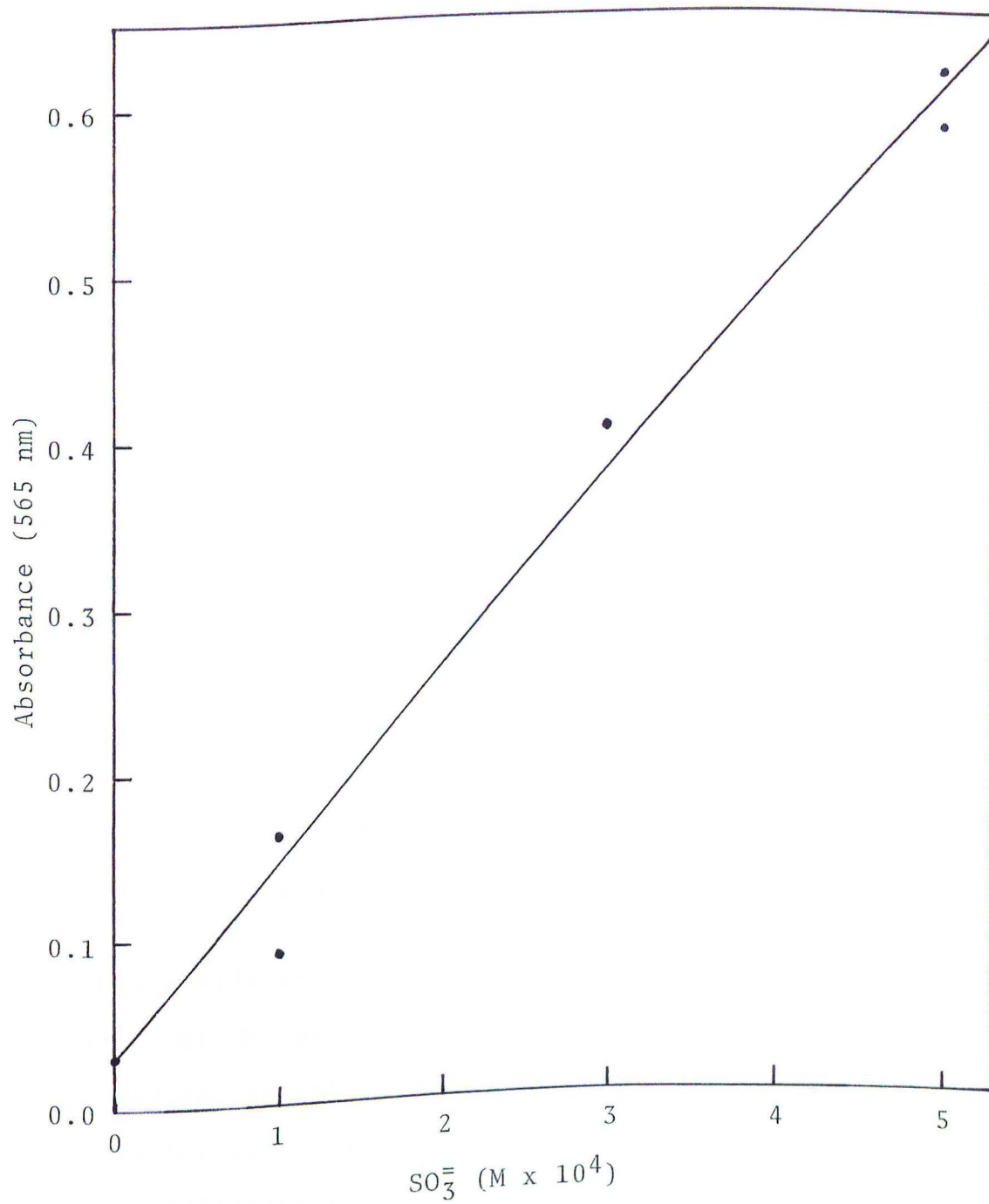


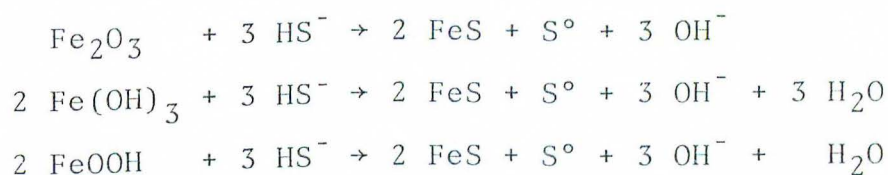
Figure 7: Sample  $\text{SO}_3^{2-}$  Calibration Curve

for one hour, then made up to 10 ml. The absorbance was measured at 510 nm. The calibration curve was linear from 1-50 ppm and had a detection limit of 1 ppm or  $1.79 \times 10^{-5}$  M.

Tests with dissolved iron standards were not affected by the zinc chloride treatment to remove dissolved sulfide. However, several times during the reaction runs, the iron test was conducted with and without the zinc chloride treatment. The untreated samples always showed higher concentrations of iron. This would indicate that the precipitation of zinc sulfide caused a coprecipitation or adsorption of iron from the solution. (Calibration curve in Figure 8.)

f. Hydrogen ion ( $H^+$ )

The reaction of iron oxides, hydroxides and oxyhydroxides results in the formation of hydroxide ions, according to the following reactions:



A pH change will be observed as a result during the reaction. The amount of  $OH^-$  produced can be determined from the pH change and the buffer capacity of the system. The integral of the buffer capacity  $\beta$ , from  $pH_{initial}$  to  $pH_{final}$  will yield the titration curve for the buffer. The titration curve for the borax-borate buffer (Perrin et al., 1974) was determined experimentally by titrating a solution of the

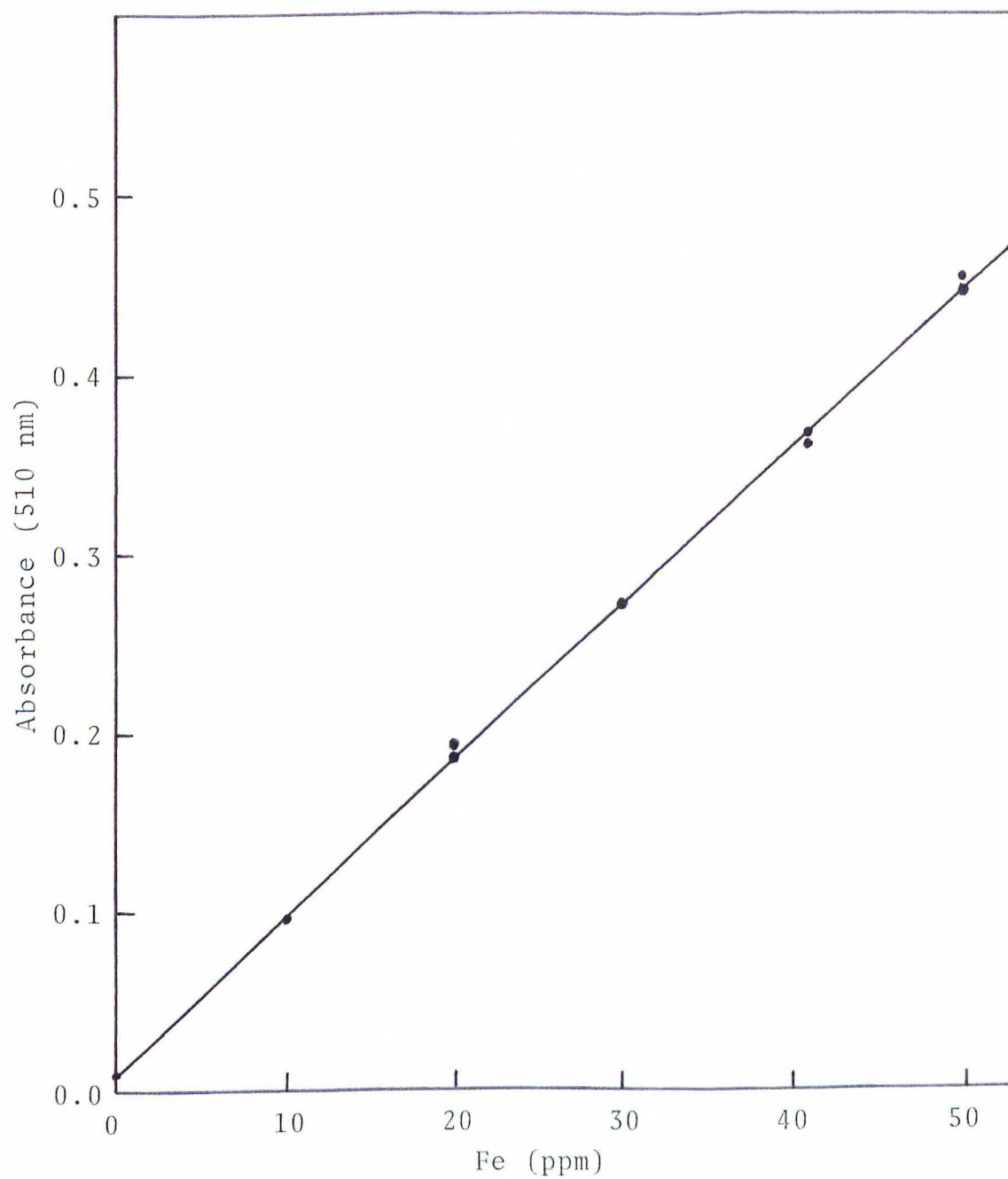


Figure 8: Sample Fe Calibration Curve



buffer, salt solution and distilled water (in the proportions used in the reaction runs) with a strong base. The titration curve for the region 7.2 to 8.0 is shown in Figure 9. The equation for the line is

$$y = 376 - 106.7 x + 7.76 x^2$$

where  $y$  is the number of millimoles per liter of added hydroxide, and  $x$  is the pH. In addition to the borate buffer, the reaction solution is buffered by the  $H_2S$ - $HS^-$  system, since the  $pK_1$  for this weak acid is 6.75 at the ionic strength of the reaction system (Goldhaber and Kaplan, 1975). The buffering capacity however, is small due to the low total sulfide concentrations used in this series of experiments ( $2-9 \times 10^{-3} M$ ). The buffering by this couple is based on the fact that the reacting species in the equations is  $HS^-$ , the predominant species at pH greater than 6.75. As a result, a change in the total sulfide concentration or a pH change will result in the release of the excess hydrogen ion which can then react with excess hydroxide ions. The amount of excess hydrogen ion that is released can be determined by the following expression

$$+\Delta(H^+) = -\Delta(OH^-) = (C_{St} \alpha_o)_{pH_i} - (C_{St} \alpha_o)_{pH_f}$$

where  $C_{St} = (H_2S) + (HS^-)$ , and

$$\alpha_o = \frac{1}{(1 + K_1/(H^+) + K_1K_2/(H^+)^2)}$$

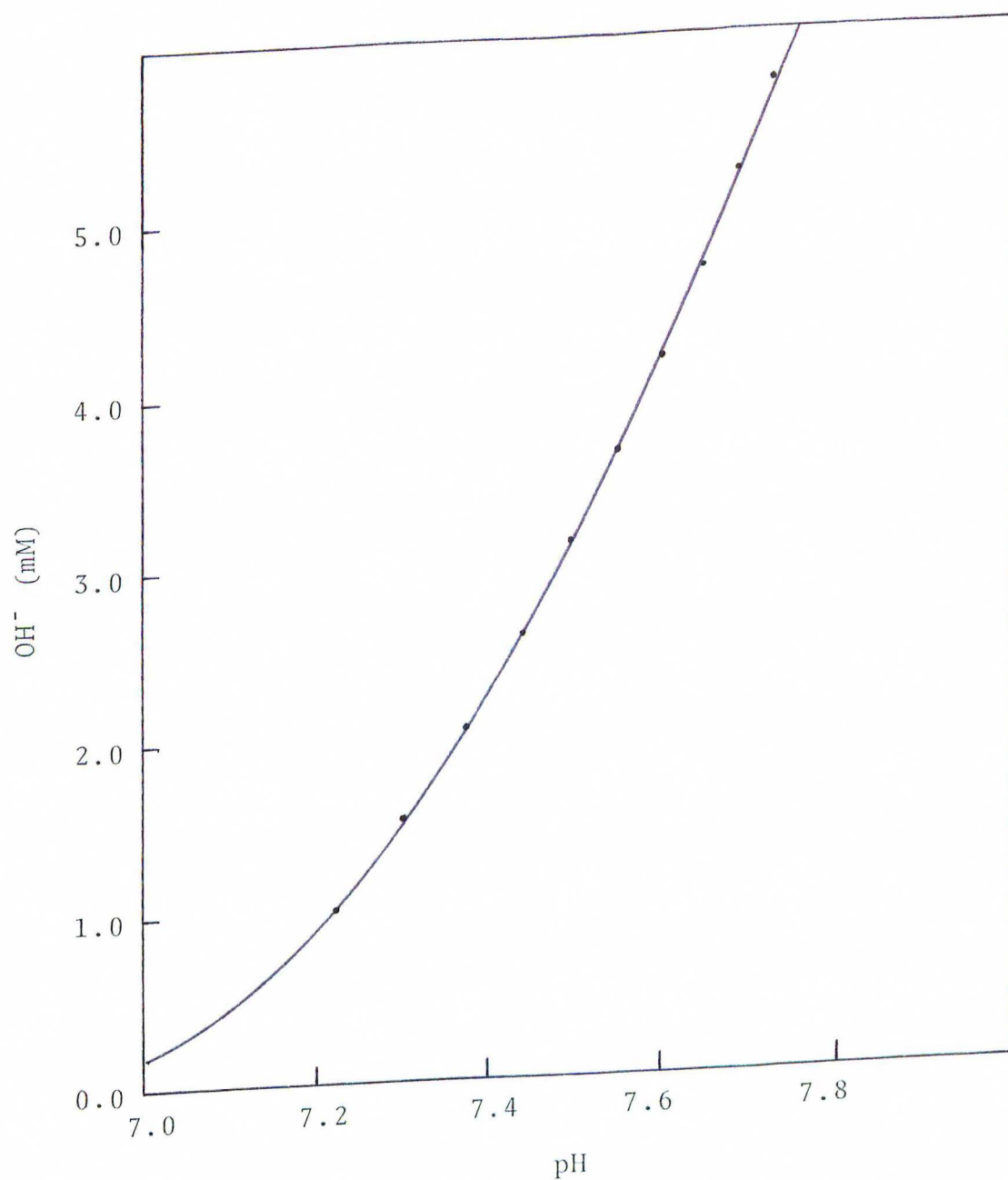


Figure 9: Titration Curve for Borax-Borate Buffer

$$[\text{OH}^-]_{\text{(mM)}} = 367 - 106.7 \text{ pH} + 7.76 \text{ pH}^2$$

where  $K_1$  and  $K_2$  are the first and second dissociation constants for hydrogen sulfide. At the pH conditions used in this study, the denominator simplifies because the third term is small and the equation reduces to

$$\alpha_o = \frac{1}{(1 + K_1/(H^+))}$$

The buffer capacity of the system is thus the sum of the two buffers (Perrin et al., 1974).

#### g. Polysulfides

The concentrations of the polysulfide ions,  $S_4^{=}$  and  $S_5^{=}$ , were determined from hydrogen ion, total sulfide and elemental sulfur concentrations, ultraviolet absorption measurements at 300 nm and 370 nm, and equilibrium calculations. At any wavelength, the total absorbance is equal to the sum of the absorbances for all of the absorbing species. At 300 nm and 370 nm, polysulfides are the only known absorbing species that are expected to be present in the reaction solutions. UV spectra of thiosulfate, sulfide, buffer solutions, sulfite, ferrous and ferric chloride solutions showed no absorbances over the range 290-400 nm. Thus, the polysulfide concentrations can be determined from the equation

$$A = ([S_4^{=}] \epsilon_4 + [S_5^{=}] \epsilon_5) l$$

where  $l$  is the cell path length,  $\epsilon_4$  and  $\epsilon_5$  are the molar absorptivities for the  $S_4^{=}$  and  $S_5^{=}$  species respectively, and



$[S_4^{=}]$  and  $[S_5^{=}]$  are the concentrations of the respective species. The molar absorptivities of the polysulfides are 3420 and 8000  $\text{cm}^{-1} \text{M}^{-1}$  at 300 nm, and 960 and 2560  $\text{cm}^{-1} \text{M}^{-1}$  at 370 nm for  $S_4^{=}$  and  $S_5^{=}$  respectively (Giggenbach, 1972). At the conditions of the reaction for pH, sulfide concentration and sulfur concentration, the tetra- and pentasulfide species are the only polysulfide species present. The amount of each can be determined with the aid of the expression:

$$\beta = (\text{HS}^-) (\text{OH}^-) / (\text{S}^0)$$

The  $\beta$  range for the experimental runs was -4.5 to -6.6, with the tetrasulfide predominating below -6.0. The  $\beta$  value can then be used with Figure 10 from Giggenbach (1972).

The ratio between the two peaks at 300 nm and 370 nm can be calculated to range from 3.35 to 3.12. However, early experiments showed that the ratio between the two peaks was always less than 3.1. Either an unknown absorbing species was present or small particles were present which scattered the light and raised the background equally over the entire spectral range. Tests were conducted to evaluate the two possibilities. Polysulfide solutions which had the proper ratio for the two peaks were used. Product material from the reaction of ferrous iron and sulfide solution were added. This solution was used to remove the possibility that submicron goethite particles were responsible for the observed phenomenon. The addition of small aliquots of

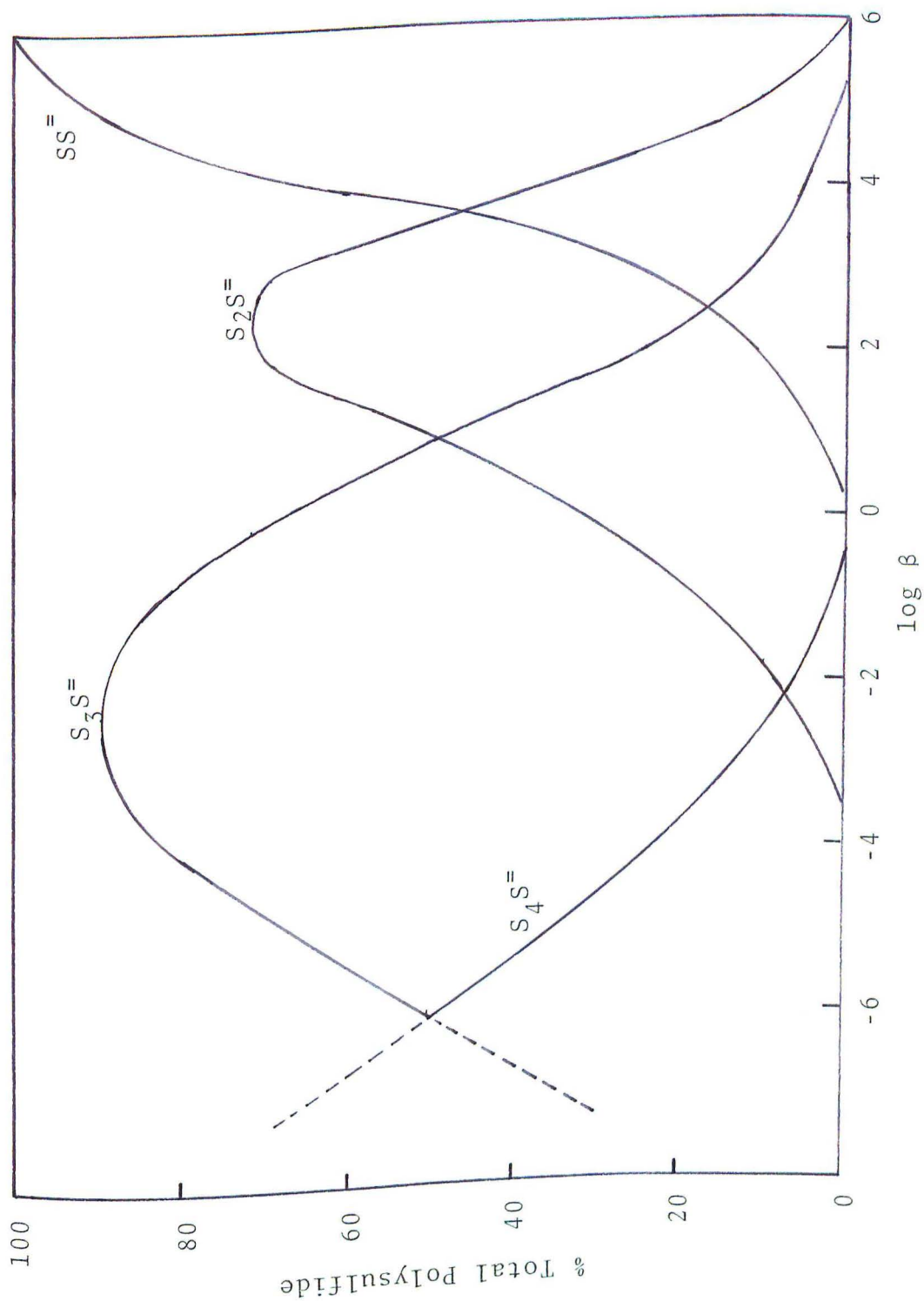


Figure 10: Equilibrium Distribution of Polysulfide Ion  $S_n S_n^{=}$

this suspension resulted in the raising of the entire UV spectrum over the desired range. The difference between the peaks and the shape of the spectrum did not change. The ratio between the two peaks decreased with the addition of each aliquot. Thus the correct possibility was the scattering by submicron particles of iron sulfide product. This would be consistent with the fact that as the reaction proceeded the background increased.

The polysulfide concentrations were then determined by subtracting the same amount from both peaks until the proper ratio was obtained. The proper ratio was determined from the following expression

$$Y = \frac{x \frac{8000}{2560} + y \frac{3420}{960}}{x \frac{8000}{2560} + y \frac{3420}{960}}$$

where  $x$  is the percentage of  $S_5^{=}$  and  $y$  is the percentage of  $S_4^{=}$ . The percentages  $x$  and  $y$  can be determined from the value of  $\beta$  and Figure 10 from Giggenbach (1972).

A check of this entire procedure was made by taking the concentrations determined for the two polysulfide species, the peak positions, the molar absorptivities, and the peak widths to synthesize a spectrum. This synthesis was performed on a Dupont curve resolver, which was provided by the Center for Materials Research. Figure 11 shows the validity of the method by the good fit that was achieved by the synthetic curve and the "real spectrum", over the significant region 300-380 nm.



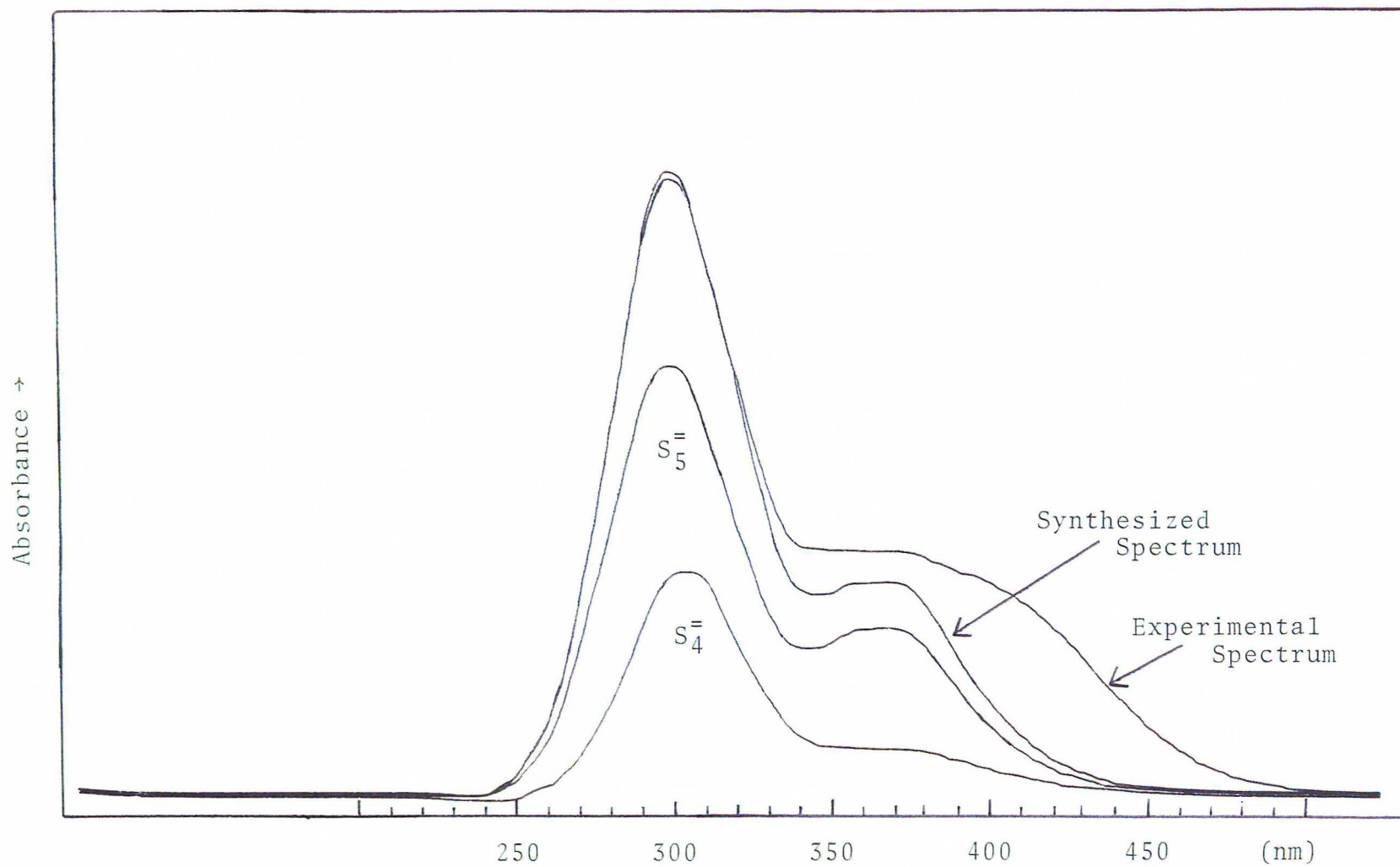


Figure 11: Real and Synthesized Polysulfide Spectra

The peak characteristics for the polysulfides are:

Species	$\nu'_n$	$\epsilon'_n$	$\nu'_{1/2}$	$\nu''_n$	$\epsilon''_n$	$\nu''_{1/2}$
$S_4^{=}$	3030	3420	595	3676	960	595
$S_5^{=}$	2990	8000	520	3740	2560	520

where the  $\nu$  values are the wavelengths of the two peaks, the  $\epsilon$  values are the molar absorptivities, and the  $\nu_{1/2}$  values are the halfwidths of the peaks. Peaks and halfwidths are in angstroms (Giggenbach, 1972).

#### 6. Dilution effects

The pH of the medium was observed to increase upon the addition of the ferric reactants. A significant portion of this change was probably due to the dilution of the buffer. In order to determine the magnitude of this effect, a series of measurements was made. Results showed that the dilution effect was +0.01 pH units / 10 ml of solution added to 500 ml final volume. There was no significant difference between the addition of deoxygenated distilled water or goethite suspension. (Figure 12.)

#### E. Particle Size Study

Determination of the size of submicron particles of FeS was attempted by successive filtration of product suspensions. Several (10-15) ml of reaction product suspension was withdrawn from the reaction vessel and successively filtered through 0.8, 0.2, 0.1, and 0.01  $\mu$  filters. The

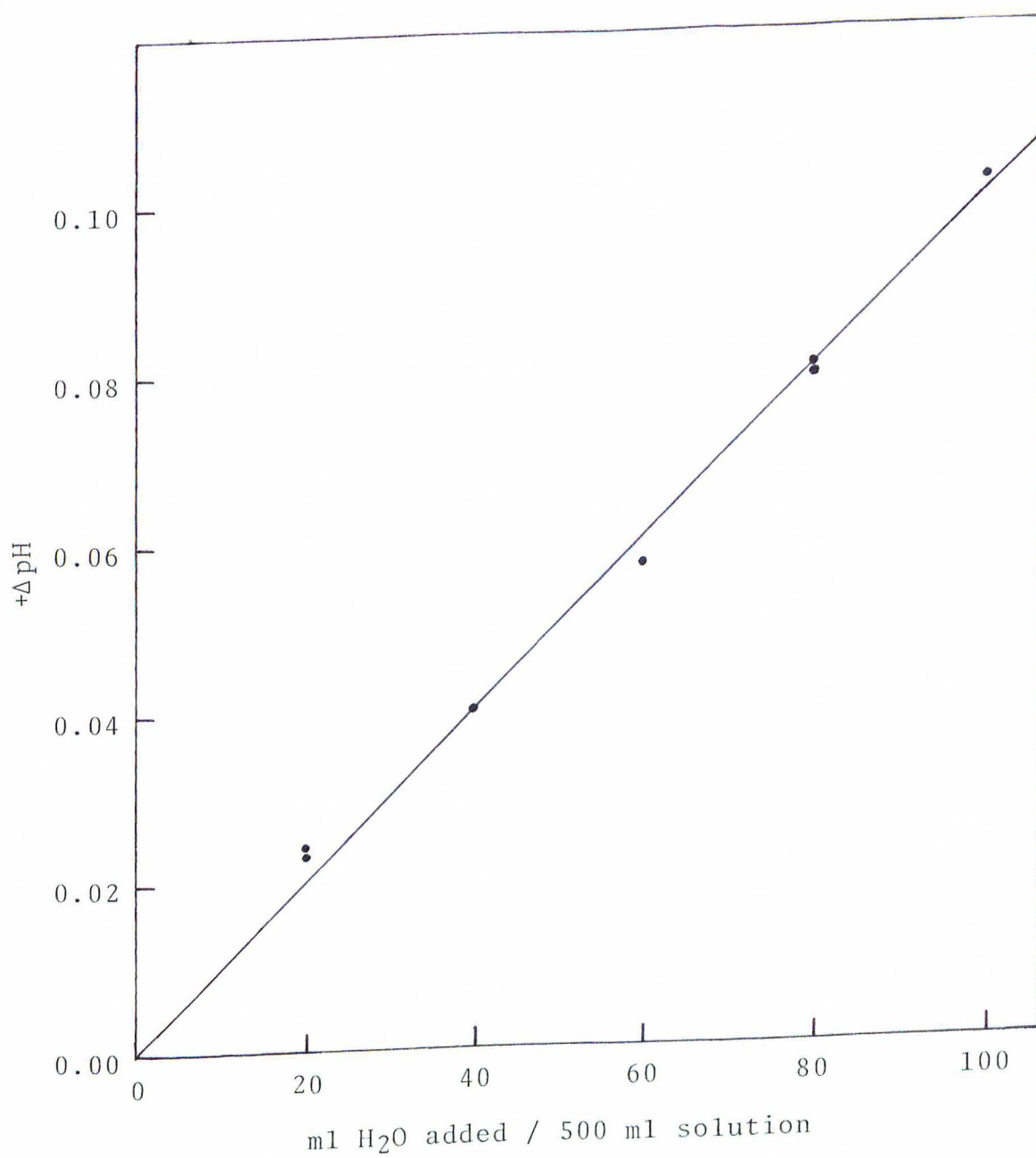


Figure 12: Change of pH Upon Dilution of Reaction Solution Due to Addition of Water



first three filters (Nuclepore) were polycarbonate while the  $0.01\mu$  filter was a membrane filter (Schleicher and Schuell).

After each filtration step, the polysulfide spectra, total "dissolved" sulfide concentration (i.e. dissolved sulfide and particulate iron sulfide smaller than the filter pore size) and iron concentrations were determined by the spectrophotometric and colorimetric methods as previously discussed.

A decrease in both iron concentration and sulfide concentration would be attributed to filtration of iron sulfide particles. Measurements of sulfide concentrations were complicated by the results which showed a decrease of dissolved sulfide without a concomitant decrease in iron concentration in the  $0.8$  and  $0.2\mu$  filtration steps. This effect was attributed to the outgassing of  $H_2S$  from solution during the filtration process. As a result it was necessary to provide a blank to correct for the outgassing. The  $0.1\mu$  filtration was repeated two times in parallel with the  $0.01\mu$  filtration to correct for this effect. The amount of  $H_2S$  lost was assumed to be independent of the filter size and only dependent on the filtration process itself. Investigation of this result indicates that this was not a good assumption. Consequently, the sulfide values are not very accurate and cannot aid in the interpretation of the result. Only the iron curve and absorbance values were used in the particle size analysis.

## RESULTS AND DISCUSSION

The results of 19 reaction runs were studied by the initial rate method to determine the rate expression and rate constant for the formation of sedimentary iron sulfides. Concentration-time curves, electron transfer balance, hydrogen balance, and stoichiometric relationships were used to determine a consistent mechanism.

Data for the reaction runs used can be found in Appendix A. All but two of the reaction runs used goethite,  $\alpha$ -FeOOH, as the reactant iron material. Amorphous  $\text{Fe}(\text{OH})_3$  was used in runs 11 and 12. The goethite suspension used in all the other runs was prepared by the same method, but three reaction runs (33, 35, and 36) used material which was prepared at a different time.

Studies by Jefferson et al. (1975) showed that coatings on the surface of iron stained kaolinite minerals consisted of crystalline goethite and amorphous iron oxide coatings. The equivalent spherical diameter of the goethite particles was determined to be 300 Å.

Figure 13 shows a sample concentration-time curve for the various reactants and products. This semi-logarithmic plot is used to show the behaviour of all the species measured during the reaction. The concentration of reactant bisulfide ion (i.e. solution sulfide) decays rapidly at first and then slows. This type of behaviour is typical of a

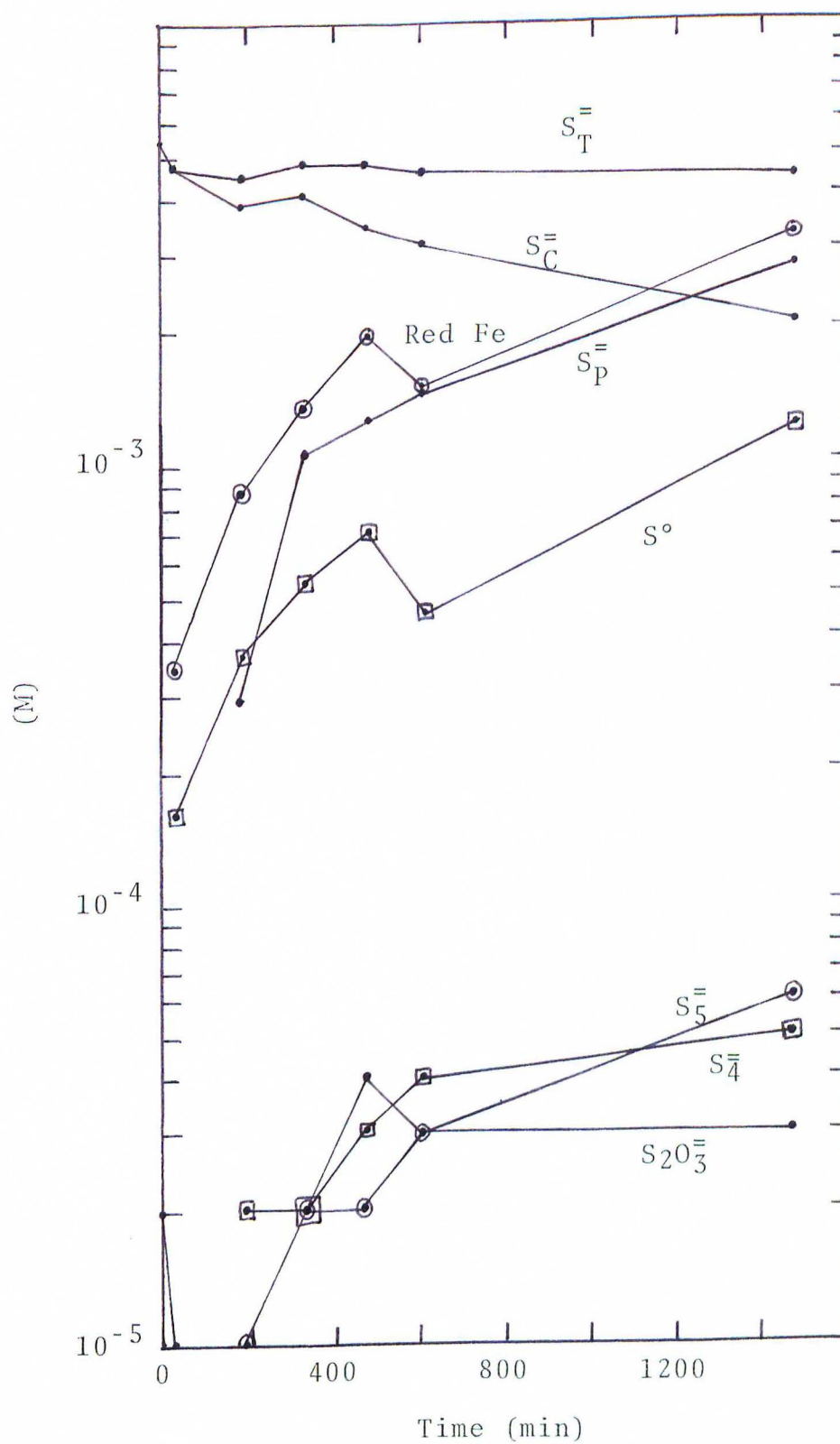


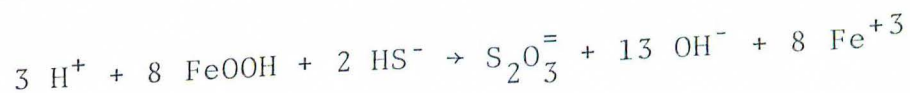
Figure 13: Concentration-Time Curves for Reactants and Products (Run 31)



multiorder rate expression. Similar polynomial growth curves are observed for the product species.

#### Oxidation products

The reaction between goethite and aqueous bisulfide ions resulted in the formation of several sulfur oxidation products: elemental sulfur, polysulfides, and thiosulfate. Thiosulfate was found to comprise  $14 \pm 8\%$  (mean of 18 runs) of the oxidation products on the basis of total electrons transferred. The reaction which can produce thiosulfate is



Variation of percent thiosulfate as a function of initial sulfide, hydrogen ion concentration, and total goethite initial surface area is shown in Table 4. A linear correlation coefficient of  $r = .97$  was found for the initial sulfide concentration vs. % thiosulfate. A linear correlation coefficient of  $r = .74$  was found for initial goethite surface area vs. % thiosulfate. The linear correlation coefficient between initial hydrogen ion and % thiosulfate was  $r = .091$ . These correlations will be explained later in terms of the initial reduction reaction.

Unfortunately, such a comparison of the data of oxidation products (concentration and %) with data from sediments is limited since there is only one study (Rozonov et al., 1971) in which possible sulfide oxidation products are reported. The lack of information in this area may be a

Table 4

Variation of % Thiosulfate with Initial Reaction Conditions

 $[S_T^{=}]_i$  and % Thiosulfate

$[S_T^{=}]_i$ (mM)	1.8	2.6	4.7	8.7
--------------------	-----	-----	-----	-----

% thiosulfate	4	3	7	18
---------------	---	---	---	----

$$\% \text{ thiosulfate} = -1.35 + 2.14 \times 10^{-3} [S_T^{=}]_i \quad r = .97$$

Initial Surface Area ( $A_i$ ) and % Thiosulfate

$A_i$ ( $m^2$ )	2.51	5.45	6.52	15.2	18.5	32.6
-----------------	------	------	------	------	------	------

% thiosulfate	22	22	36	7	5	6
---------------	----	----	----	---	---	---

$$\% \text{ thiosulfate} = 27.3 - .824 A_i \quad r = .74$$

 $[H^+]_i$  and % Thiosulfate

$[H^+]_i$ ( $M \times 10^8$ )	1.06	1.86	2.79	3.81	4.65	6.75	9.30
-------------------------------	------	------	------	------	------	------	------

% thiosulfate	10	20	36	25	17	19	22
---------------	----	----	----	----	----	----	----

$$\% \text{ thiosulfate} = 20.1 + 2.52 \times 10^7 [H^+]_i \quad r = .091$$

result of several experimental difficulties or theoretical preconceptions. Experimentally, interstitial waters of reducing sediments are difficult to study due to problems of rapid air oxidation (Troup et al., 1974; Bray et al., 1973). Difficulties in measurement of small quantities ( $<1$  mM) of sulfate, sulfite or thiosulfate may also be a factor in the small number of studies of sulfide oxidation products. An additional reason for the lack of data for thiosulfate concentrations in sediments is that Desulfovibrio can utilize thiosulfate ion as well as sulfate ion for its respiratory processes (Murakami, 1952). Thus, thiosulfate could be recycled back to sulfide and would not be observed as an oxidation product.

Rozanov et al. (1971), however, measured the concentration of  $H_2S$  and thiosulfate in interstitial waters of anoxic marine sediments. Concentrations of thiosulfate and sulfide ranged from  $4 \times 10^{-6}$  to  $3.5 \times 10^{-4}$  M, and from  $1 \times 10^{-5}$  to  $4.5 \times 10^{-3}$  M respectively. Calculations were made using this data to determine the importance of thiosulfate as an oxidation product in the sediment. Elemental sulfur and thiosulfate were assumed to be the only sulfide oxidation products. Elemental sulfur and thiosulfate were also assumed to be produced only by the reduction of  $FeOOH$  by  $H_2S$ . These calculations showed that 0.9-32% of the oxidation products are thiosulfate (on the basis of electron transfer balance) with an average of 6% for 15 values. This is low compared to the 14% found in the present study, but



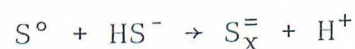
considering the fact that some elemental sulfur may be derived from the microbial oxidation of  $\text{HS}^-$  by Desulfovibrio and Thiobacillus (Zajic, 1969) the agreement is rather good.

In addition, a linear regression analysis was conducted on the concentration of sulfide and % thiosulfate (electron balance-wise) reported by Rozonov et al. (1971) to see if any correlation existed. Calculations using 15 points yielded a straight line, with the equation

$$[\text{S}_2\text{O}_3^{=}] = .783 + 4.32 \times 10^3 [\text{S}_{\text{T}_i}^{=}]$$

This line had a linear correlation coefficient of  $r = .77$ , and these results agree with those of this study which showed a linear relationship between % thiosulfate and total initial sulfide concentration.

Polysulfides,  $\text{S}_4^{=}$  and  $\text{S}_5^{=}$ , and elemental sulfur were grouped together since polysulfides are formed by the following rapid reaction of elemental sulfur with dissolved sulfide ions (Teder, 1971):

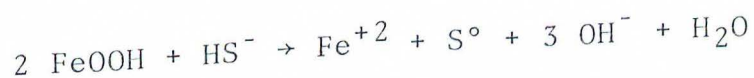


where  $x = 2, 3, 4$ , or  $5$ . At the pH, sulfide, and elemental sulfur concentrations used in this study, the predominant polysulfide species are  $\text{S}_4^{=}$  and  $\text{S}_5^{=}$ . Other possible polysulfides are present only at higher pH values (Giggenbach, 1972). The total concentration of elemental sulfur can be determined from the following equation:

$$[S^{\circ}]_t = [S^{\circ}] + 3 [S_4^{\equiv}] + 4 [S_5^{\equiv}]$$

where  $[S^{\circ}]$  is the free sulfur as determined by the acetone extraction. The last two terms represent the complexed elemental sulfur.

The overall reaction responsible for the formation of the elemental sulfur as the oxidation product is:



Polysulfides are formed by the rapid subsequent reaction of the elemental sulfur as shown above.

Elemental sulfur is the major oxidation product in the reaction and as such can serve as a quantitatively significant source of  $\text{S}^{\circ}$  in the sediment. However, the above reaction for the chemical production of elemental sulfur could provide only half the elemental sulfur needed for the transformation of iron monosulfide, mackinawite or amorphous  $\text{FeS}$ , to pyrite. This assumes that all of the ferrous iron is initially reduced by sulfide species. Microbial processes are probably responsible for the bulk of elemental sulfur in anoxic sediments. Thiobacillus denitri-  
ficans and other sulfide oxidizing anaerobes can oxidize sulfide to elemental sulfur, although these bacteria prefer to oxidize elemental sulfur to thiosulfate and sulfate (Zajic, 1969).

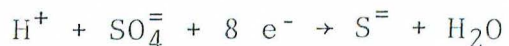
Data by Berner (1964 and 1970) and Kaplan et al. (1963) shows that pyrite was the major iron sulfide found

in recent marine sediments. Sulfur derived from the chemical oxidation of sulfide could have accounted for only 50% of the elemental sulfur found as free and pyrite sulfur. This calculation is based on the amount of total iron sulfides, both mono- and disulfides, and the concentration of total elemental sulfur.

#### Reduced iron

What, then, is the predominant reaction responsible for the reduction of iron in the sediment? Several bacteria of the genus Pseudomonas can reduce large quantities of ferric to ferrous iron in soils and bogs. However, little is known about the iron reducing capabilities of microbes in anoxic sediments.

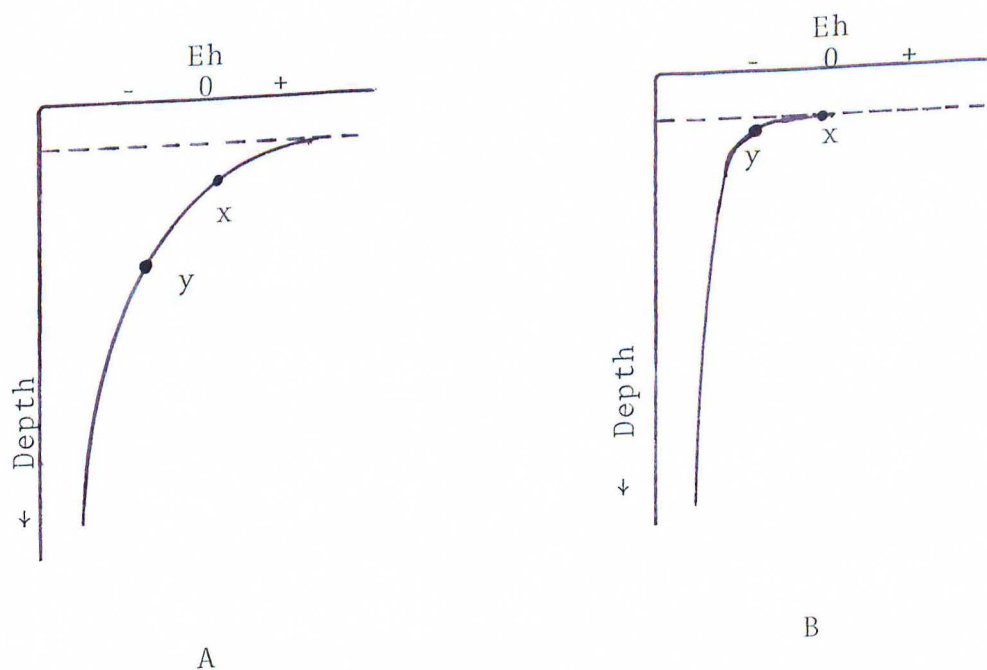
Thermodynamically, the reduction of iron should occur prior to the reduction of sulfate (and formation of sulfide). The redox reactions for these two species are:



(Stumm and Morgan, 1970)

Thus the reduction of iron would not proceed by the concomitant oxidation of sulfide species. The thermodynamic sequence of reactions above would occur in the sediment in which the oxic-anoxic boundary occurs well below the sediment-water interface. This type of sediment column would have an Eh profile as shown in Figure A below.



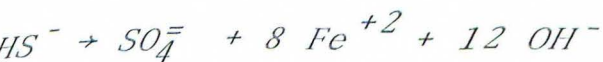
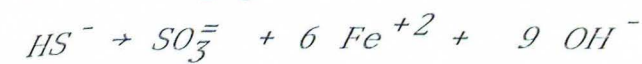
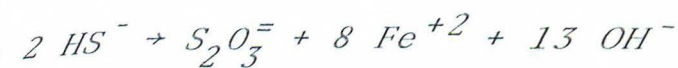
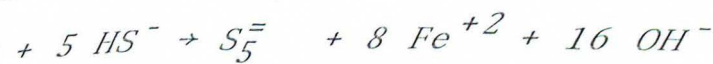
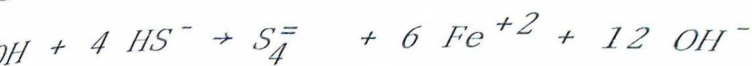


At point x, the reduction of ferric iron would occur, while sulfate reduction would occur at point y.

In many anoxic sediments, the boundary between the oxidizing and reducing zones occurs at or slightly above the sediment-water interface, and the entire sediment column has a negative Eh. An Eh profile for such a sediment column is shown in Figure B above. In this environment, both sulfate ion and ferric iron species could be reduced simultaneously. In this type of anoxic sediment, the reduction of  $\text{Fe}^{+3}$  by  $\text{HS}^-$  could occur, producing elemental sulfur. In extreme cases, the overlying bottom waters are anoxic, and  $\text{H}_2\text{S}$  is found in the water column. (The Black Sea is the classic example of this type of environment.) Here the reduction process can occur in the water column. Brewer and Spencer

(1974), studied the partition of trace metals between dissolved and particulate phases in the water column. They observed a rapid rise in the concentration of trace metals in the anoxic part of the water column, followed by a rapid decrease, as they descended into the anoxic region of the water column. This behaviour provides evidence for the rapid reduction and dissolution of iron sulfides. Saturation with respect to iron sulfides was exceeded when the rate of formation of iron sulfides exceeded the rate of dissolution.

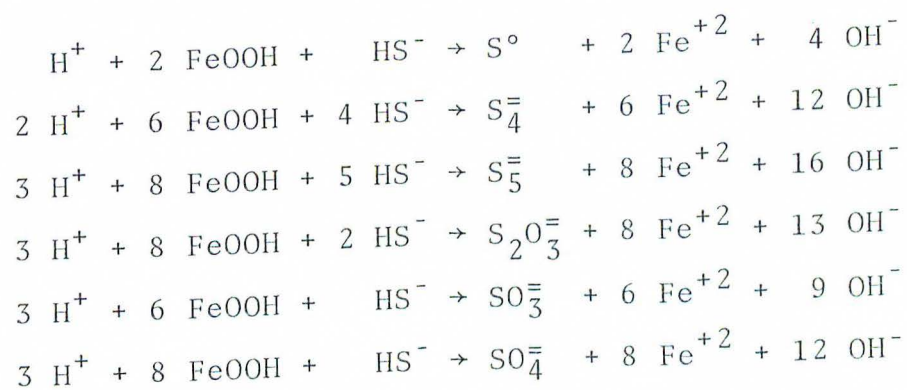
The amount of ferrous iron can be determined from the amount of the sulfide oxidation products and the changes that occur in the specific redox potential. The oxidation number changes for the following reactions are 6, 8, 8, 6, and 8.



that are transferred from the reagent, which in these reactions is determined from the following

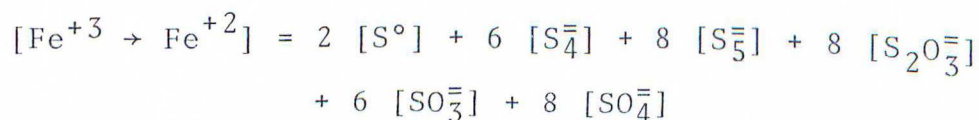
(1974), studied the partition of trace elements between the dissolved and particulate phases in the Black Sea. They observed a rapid rise in the concentration of dissolved iron in the anoxic part of the water column, which was followed by a rapid decrease, as they descended into a more anoxic region of the water column. This behaviour was interpreted as evidence for the rapid reduction and dissolution of  $\text{Fe}^{+3}$ , until saturation with respect to iron sulfides occurred. Precipitation of iron sulfides occurred when the  $K_{sp}$  for their formation was exceeded.

The amount of ferrous iron can be determined from the concentration of the sulfide oxidation products and the oxidation number changes that occur in the specific redox reactions. The oxidation number changes for the following reactions are 2, 6, 8, 8, 6, and 8.



Thus the number of electrons that are transferred from the sulfide ion to the oxidizing agent, which in these reactions is the ferric ion, can be determined from the following equation:





This is based on the assumption that iron is the only oxidizing agent present. One method of testing this assumption is to see if the electron balance exceeds the initial concentration of oxidizing agent - the concentration of goethite. A check of 90 electron balance measurements showed that 74% of the measurements indicated an electron balance less than the initial iron concentration. The remaining 26% of the readings, which exceeded the theoretical limit, were taken during reaction runs in which the rate of sulfide formation was high. This is shown by the high reduced iron values in reaction runs 11, 12, 33, 34, and 35, which are shown in Appendix A. This excess is too large to be attributed to experimental error.

Complete conversion of goethite to iron sulfide was observed within 30 minutes for runs 11 and 12. In these two runs, the electron balance exceeded the total reducible iron by 1.8 mM. The electron balance in these two runs, however, decreased over 24 hours until the values were 1.8 and 0.7 mM for runs 11 and 12 respectively. A similar decrease was also observed in the acid extractable solid sulfide ( $\text{S}_p^{\bar{2}}$ ) from a maximum of 1.46 mM to 1.03 mM (in reaction run 11). This adsorbed or coprecipitated sulfide could have been oxidized during the acetone extraction to form elemental sulfur. This would have increased the elemental sulfur

concentration and total reduced iron values. "Excess" reduced iron was also observed in runs 33, 34, and 35, in which 1.3, 0.4, and 0.5 mM of excess reduced iron were measured. These three runs had the highest rate constant for formation of iron sulfide. During this rapid formation, bisulfide ion could have been coprecipitated as in runs 11 and 12. This adsorbed sulfide could explain in a similar fashion the high levels of reduced iron calculated for runs 33, 34, and 35. Such a phenomenon was observed by Berner (1969) in a study of California coastal sediment.

Rickard's (1974) suggested mechanism for the formation of sedimentary iron sulfides included dissolution, reduction, and precipitation steps. Ideally, the way to determine the order of the sequence would be to determine the rates of the individual reactions. Qualitative analysis of the concentration-time plots for the reaction runs may give some insight into the reactions involved. Plots of reduced iron vs. acid extractable sulfide ( $S_p^=$ ) for several reactions are given in Figure 14. The line indicates equality between the amount of reduced iron and the amount of FeS produced. If the points fall above the line, this indicates the sequence of precipitation (adsorption) followed by reduction. Conversely, if the points fall below the line, reduction precedes precipitation. The time interval between the two reactions is proportional to the distance of the point from the line. This plot shows that reduction precedes the precipitation reaction by a significant time interval.

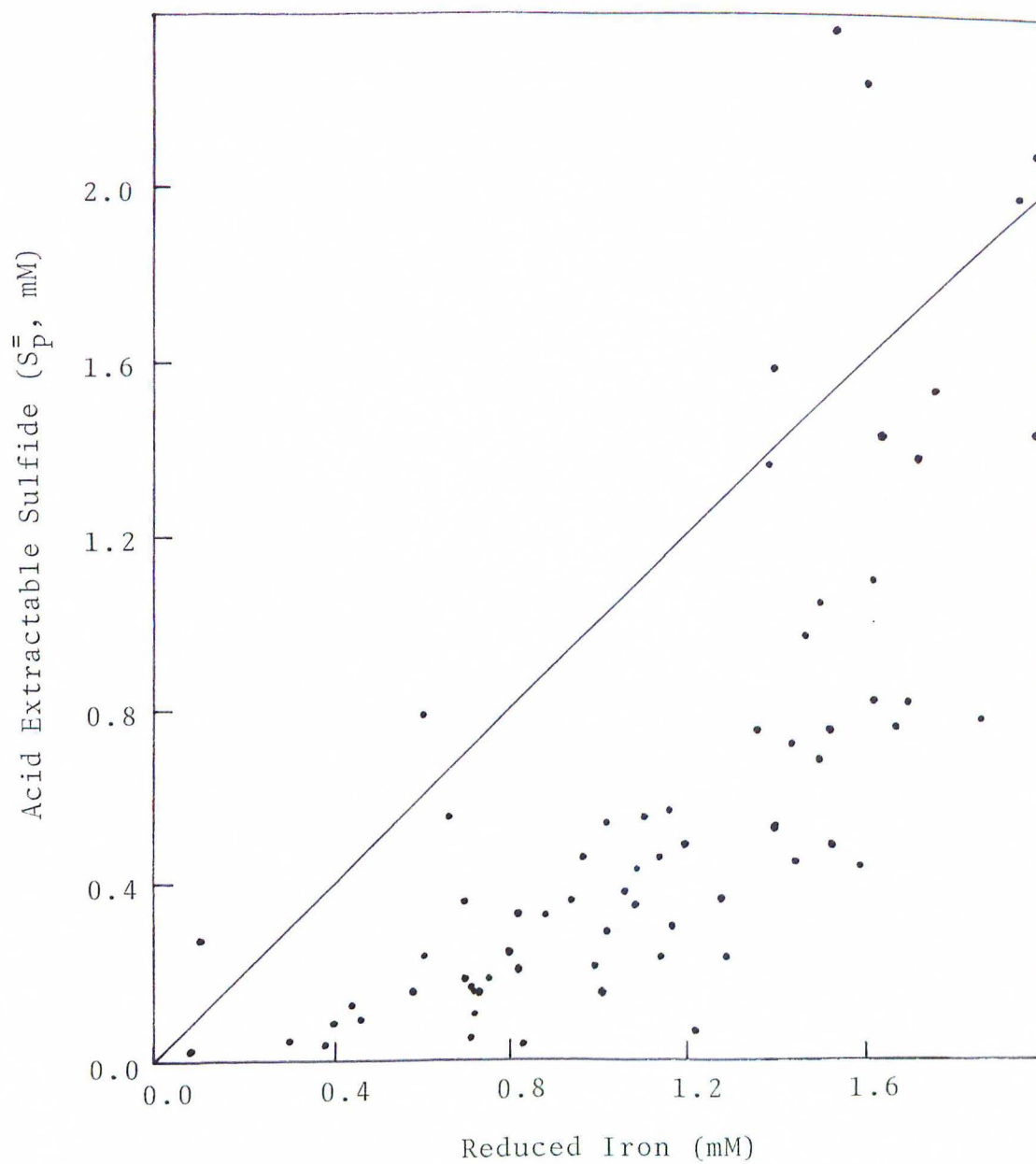


Figure 14: Plot of Acid Extractable Sulfide Concentration vs. Reduced Iron Concentration



Several concentration-time plots of FeS and electron balance are shown in Figures 15, and 16. These plots also show that reduction preceeds precipitation. The reduction process occurs rapidly at first but then slows down as the available reducible iron (i.e. surface iron) is depleted. Additional reduction of iron can only occur after the dissolution of the surface ferrous iron.

Quantitatively, the reduction reaction was studied by analyzing the electron balance-time plots by the initial rate method. A detailed description of the initial rate method can be found in Appendix B. Slopes of the plots were first determined by simple linear regression. All but four reaction runs exceeded the 95% confidence level for the correlation coefficient; those rejected were not used in the determination of the rate constant. The slopes were then plotted against the initial concentrations to determine the reaction order with respect to the particular species. Thus, log-log plots are shown in Figures 17, 18, and 19 for  $\text{HS}^-$ ,  $\text{H}^+$ , and  $\text{A}_{\text{FeOOH}}$ . The reaction orders were determined to be 0.60, 0.49, and 0.89, respectively. The rate constant was calculated on the basis of 10 runs (Table 5) to be  $0.0179 \pm 0.0015 \text{ M}^{-1} \text{ l}^{-1} \text{ m}^{-2} \text{ min}^{-1}$ . Thus the rate expression was determined to be:

$$d[\text{Red Fe}]/dt = k [\text{HS}^-]_i^{.60} (\text{H}^+)_i^{.49} \text{A}_{\text{FeOOH}}^{.89}_i$$

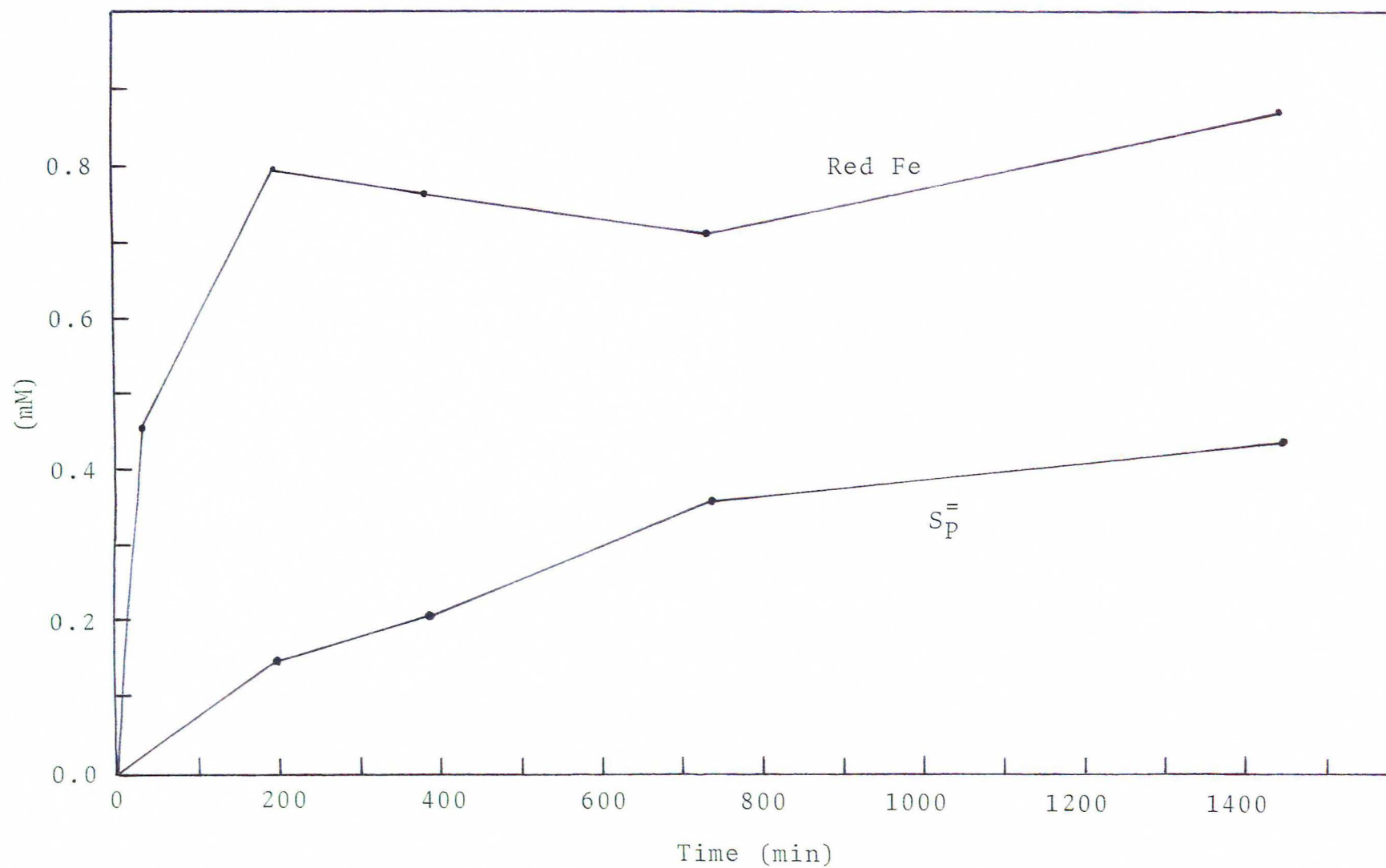


Figure 15: Plot of Reduced Iron and Acid Extractable Sulfide,  $S_P^=$ , vs. Time (Run 6)

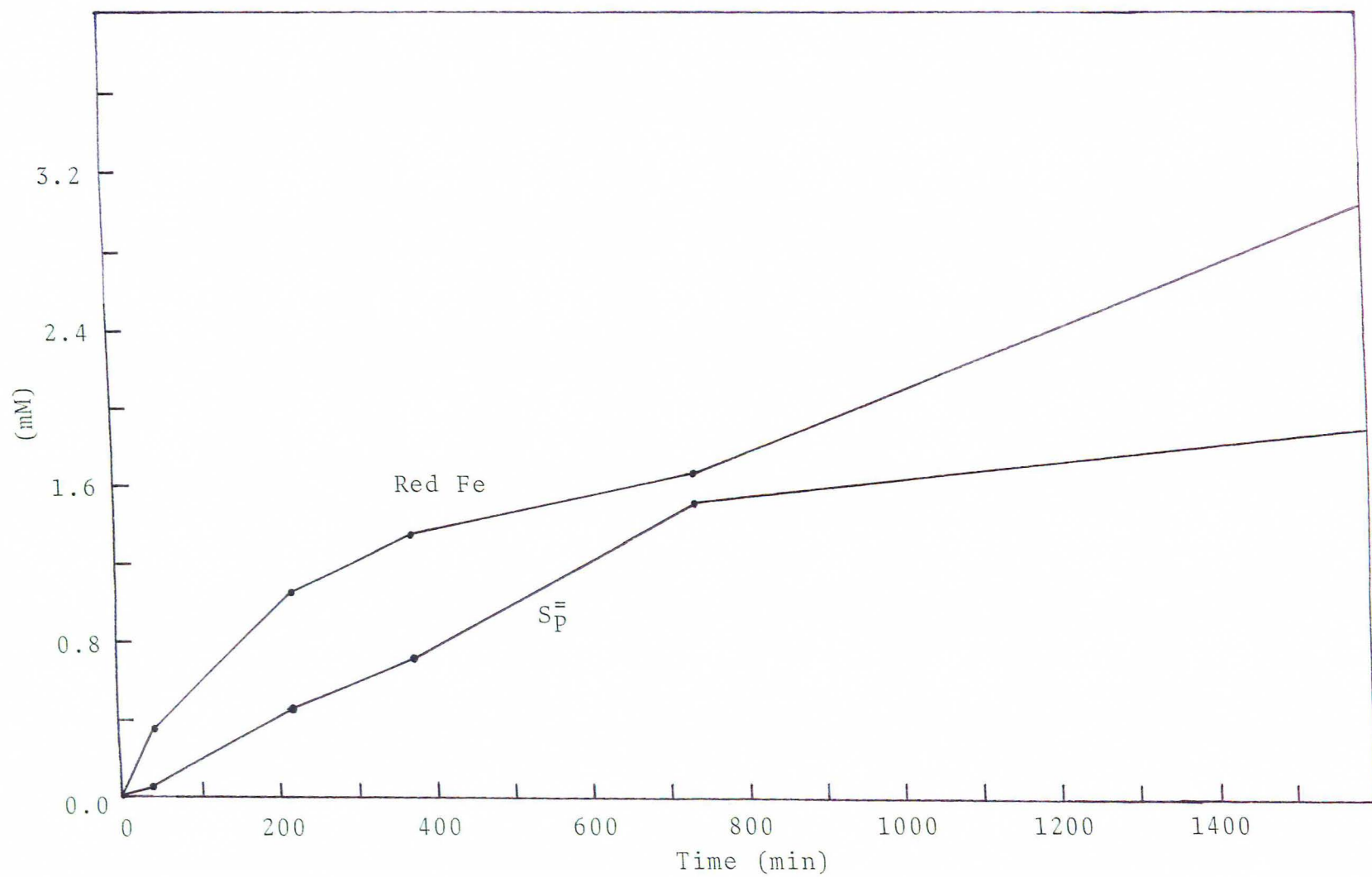


Figure 16: Plot of Reduced Iron and Acid Extractable Sulfide,  $S_p^=$ , vs. Time (Run 24)



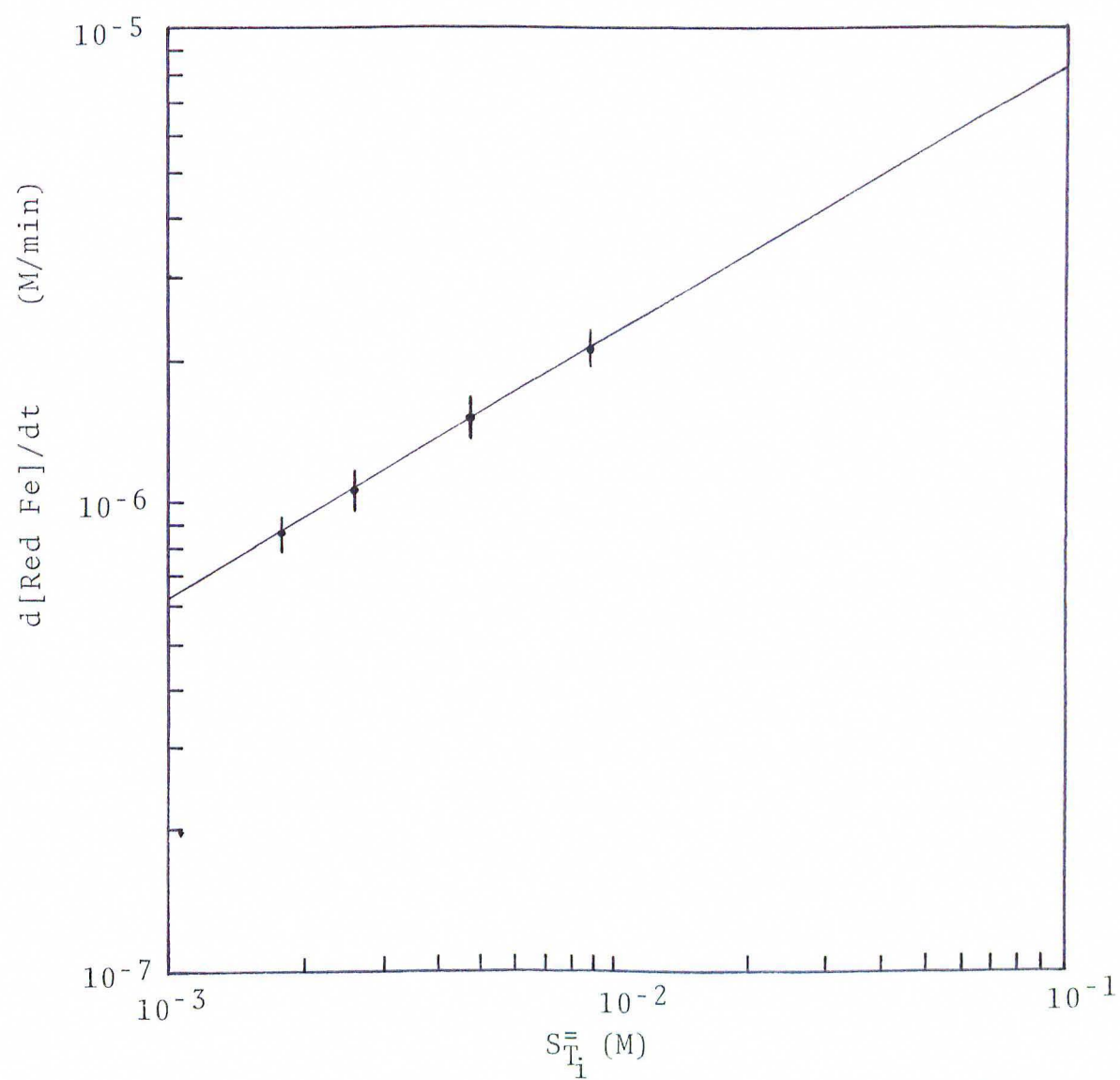


Figure 17: Plot of Rate of Fe Reduction vs.  $S_{T_i}^{=}$

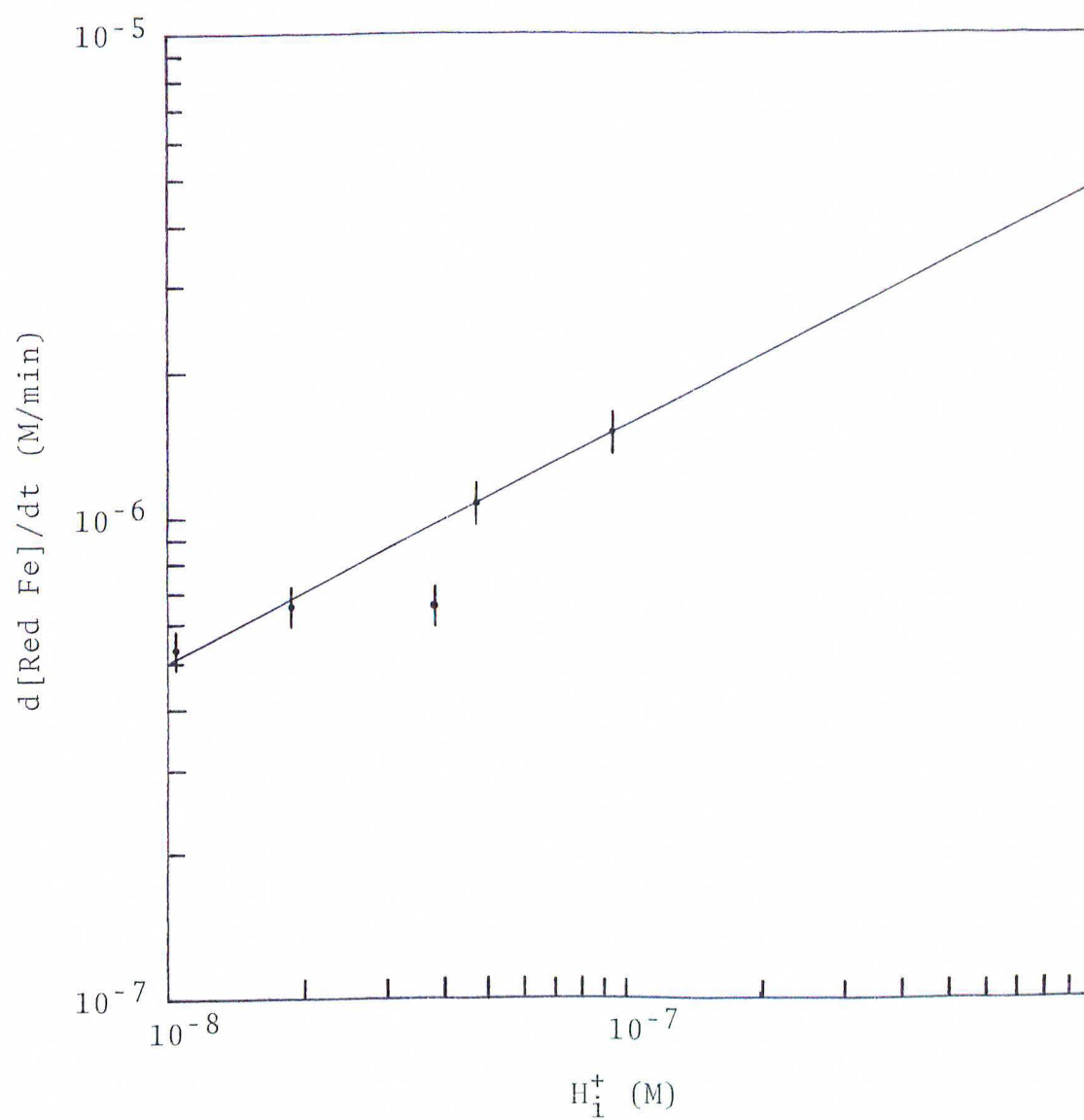


Figure 18: Plot of Rate of Iron Reduction vs. Initial Hydrogen Ion Concentration

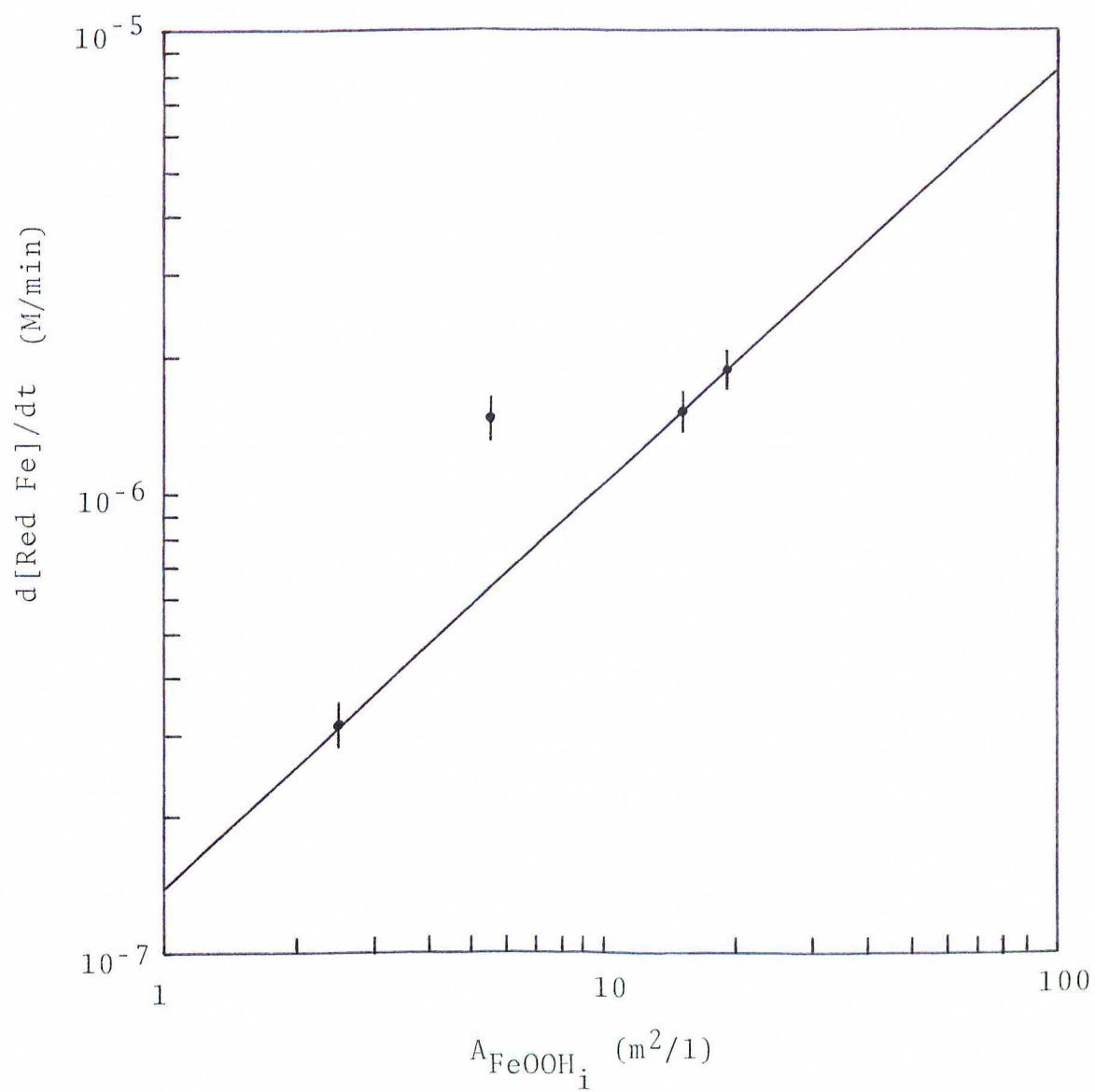


Figure 19: Plot of Rate of Reduction of Fe vs. Initial Goethite Surface Area

Table 5

Rate of Reduction During Phase II (Rate of Dissolution)

$$d[\text{Red Fe}]/dt = k_{\text{red}} [\text{HS}^-]_i^{.60} (\text{H}^+)_i^{.49} A_{\text{FeOOH}_i}^{.89} = mt + b$$

Run	m	b	$k_{\text{red}}$	Correlation Coefficient r
6	$1.10 \times 10^{-7}$	$6.50 \times 10^{-4}$	$2.68 \times 10^{-3}$	.72
7	$5.30 \times 10^{-7}$	$1.40 \times 10^{-4}$	$2.04 \times 10^{-2}$	.96
9	$6.25 \times 10^{-7}$	$6.50 \times 10^{-4}$	$4.02 \times 10^{-3}$	.75*
17	$1.40 \times 10^{-6}$	$1.40 \times 10^{-4}$	$4.37 \times 10^{-2**}$	.99
21	$3.07 \times 10^{-7}$	$5.90 \times 10^{-4}$	$1.62 \times 10^{-2}$	.99
22	$6.50 \times 10^{-7}$	$3.90 \times 10^{-4}$	$1.84 \times 10^{-2}$	.97
24	$1.50 \times 10^{-6}$	$6.00 \times 10^{-4}$	$1.69 \times 10^{-2}$	.98
25	$1.09 \times 10^{-6}$	$2.86 \times 10^{-4}$	$1.98 \times 10^{-2}$	.96
28	$1.03 \times 10^{-6}$	$5.25 \times 10^{-4}$	$1.66 \times 10^{-2}$	.96
29	$2.18 \times 10^{-6}$	$6.90 \times 10^{-4}$	$1.64 \times 10^{-2}$	.98
30	$8.49 \times 10^{-7}$	$9.30 \times 10^{-4}$	$1.68 \times 10^{-2}$	.97
31	$1.88 \times 10^{-6}$	$5.50 \times 10^{-4}$	$1.73 \times 10^{-2}$	.96
32	$1.78 \times 10^{-6}$	$4.70 \times 10^{-4}$	$2.05 \times 10^{-2}$	.42*
33	$1.48 \times 10^{-6}$	$3.28 \times 10^{-4}$	$1.99 \times 10^{-2}$	.96
34	$7.50 \times 10^{-7}$	$6.70 \times 10^{-4}$	$1.12 \times 10^{-2}$	.79*
35	$6.69 \times 10^{-7}$	$6.70 \times 10^{-4}$	$1.24 \times 10^{-2}$	.89
36	Not Determined			

\*not statistically significant

\*\*discarded



Visual examination of the plots of electron transfer balance against time, revealed that the data points were more likely to be fitted by a quadratic curve. (See Figures 15, 16, 20.) The curves through these points were determined by a least squares polynomial fit. However, when the initial slopes were used to determine the coefficients for the rate expression, no significant linear fit was obtained. As a result, the obviously polynomial curves were analyzed with the reactions responsible for the generation of this data. It was noted that the initial electron balance measurements (taken at times less than 40 minutes) were in some reaction runs, as much as 30% of the final electron balance measurements. Therefore, the polynomial curve was interpreted as resulting from a two step reduction reaction, which is graphically represented in Figure 21. In the first step of the reaction, Phase I, the rapid reduction of surface iron occurs. This is indicated by the large initial slope of the curve at time zero. In the second step, Phase II, the underlying layers of the ferric iron are reduced as the surface layer of ferrous ions is dissolved. Thus the rate of reduction in Phase II is actually controlled by the rate of dissolution of the reduced surface layers, and the rate of reduction during Phase II gives the rate of dissolution.

The rate of the initial surface reduction of iron in Phase I is difficult to assess because of the rapidity of the reaction, and the insufficient number of data points during the first 30 minutes. Additional studies, however,

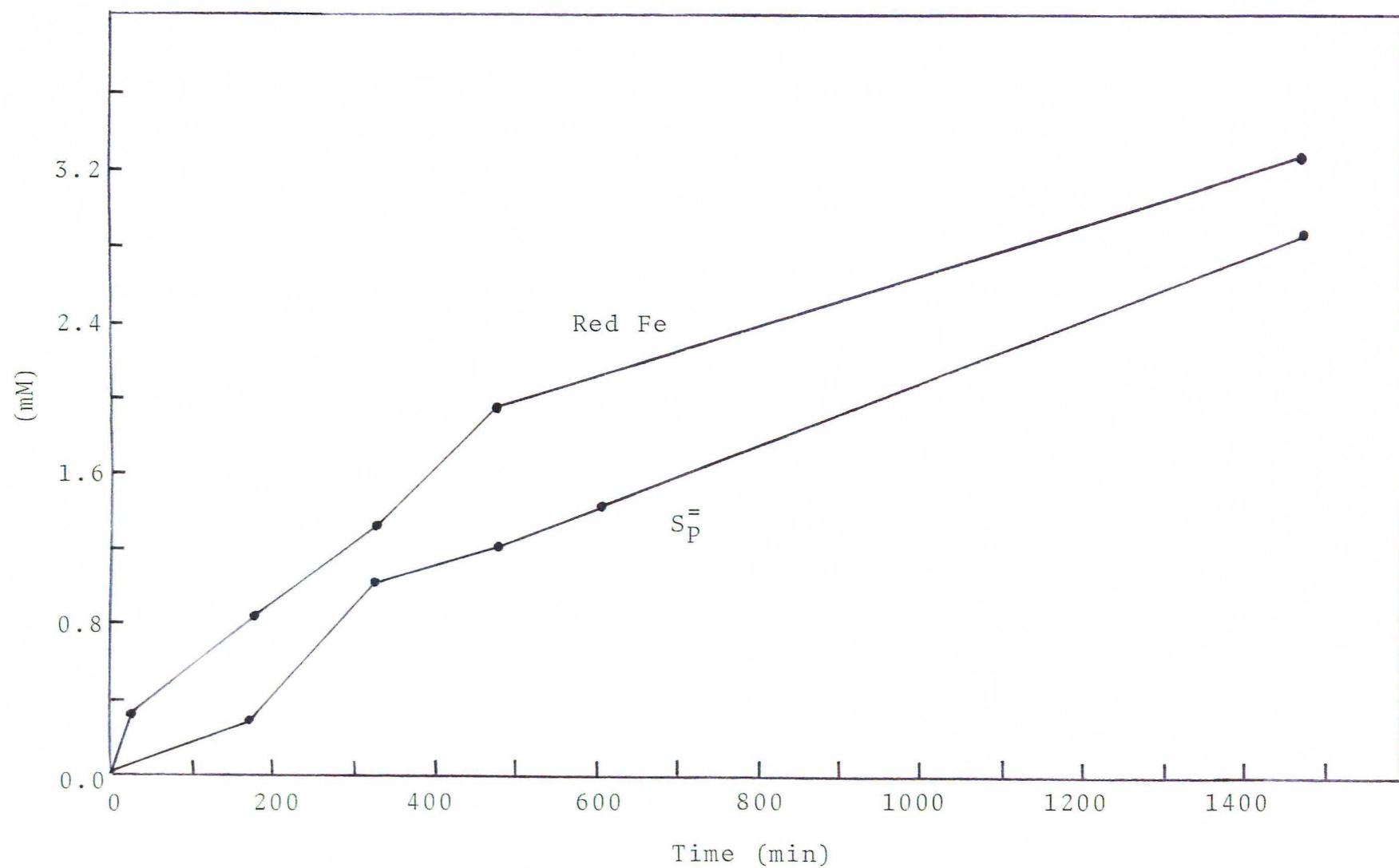


Figure 20: Plot of Reduced Iron and Acid Extractable Sulfide,  $S_P^=$ , vs. Time (Run 31)

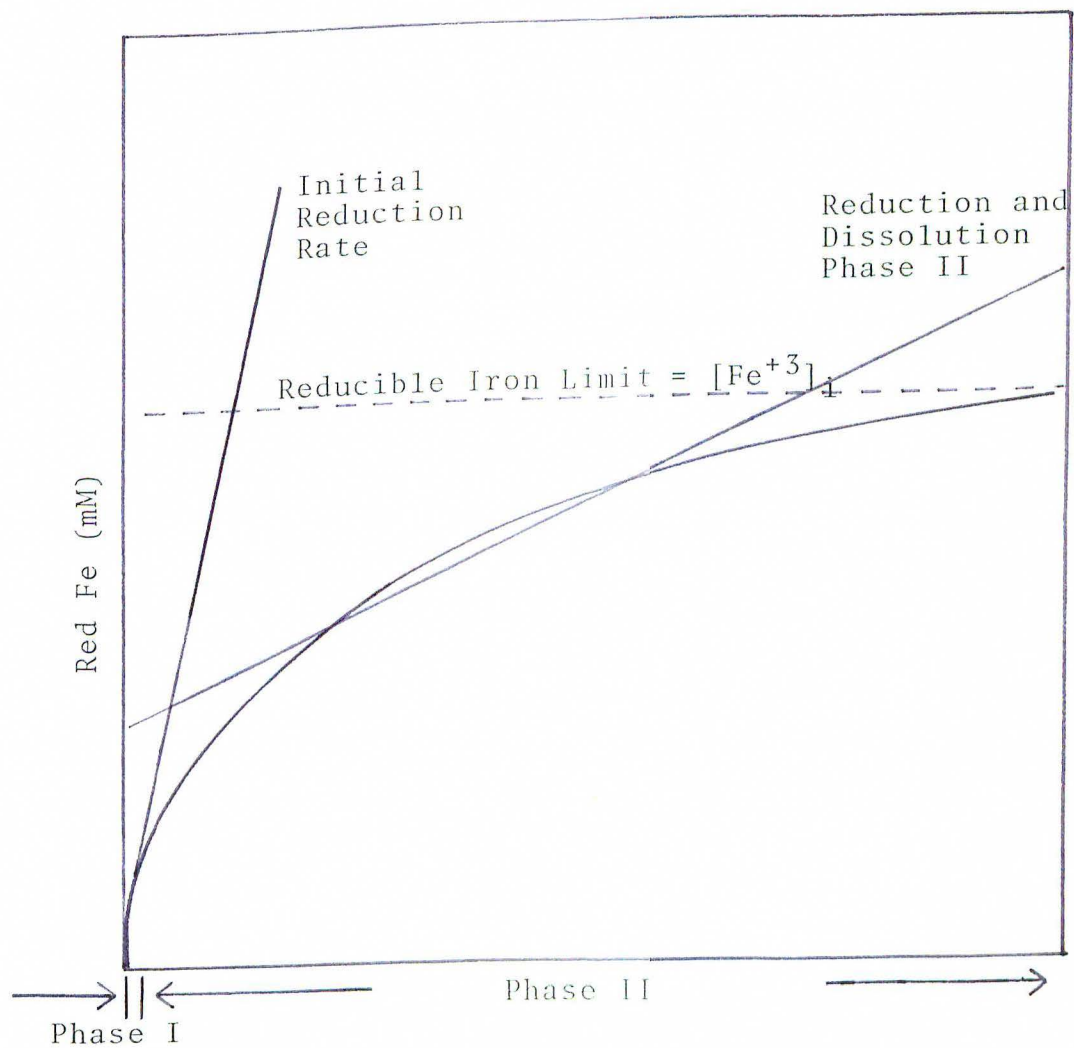


Figure 21: Idealized Reduction-Dissolution Curve

may be able to determine the rate expression and rate constant for the reduction process.

Any postulated mechanism for the reduction reaction must explain the rate expression, sulfide oxidation products, and variation in the products with respect to initial conditions. Two basic approaches can be used to develop a mechanism: the rate determining step approach, or the steady state hypothesis (Edwards et al., 1968). In this study the former was adopted, since data by Rickard (1974) indicated that a rate determining step might have been involved in the reaction.

Any complex chemical reaction proceeds by a mechanism of several elementary steps. The overall rate of the reaction is determined by the rate of the slowest step, the rate determining step.

At this point it is necessary to clarify three concepts: order, molecularity and stoichiometry. Order is an experimentally determined value in the rate expression, while molecularity is the number of reacting species or molecules involved in the formation of the activated complex (Pilling, 1975). Stoichiometry is the value of the coefficients in the reaction. These three quantities may or may not have the same numerical value, depending on the reaction.

The redox reaction between  $\text{FeOOH}$  and aqueous sulfide species required the approach of reduced sulfide species to the surface of the goethite, where the electron transfer can occur. The rate of approach and distance from the



surface are affected by the surface charge of the solid and possibly by physical and chemical adsorption (Reynolds and Lumry, 1966). The surface of an oxide or oxyhydroxide has a surface charge as a result of the interaction of the surface oxygen atoms with water in the bulk solution. Basically, the mechanism for this reaction involves the protonation and deprotonation of surface adsorption sites (Parks and De Bruyn, 1962). The surface charge is a function of pH, and the pH at which the surface charge is zero is called the zero point of charge. However, when  $H^+$  and  $OH^-$  are the potential determining ions, this pH is called the isoelectric point (IEP) (Berner, 1970).

The double layer consists essentially of a charged surface layer of potential determining ions, and a layer of oppositely charged counterions in solution parallel to the surface of the solid. This layer of mobile counterions is called the Gouy layer. The thickness of the Gouy layer is affected by the ionic strength and stirring of the solution. An increase in either or both of these factors will reduce the thickness of the Gouy layer. The composition of both the Helmholtz layer of potential determining ions and the Gouy layer of counterions can change in response to changes in the composition of the bulk solution (Berner, 1971).

Physical and chemical adsorption may also affect the rate of electron transfer across the solid-solution interface.

$\alpha\text{-Fe}_2\text{O}_3$  has been shown to chemisorb  $\text{H}_2\text{S}$  from the gas phase resulting in the formation of  $\text{HS}^-$  and  $\text{H}^+$  (Blyholden and Richardson, 1962). No similar studies have been conducted on the  $\text{H}_2\text{S}$ -goethite system, but results by Gast et al. (1974) showed that goethite hydrogen bonds the first layer of adsorbed water to the surface. This hydrogen bonding was shown to be stronger than observed in  $\alpha\text{-Fe}_2\text{O}_3$ . The adsorbed water on goethite was also shown to be readily exchanged with  $\text{D}_2\text{O}$ .

The physical adsorption of ions is dependent on the charges of the ions and the surface of the particles. As shown above, the surface of goethite is negatively charged above pH 6.7. Therefore, the physical adsorption of water is hindered above pH 6.7 by coulombic interaction. Below the IEP however, the surface is positively charged and physical adsorption should be rapid --- consequently reduction would be rapid if the adsorption of  $\text{HS}^-$  were the rate determining step in the reaction.

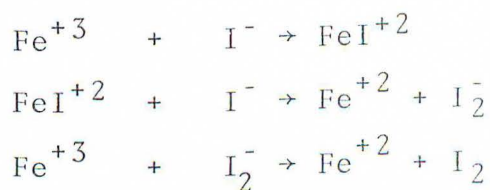
The rapid adsorption of  $\text{HS}^-$  below the IEP was demonstrated in reaction runs 11 and 12, where  $\text{Fe}(\text{OH})_3$  was used as the reactant iron phase. The IEP for  $\text{Fe}(\text{OH})_3$  is 8.5 (Parks, 1968). Results for these two runs showed that the formation of iron sulfide was essentially complete within the first 30 minutes even at pH 8.5.

A comparison of reaction run 11 with one of comparable conditions with goethite as a reactant (run 6) shows a dramatic difference in the rate of iron sulfide formation. At

30 minutes, 1.48 mM of FeS was produced in reaction run 11 (pH = 7.58) while in run 6 (pH = 7.554), only 0.02 mM of FeS was produced (extrapolated from Figure 15). Although there is a difference between the surface areas of the reactant iron phases ( $6.5 \text{ m}^2/\text{l}$  in run 6, and  $14 \text{ m}^2/\text{l}$  in run 11), this difference in initial surface area could only account for 1% of the difference in the amount of FeS produced. This would then indicate that the rapid adsorption of  $\text{HS}^-$  does occur in the case of run 11, with a pH below the IEP of  $\text{Fe}(\text{OH})_3$ . Adsorption of  $\text{HS}^-$  does occur above the IEP of goethite, but to a lesser extent than it would below the IEP.

The reduction of haematite would also be expected to occur rapidly, since the IEP for haematite is 8.5 (Parks, 1968). Thus  $\text{HS}^-$  can exchange with  $\text{OH}^-$  in the potential determining layer but the exchange would be favored at pH conditions either near or below the IEP. This would explain the increase in the rate of the reduction as the initial pH is reduced. Once  $\text{HS}^-$  is present in the potential determining layer, the electron transfer can occur. However, the oxidation change for  $\text{Fe}^{+3}$  going to  $\text{Fe}^{+2}$  and  $\text{S}^-$  to  $\text{S}^0$  (principal oxidation product) differs by 1. Therefore, the reduction of one ferric iron by one bisulfide ion will result in a highly unstable oxidation state of -1 for sulfur (Laurence and Ellis, 1972). These authors studied the oxidation of aqueous iodide ions by aqueous ferric ion. The mechanism they postulated required the formation of  $\text{I}_2^-$  which reacted with ferric ion by the reaction:





$\text{HS}^{-}$  could react as does  $\text{I}^{-}$  in the above reactions, to yield  $\text{HS}^{\circ}$ , equivalent of  $\text{I}_2^{-}$ . However, in the reaction of goethite with aqueous sulfide species, the interaction of  $\text{HS}^{\circ}$  with another ferric iron coordination sphere is not necessarily required, as it's analog in the above mechanism. Then  $\text{HS}^{-}$  can be thought of as being associated with a surface adsorption site, since the purpose of the fixed layer is to balance the charge of the protonated site. The structure of goethite consists of hexagonally close-packed oxygen atoms with iron in the octahedral interstices (Deer, Howie, and Zussman, 1966). Thus, each surface oxygen is shared by two iron octahedra, and the potential determining  $\text{HS}^{-}$  is associated with two iron octahedra. Both octahedra contain ferric ion which can be reduced.  $\text{HS}^{-}$  would then transfer one electron to one of the ferric ions, resulting in the formation of  $\text{HS}^{\circ}$ .  $\text{HS}^{\circ}$  reacts immediately by transferring an electron to the other ferric ion with which it is associated. This would produce elemental sulfur,  $\text{S}^{\circ}$ , hydrogen ion, and two ferrous ions. The structure of the goethite favors a two electron exchange. This mechanism would explain why sulfur is the principal oxidation product.

How, then, is thiosulfate produced? The formation of thiosulfate would require conditions which favor



interaction between two or more unstable oxidation species  $\text{HS}^\circ$ . An increase in  $\text{HS}^-$  concentration would increase the number of  $\text{HS}^\circ$ -occupied surface adsorption sites, which would also increase the number of  $\text{HS}^\circ$  species. An increase in the total dissolved sulfide, at constant iron reactant surface area, should result in an increase in % thiosulfate. This was observed in the results of the present study and in the results of Rozanov et al. (1971).

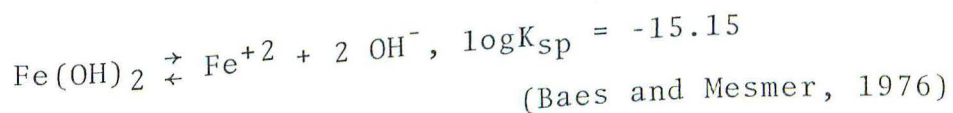
Conversely, an increase in the total number of surface adsorption sites would decrease the % thiosulfate of the oxidation products, by decreasing the interaction between  $\text{HS}^\circ$  species. A low correlation ( $r = 0.09$ ) was observed between the % thiosulfate and the initial pH. This would indicate that sulfide speciation was not an important factor in the formation of oxidation products.

It appears that both  $\text{H}_2\text{S}$  and  $\text{HS}^-$  are equally reactive. This interpretation was made in view of the fact that the relative proportions of  $\text{H}_2\text{S}$  and  $\text{HS}^-$  change significantly over the pH range of this study. If the speciation of reduced sulfur was important, the relative proportion of oxidation products should change in response to a variation in pH.

Thus the mechanism for the reduction reaction is postulated to be:

- (1) protonation of surface adsorption sites
- (2) exchange of  $\text{SH}^-$  with  $\text{OH}^-$  in the fixed layer of the iron phase
- (3) consecutive transfer of two electrons from adsorbed  $\text{HS}^-$  to surface ferric iron
- (4) formation of a protonated layer of  $\text{Fe}(\text{OH})_2$
- (5) dissolution of a  $\text{Fe}(\text{OH})_2$  layer.

After reduction of the surface layer of ferric iron, the reduction of ferric ions in the underlying bulk of solid can only occur after dissolution of the surface layer of ferrous ions. Ferrous hydroxide,  $\text{Fe}(\text{OH})_2$  is metastable at the pH values of this study, and in natural anoxic sediments. The solubility product for  $\text{Fe}(\text{OH})_2$  is

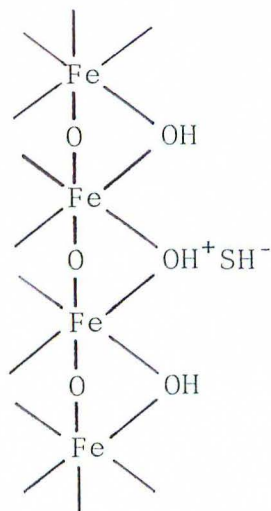


The concentration of iron in equilibrium with solid  $\text{Fe}(\text{OH})_2$  at pH 7-8 is  $10^{-1.15}$  to  $10^{-3.15} \text{ Fe}^{+2}$ . Thus the surface layer should dissolve and expose the remainder of the solid (Walton, 1967). Kinetics of diffusion controlled dissolution are first order with respect to surface area. However, there is ample precedent for reactions in which dissolution is controlled by the chemical reaction (Moelwyn-Hughes, 1933). The rate expression for the reduction and dissolution phase was determined to be

$$d[\text{Red Fe}]/dt = d \text{ Dissolution}/dt = k_D [\text{HS}^-]_i^{.60} (\text{H}^+)_i^{.49} A_{\text{FeOOH}_i}^{.89}$$

Here, a first order (0.89) dependance on surface area was seen, but a half-order dependance on both  $\text{HS}^-$  (0.60) and  $\text{H}^+$  (0.49) was also observed. This higher order kinetics indicates a chemical control for the dissolution reaction.

From rate determining step theory, the composition of the activated complex is  $\text{FeOOH} \cdot 1/2 \text{HS}^- \cdot 1/2 \text{H}^+$ . Since molecules do not react by halves, the composition is therefore  $2 \text{FeOOH} \cdot \text{HS}^- \cdot \text{H}^+$ . This is the activated complex for the reduction reaction.



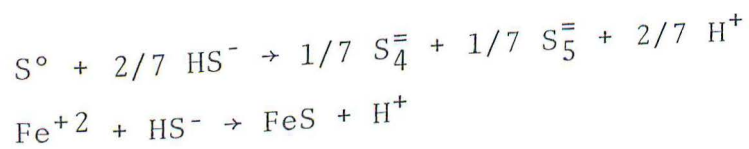
After reduction, the product elemental sulfur would diffuse out of the surface of the solid (Moelwyn-Hughes, 1933). The hydrogen ion from the  $\text{HS}^-$  would remain to protonate the surface since the IEP for  $\text{Fe}(\text{OH})_2$  is 12 (Parks, 1965).

#### Hydrogen balance

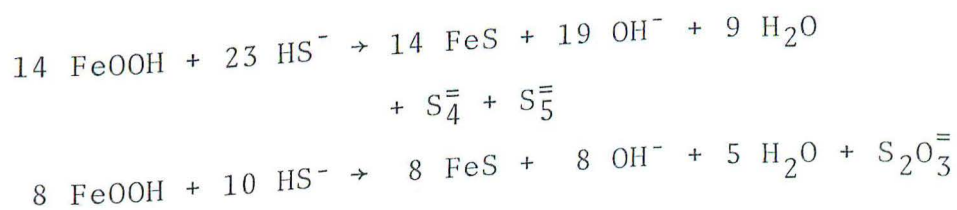
Large quantities of hydroxyl ion are produced by the reduction reaction of goethite by  $\text{HS}^-$ . In addition, hydroxyl ions are produced by the precipitation reaction of ferrous iron with aqueous bisulfide and the formation of



polysulfide from elemental sulfur.



The overall reactions therefore would be



Thus the hydroxyl:iron sulfide product ratio should be 1.36 and 1 respectively. Since sulfur was the principal oxidation product, the ratio should be closer to 1.36. Table 6 gives the ratio of millimoles of hydroxyl ion and the millimoles of FeS as  $\text{S}_\text{P}^{=2-}$ . For all but two runs, the ratios of these values is less than one. Either there exists an additional sink for  $\text{OH}^-$  or the reaction does not proceed as simply as is stated above.

Chemical analysis by Berner (1964a) of his product, iron monosulfide, showed that the ratio of Fe:S was not 1:1, but rather 0.9:1 to 1.1:1. The iron deficient monosulfide was hypothesized to form by the adsorption or coprecipitation of  $\text{Na}_2\text{S}$  with the FeS. Analyses of the product iron sulfide were conducted for Fe, Na and S. The excess sulfide was then determined by subtracting  $0.5 \text{Na}^+$ . The ratio was then determined as 0.9 at a minimum. However, the excess sulfide was assumed to be present as  $\text{Na}_2\text{S}$ , but Goldhaber and Kaplan (1975) have shown that  $\text{S}^{=2-}$  does not



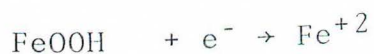
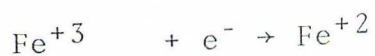
Table 6

Hydrogen Balance							
Time (min)	<u>~ 30</u>	<u>~200</u>	<u>~350</u>	<u>~400</u>	<u>~600</u>	<u>~750</u>	<u>~1440</u>
Run							
6	-	0	-	0.30	-	0.30	0.62
9	-	0.40	-	0.74	-	0.59	0.84
22	6.80	1.16	-	2.95	-	1.19	1.2
24	0	0	-	0.32		0.40	0.54
25	0.37	-	-	1.48		0.74	0.51
28	0	0	0.10	0.10	-	0.19	0.54
29	-	0.71	0.52	0.36		0.50	0.57
30		0.33	0.14	-	0.10	0.19	0.19
31		1.29	0.48		0.41	0.57	0.46
33		0.64	1.07	0.88	0.80		0.71
34		1.36	1.47	1.49	0.84		0.94
35		6.60	4.00	-	0.93		1.34
36		2.40	1.70	1.26	0.93	0.43	1.27

Ratio of mM  $+\Delta\text{OH}^-/\text{mM } \text{S}_{\text{P}}^-$

Exact times may be found in Appendix A.

exist at neutral pH values. Rather, NaHS would be present, and the Na:HS ratio would be 1:1. Thus the minimum ratio of Fe:S would be 0.8. This factor of 0.8 would reduce the  $\text{OH}^-:\text{FeS}$  in a large number of data sets but still some of the data would not have the required ratio of 1 to 1.36. Previous mechanisms and reactions for the formation of iron sulfide (Rickard, 1974, Berner, 1962) did not account for the product  $\text{OH}^-$  ions, as in Rickard's (1974) mechanism



An additional sink for hydroxyl might be adsorption of hydroxyl within the structure of the iron monosulfides. This process would remove additional hydroxide ion from solution so that it would not be measured by the hydrogen electrode. Quantitatively this could only account for a few percent of the excess hydroxyl ions. This coprecipitated hydroxyl might account for the fact that the initial iron sulfide is amorphous (Berner, 1964a) by hindering crystallization. Adsorbed hydroxyl could possibly be determined by infrared spectroscopy, but there are no available data for the presence of hydroxyl groups in iron sulfides. In addition, two experimental problems would interfere with the determination of adsorbed  $\text{OH}^-$ . Initially formed iron sulfides are extremely susceptible to air oxidation (Berner, 1964a), thus great care must be taken to prevent oxidation. Also, hydroxyls are present in the reactant iron phases,

FeOOH and Fe(OH)<sub>3</sub>. The product sulfide material must be free from contamination with reactant material which would give a positive test for hydroxyl.

#### Formation of iron sulfide

After reduction of goethite, the ferrous hydroxide dissolves to produce aqueous ferrous ions and hydroxide ions. Solubility product calculations for Fe(OH)<sub>2</sub> ( $K_{sp} = 10^{-15.15}$ ; Baes and Mesmer, 1976) show that the equilibrium concentration of Fe<sup>+2</sup> at pH 8 is  $10^{-3.15}$  M. The concentration of S<sup>=</sup> species at these conditions (pH 8 and  $S_T^= = 4 \times 10^{-3}$  M) can be calculated from the expression

$$[S^=] = \frac{S_T^=}{[H^+]^2/K_1K_2 + [H^+]/K_2 + 1}$$

where  $K_1 = 10^{-7.1}$  and  $K_2 = 10^{-14}$  are the first and second dissociation constants for H<sub>2</sub>S respectively (Stumm and Morgan, 1970). These calculations showed that the concentration of S<sup>=</sup> is  $10^{-7.5}$  or  $3.16 \times 10^{-8}$  M. The solubility product of FeS has a value of  $10^{-10.65}$ , or six orders of magnitude greater than the most soluble sulfide, amorphous iron sulfide, with an ion activity product of  $10^{-16.9}$  (Doyle, 1968). As a result of the dissolution of Fe(OH)<sub>2</sub>, the solution is supersaturated with respect to iron sulfide and precipitation should occur rapidly.

The rate of formation of iron sulfide was studied by the initial rate method. Quadratic equations were de-

terminated by a least squares regression analysis, which described the concentration-time curves for acid extractable sulfide sulfur. The initial rate for each reaction run was determined by the method described in Appendix B.

Log-log plots of the initial rates for the formation of FeS vs. the initial bisulfide ion concentration, the initial hydrogen ion concentration, and the initial surface area of goethite, can be found in Figures 22, 23, and 24. The slopes, and hence the reaction orders for these species, were found to be 0.97, 0.82 and 1.1 respectively. This resulted in a rate expression:

$$d[\text{FeS}]/dt = k [\text{HS}^-]_i^{.97} (\text{H}^+)_i^{.82} A_{\text{FeOOH}_i}^{1.1}$$

The rate constant,  $k$ , was calculated on the basis of 16 experimental runs to have a mean value of  $31 \pm 10 \text{ M}^{-1} \text{ l}^{-1} \text{ m}^{-2} \text{ min}^{-1}$ . The rates and rate constants for the 16 individual runs may be found in Table 7.

A comparison of the results of this study with those obtained in a previous kinetic study by Rickard (1974), reveals some disagreement. Rickard determined the overall reaction to be 9/2 order: first order in goethite surface area, 3/2 order in total sulfide concentration, and second order in hydrogen ion activity. Results of the present study indicate a third order reaction, first order in each of the three reactants: goethite surface area, total initial sulfide concentration, and hydrogen ion activity. Comparison



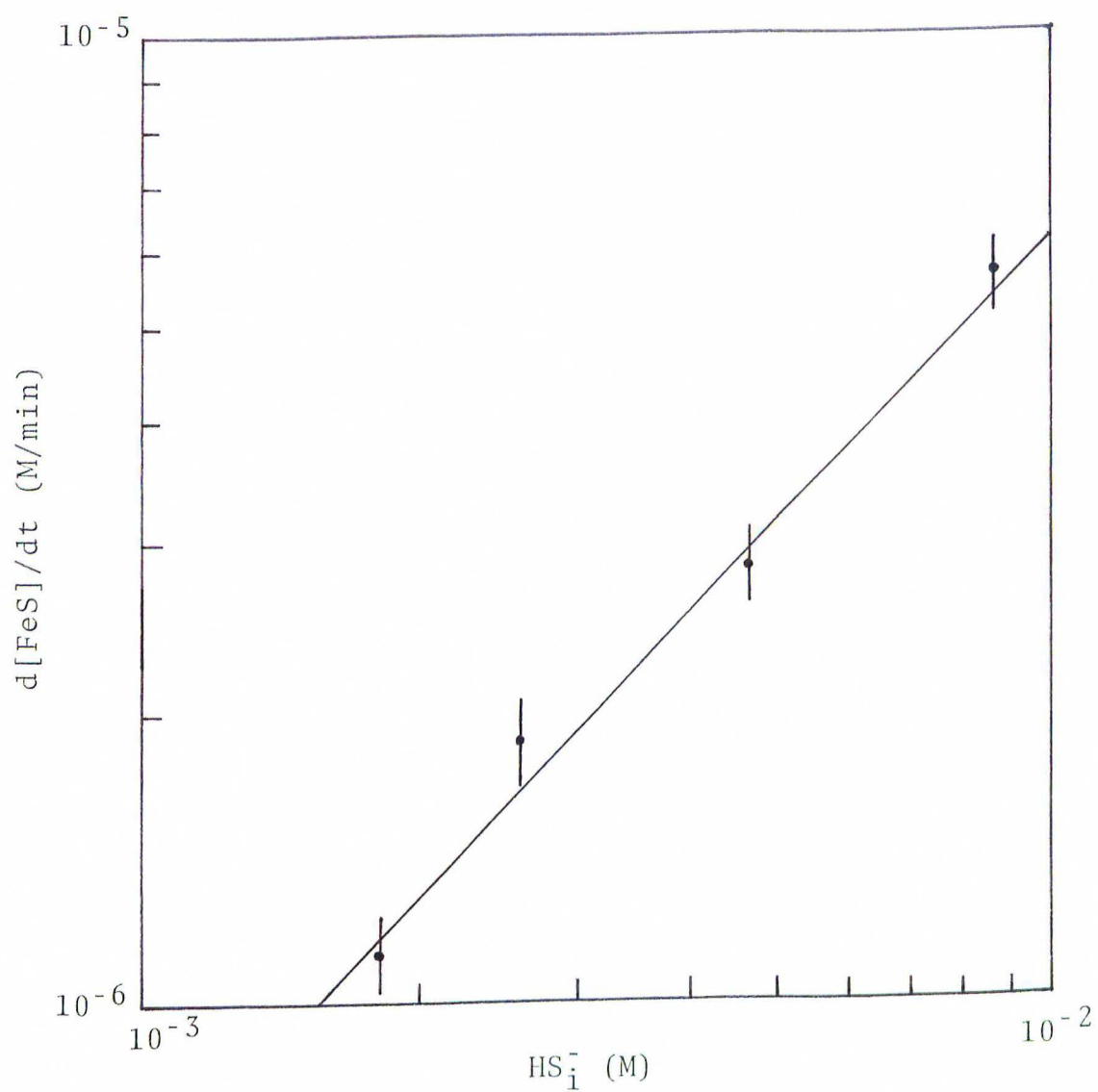


Figure 22: Plot of Rate of Iron Sulfide Formation vs. Initial Bisulfide Ion Concentration

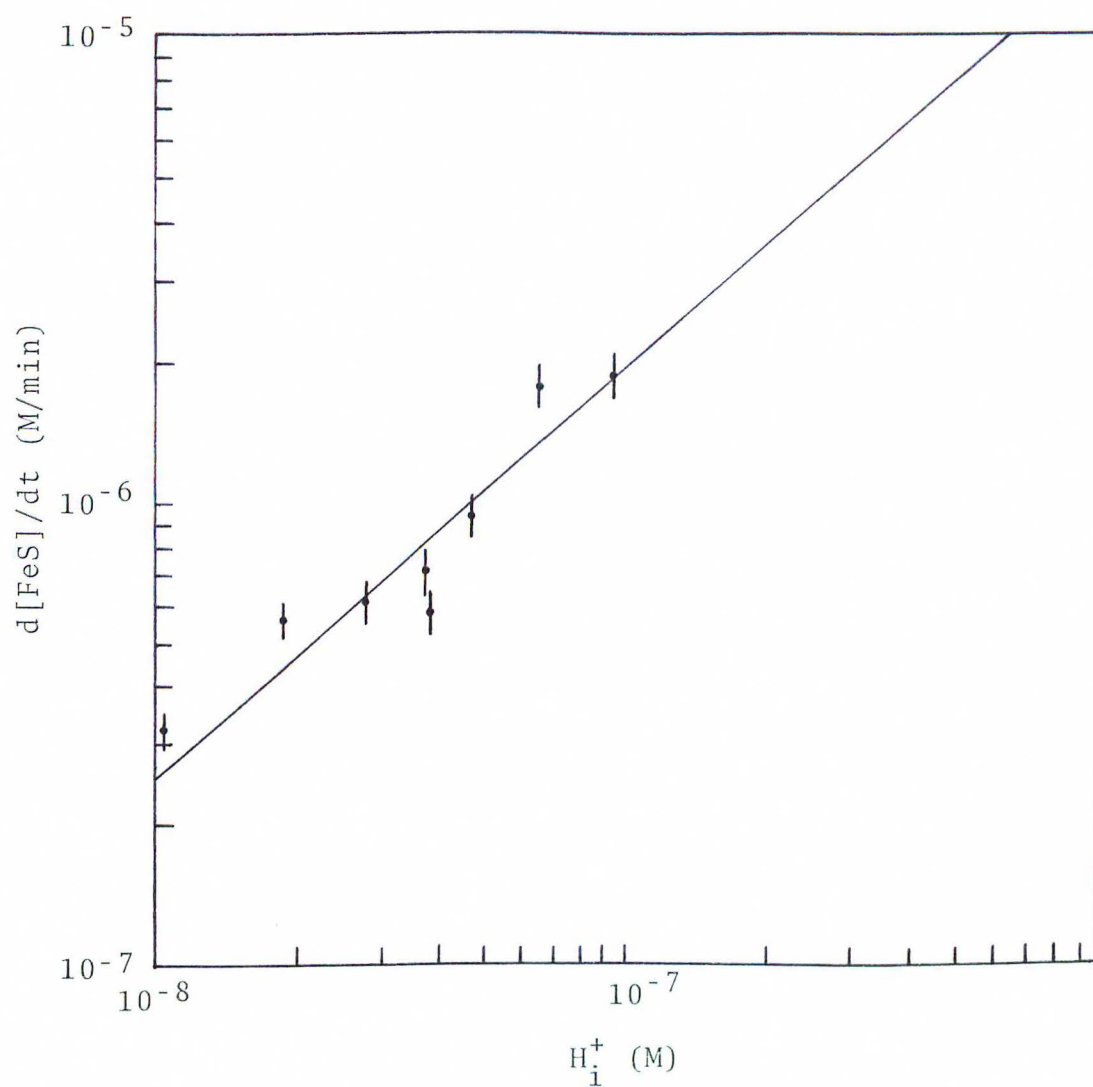


Figure 23: Plot of Rate of Iron Sulfide Formation vs. Initial Hydrogen Ion Concentration

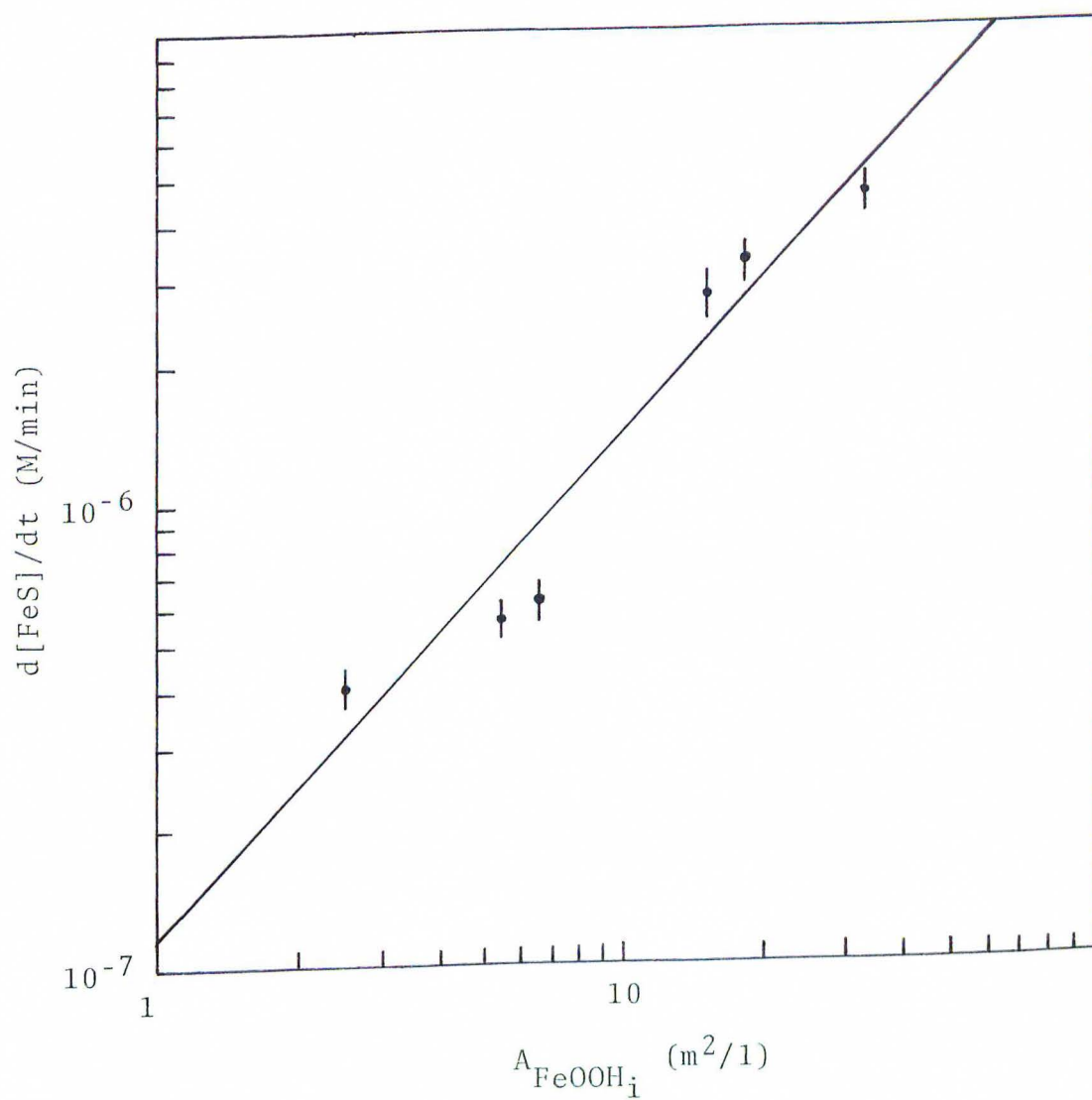


Figure 24: Plot of Rate of Iron Sulfide Formation vs. Initial Goethite Surface Area

Table 7

## Rate of FeS Formation

$$d[\text{FeS}]/dt = k [\text{HS}^-]_i^{.97} (\text{H}^+)_i^{.82} A_{\text{FeOOH}_i}^{1.1}$$

$$k = 31 \pm 10 \text{ M}^{-1} \text{ l}^{-1} \text{ m}^{-2} \text{ min}^{-1}$$

$$d[\text{FeS}]/dt = a + bt + ct^2$$

Run	a	b	c	k	mean % thio- sulfate
6	$2.70 \times 10^{-5}$	$6.07 \times 10^{-7}$	$-2.26 \times 10^{-10}$	23.0	36
7	$-1.55 \times 10^{-5}$	$3.11 \times 10^{-7}$	$-6.49 \times 10^{-11}$	25.0	10
9	$-3.14 \times 10^{-5}$	$4.58 \times 10^{-6}$	$-1.98 \times 10^{-9}$	34.6	6
17	$-2.85 \times 10^{-5}$	$5.52 \times 10^{-7}$	$-1.10 \times 10^{-11}$	29.3	22
21	$-1.01 \times 10^{-4}$	$3.97 \times 10^{-7}$	$-4.46 \times 10^{-11}$	38.5	22
22	$2.43 \times 10^{-5}$	$5.55 \times 10^{-7}$	$-1.77 \times 10^{-11}$	26.8	20
24	$-1.15 \times 10^{-4}$	$2.83 \times 10^{-6}$	$-9.34 \times 10^{-11}$	40.4	7
25	$3.97 \times 10^{-5}$	$9.19 \times 10^{-7}$	$r = 0.99 **$	21.3	17
28	$-8.37 \times 10^{-5}$	$1.86 \times 10^{-6}$	$-5.64 \times 10^{-10}$	48.1	4
29	$-1.65 \times 10^{-4}$	$5.54 \times 10^{-6}$	$-1.53 \times 10^{-9}$	42.6	18
30	$-9.76 \times 10^{-5}$	$1.13 \times 10^{-6}$	$-3.78 \times 10^{-10}$	40.9	4
31	$-1.53 \times 10^{-4}$	$3.24 \times 10^{-6}$	$-8.56 \times 10^{-10}$	36.0	5
32*	$8.44 \times 10^{-5}$	$1.61 \times 10^{-7}$	$1.53 \times 10^{-10}$	3.4	3
33	$-1.65 \times 10^{-4}$	$1.81 \times 10^{-6}$	$-7.67 \times 10^{-10}$	26.1	22
34	$-1.01 \times 10^{-4}$	$1.76 \times 10^{-6}$	$-7.21 \times 10^{-10}$	28.2	19
35	$-1.67 \times 10^{-3}$	$5.68 \times 10^{-7}$	$r = 0.91 **$	13.6	25
36	$-5.07 \times 10^{-5}$	$6.99 \times 10^{-7}$	$r = 0.99 **$	17.1	--

\*run conducted without stirring

\*\*linearly fitted



of rate constants from the two studies is not meaningful, since the rate expressions are of different orders.

The difference in the two rate expressions for the formation of iron sulfide can be explained by the specie that was measured to determine the rate of formation. Rickard (1974) measured the amount of  $\text{OH}^-$  produced. These experimental values were then used in mass balance and equilibrium expressions to calculate the amount of product  $\text{FeS}$ . Hydroxyl is produced (or  $\text{H}^+$  consumed) by several reactions in Rickard's mechanism:



Thus, the rate of formation of  $\text{OH}^-$  is a measure of the entire mechanism - dissolution, reduction, and precipitation. In the present study, the rate expression for the dissolution and precipitation reactions were determined separately; that is, Rickard's rate expression was separated into two parts in the present study.

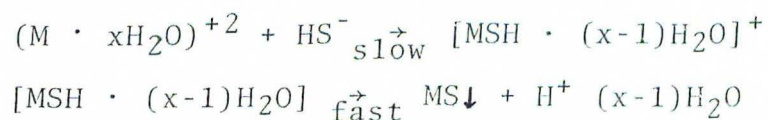
As stated previously, the number of species in the activated complex is given by the order of the rate expression. Rickard's (1974) rate expression implies an activated complex of 9/2 molecules which could form by preequilibrium prior to the rate determining step, the dissolution of goethite. The rate expression determined in the present study indicates a three molecule activated complex, of the

form  $\text{FeOOH} \cdot \text{HS}^- \cdot \text{H}^+$ .

Termolecular activated complexes usually form by an equilibrium step prior to the rate determining step (Wilkins, 1974). It is unusual that the initial surface area of goethite is involved in the precipitation of the two dissolved species  $\text{Fe}^{+2}$  and  $\text{S}^{=}$ . Yet, if the protonation of the  $\text{Fe}(\text{OH})_2$  is considered to be the pre-equilibrium step, the effect of the surface area may be explained. The protonation of  $\text{Fe}(\text{OH})_2$  at pH 7-8 does occur, since the IEP for ferrous hydroxide is 12 (Parks, 1965). After protonation the ferrous hydroxide dissolves to form either  $\text{Fe}^{+2}$  or  $\text{FeOH}^+$  (Baes and Mesmer, 1976; Kester et al., 1975) depending upon which stability constants are used.  $\text{Fe}^{+2}$  is indicated in this mechanism since the protonation of the  $\text{Fe}(\text{OH})_2$  surface layer would yield  $\text{FeO}_2\text{H}_4^{+2}$  or  $\text{Fe}^{+2} \cdot 2 \text{H}_2\text{O}$ . The second, and rate determining step, in the reaction is:



This reaction is in agreement with Pohl (1954). His study of dissolution and precipitation of metal sulfides indicated that  $\text{HS}^-$  was the sulfide specie involved in the formation of the activated complex, by the reactions:



Previously proposed reactions and mechanisms (Berner, 1964a; Rickard, 1974) used either  $\text{H}_2\text{S}$  or  $\text{S}^{=}$  as the reactant sulfur-containing species.

The reaction for the formation of iron sulfide is initially an equilibrium reaction, since it involves the formation of small (5-20 Å) ionic clusters of FeS (Walton, 1967). These clusters grow and decay until a critical cluster size is achieved. The critical cluster size is defined as the largest cluster which can exist before spontaneous crystallization occurs (Walton, 1967).

#### Particle size study

Sequential filtration studies were conducted at the ends of four reaction runs to determine the size of the submicron particles of iron sulfide in solution. The results of these measurements (Table 8) showed that the predominant particles size of FeS was  $<0.01\mu$ , but a significant number of particles were between 0.01 and  $0.1\mu$  in diameter. This was demonstrated by the  $0.01\mu$  filtration step which removed 30%, 100% and 30% of the particulate iron in runs 29, 30, and 31, respectively. Run 32 was the only reaction run that was not stirred, and it was the only run in which the particles of FeS were all  $<0.01\mu$ . This would indicate that stirring increases the size of the particles of iron sulfide formed.

These results were also supported by the UV measurements which showed meaningful changes in absorbance only



Table 8

## Particle Size Study

Run	Filter Size $\mu$	$[S_{\bar{X}}]_T$ (M)	Absorbance 300 nm	Absorbance 370 nm	[Fe] ppm	$[S_T]$ (mM)
29	0.8	$1.2 \times 10^{-4}$	1.264	0.812	6	6.36
	0.2	$1.2 \times 10^{-4}$	1.266	0.796	6	5.11
	0.1	$1.2 \times 10^{-4}$	1.264	0.789	6	3.16
	0.1*	Not Determined				
	0.01°	$1.3 \times 10^{-4}$	1.125	0.633	4	3.60
30	0.8	$3 \times 10^{-5}$	0.537	0.417	5	0.57
	0.2	$2 \times 10^{-5}$	0.507	0.419	4	0.43
	0.1	$4 \times 10^{-5}$	0.426	0.407	5	0.19
	0.1*	$4 \times 10^{-5}$	0.426	0.354	4	0.19
	0.01°	0	0.046	0.016	0	0.00
31	0.8	$1.3 \times 10^{-4}$	1.490	0.968	10	1.86
	0.2	$1.3 \times 10^{-4}$	1.502	0.968	10	1.66
	0.1	$1.3 \times 10^{-4}$	1.509	0.965	10	1.32
	0.1*	$1.3 \times 10^{-4}$	1.482	0.945	10	1.03
	0.01°	$1.1 \times 10^{-4}$	1.222	0.748	7	0.80
32	0.8	$6 \times 10^{-5}$	0.411	0.175	2	3.19
	0.2	$6 \times 10^{-5}$	0.401	0.169	2	2.72
	0.1	$6 \times 10^{-5}$	0.401	0.169	2	2.08
	0.1*	$6 \times 10^{-5}$	0.389	0.150	2	2.01
	0.01°	$6 \times 10^{-5}$	0.311	0.080	2	1.82

0.1\* filtered through 0.1 $\mu$  filter twice

0.01° Schleicher and Schuell nitrocellulose membrane filter  
All other filters polycarbonate



Table 9

"Dissolved Iron" Concentration (mM)							
Time (min)	0	~ 30	~200	~300	~400	~750	~1450
Run							
6	-	-	-	-	-	0.03	0.03
7	-	0.01	0.06	0.03	0.03	0.01	0.03
9			0.03		0.02	0.03	
11		0.01	0.01		0.01		
17					0.03	0.03	0.06
21							0.04
22						0.08	
24		-		0.02	0.02	0.03	0.03
25		0.01			0.03	0.03	0.08
28				0.01	0.02	0.06	0.12
29			0.01	0.02	0.04	0.10	0.11
30		0.01	0.01	0.01	0.01	0.01	0.01
32		-	-	-	-	-	-

$[\text{Fe}_{\text{AZ}}]$  = dissolved Fe + particulate Fe ( $<0.1 \mu$ )

Exact times for measurements may be found in  
Appendix A.

after filtration with  $0.01\mu$  filters. The decrease in absorbance after filtration was attributed to the removal of submicron particles which scattered the UV radiation, and therefore increased the absorbance. This verified, at least qualitatively, that the unusual polysulfide spectra were caused by scattering from submicron particles.

The iron concentrations in all four filtration runs were 2-10 ppm after filtration through a  $0.2\mu$  filter. Thermodynamic calculations by Brooks et al. (1968) and Presely et al. (1972) indicated that the concentration of dissolved iron at  $10^{-3}\text{M}$  total sulfide and pH 8 should be 0.03 ppb. The filtration study results show that the solution in the present study is not in thermodynamic equilibrium, or that the definition of dissolved species is incorrect. Traditionally, the definition of dissolved species was any material that passed through a  $0.45\mu$  filter. Yet the result of this study and others (Kennedy et al., 1974) showed that there are significant levels of iron-containing particles at  $<0.45\mu$ . The interpretation of concentrations of dissolved species (by the traditional definition) from interstitial waters of anoxic or oxic sediments could be seriously in error if this is not considered.

Dissolved iron ( $<0.45\mu$ ) concentrations in interstitial waters of anoxic sediments, have been measured as high as 0.2 ppm (Presely et al., 1972). The concentrations in the reaction runs (Table 9;  $0.02\text{ mM} = 1\text{ ppm Fe}$ ) and in

the particle size studies indicate a concentration of iron as much as an order of magnitude greater than that measured in natural sediments. If one considers that the reaction conditions in this study are ideal for the formation of iron sulfide, then the agreement in concentrations between natural interstitial waters and this study is quite good.

## CONCLUSIONS

The rates and rate expressions for reaction of  $\text{FeOOH}$  and  $\text{HS}^-$  leave little room for interpretation, since they are based solely on experimentally measured quantities. However, the mechanism for the reaction is open to several interpretations. This is true because the development of any mechanism is based on both experimental data and chemical insight. "Indeed it is impossible to prove any single mechanism. However, much favorable data may be amassed for a mechanism so that one can be fairly certain of validity" (Wilkins, 1974).

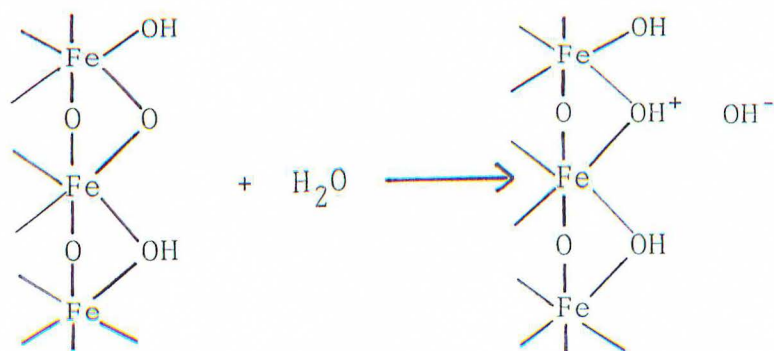
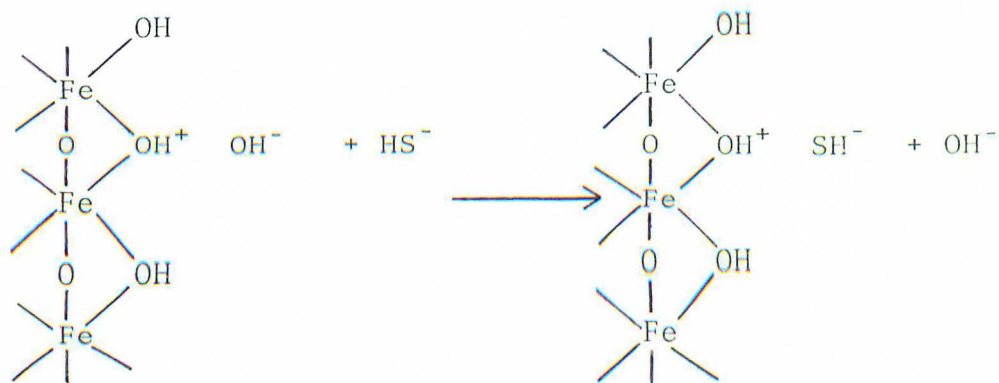
The mechanism for the formation of  $\text{FeS}$  involves dissolution, reduction, and precipitation steps. A comparison of morphology and crystallinity of reactant solids and product solids (Rickard, 1974) indicates that a mechanism includes a dissolution step, while chemical principles indicate that a precipitation reaction is necessary. In addition, there is no question of the oxidation state of iron in iron sulfides; hence, a reduction reaction is also required. The sequence of these processes is defined in the mechanism. The reduced iron-time and precipitated sulfide-time data indicated that the reduction reaction preceded the precipitation reaction. However, the composition of the activated complex for the reduction reaction was based on the assumption that the mechanism for the



Figure 25

## Detailed Reaction Mechanism

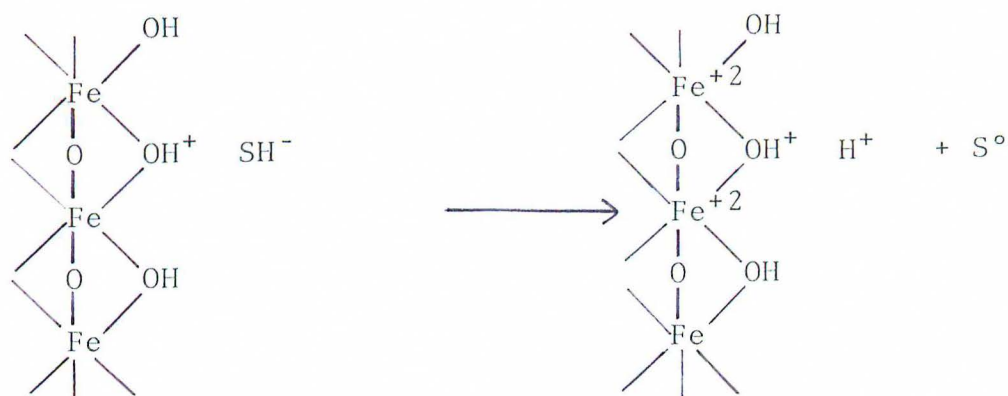
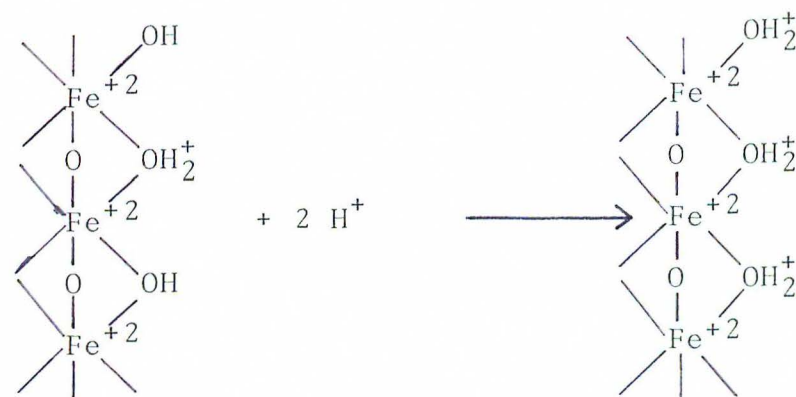
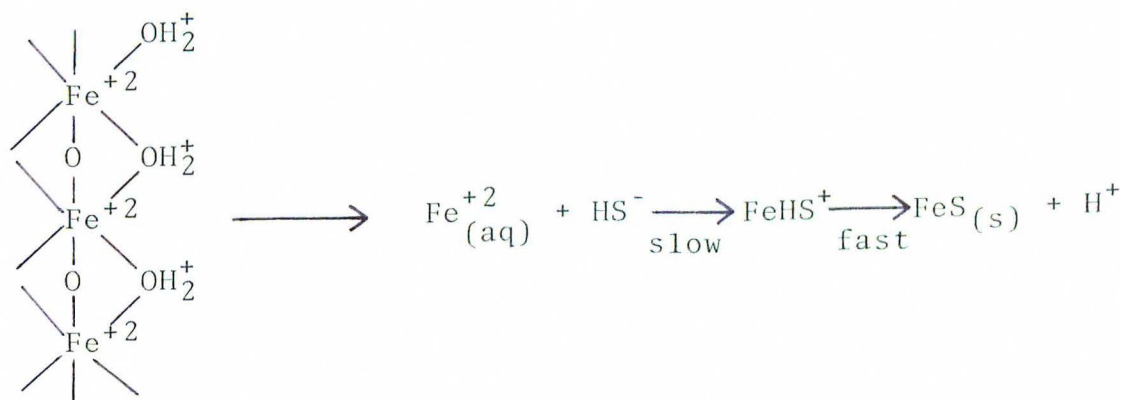
## 1) Protonation of surface adsorption site

2) Exchange of  $\text{HS}^-$  with  $\text{OH}^-$  in fixed layer

(cont.)

Figure 25 (cont.)

## 3) Consecutive reduction of iron

4) Protonation of  $\text{Fe}(\text{OH})_2$  surface layer5) Dissolution of  $\text{Fe}(\text{OH})_2^+$  and precipitation of  $\text{FeS}$ 

reduction reaction involved a rate determining step. This had to be inferred since little experimental data was available for the reduction reaction. Thus several other mechanisms may exist. One such mechanism would involve the replacement of a hydroxyl in the coordination sphere of Fe in goethite by  $\text{HS}^-$ . However, there is no data to support this mechanism.

The inclusion of the dissolution process in the mechanism was inferred on the basis of the following argument. If dissolution had preceded reduction, considerable quantities of aqueous ferric species would have been produced. These ferric species would then have been reduced rapidly to an aqueous ferrous species, as indicated by the high concentration of sulfide oxidation products, in the first several minutes of the reaction. Then these ferrous ions could have reacted rapidly with dissolved sulfide to form iron sulfide. However, there is a considerable time interval between the reduction reaction and the appearance of the precipitated iron sulfide. Thus, the dissolution reaction would have had to follow the reduction reaction. In addition, thermodynamic calculations indicate that ferric species would not be expected at these pH, Eh, and pS conditions.

The reduction reaction was inferred to occur as a two step process: the reduction of surface iron, and the reduction of the remainder of ferric iron after dissolution of the surface ferrous layer. The rate of the reduction

reaction of the subsurface iron was interpreted as being a measure of the rate of dissolution of the surface layer. A comparison of the rate of reduction during this second reduction process with the initial rate of iron sulfide formation showed that the precipitation reaction was approximately as fast as the dissolution reaction. Thus it was inferred that the dissolution step was the rate determining step for the overall reaction, since the initial rate of reduction was shown to be high.

The overall mechanism for the formation of iron sulfide was determined to be as outlined in Figure 25.

The results of this study are believed to be significant in the understanding of two geological problems. The initial rate of iron sulfide formation was found to range from  $1.6 \times 10^{-7}$  (Run 32) to  $5.54 \times 10^{-6}$  (Run 29) M/min. Conversion of this data to units comparable to Berner's (1972) would yield rates of 2.7-58.5 mg sulfur/cm<sup>2</sup>-yr. Berner (1972) reported a range of sulfur uptake by marine sediments of .05-11.3 mg/cm<sup>2</sup>-yr. The highest value was found in a polluted Maine fjord. Thus the lowest rates in the present study are well within the range of Berner's data. From his data, Berner calculated that the Black Sea could remove one megaton of sulfur per year, which combined with the six megatons of sulfur uptake for the hemipelagic sediments could not account for the input of sulfur by stream load. The use of the largest value from this study (58.5 ms/cm<sup>2</sup>-yr) and a surface area of anoxic sediment



comparable to the Black Sea ( $423,000 \text{ km}^2$ ) could remove 248 megatons of sulfur per year. This could account for the 129 megatons of sulfur per year added by stream input. However, this higher rate of sulfur uptake would not be likely. Rather, the value of  $11.3 \text{ mg/cm}^2\text{-yr}$  would be more feasible. Calculations using this latter value show that anoxic sediments with a sulfur uptake of  $11.3 \text{ mg/cm}^2\text{-yr}$  could remove 45 megatons of sulfur per year, or 35% of the oceanic sulfur budget. Iron sulfide formation could be important in the sulfur budget assuming the rate of iron sulfide formation in estuaries and deltaic sediments has this value, and surface areas of anoxic sediments are comparable to the Black Sea.

Another significant result of this study was the formation of elemental sulfur in anoxic sediments by a chemical reaction. The postulated mechanism for the formation of iron monosulfide would yield elemental sulfur in a ratio of one part sulfur to two parts iron sulfide. This sulfur could be used to convert the iron monosulfide to pyrite, the thermodynamically stable iron sulfide.

Previous studies of trace element concentrations in interstitial waters of anoxic sediments have been used to infer a solid phase controlling the solubility of the metal and hence the presence of that solid in the sediment. This study showed that the distinction between the dissolved and particulate phases is not as simple as previously thought. Particle size measurements showed that there were measurable concentrations of particulate FeS present, in the filtered

solution, even after filtering through a  $0.01\mu$  filter. These concentrations were in the ppm range, while equilibrium concentrations from the  $K_{sp}$  indicated that the dissolved iron concentrations should be in the ppb range. Iron sulfide must be controlling the solubility of Fe in the present study, since it is the only iron phase present at the end of the experiment. Thus future studies of the interstitial water chemistry must consider the presence of non-filterable particles in the solution.

All research should be open ended, that is, it should suggest several new areas to be investigated. One possible area for future investigation is the study of the effect of ionic strength on the reaction rates. The thickness of the Gouy layer, and hence the closest distance of approach of bisulfide species to the surface of the iron reactant phase, is reduced by an increase in ionic strength. Thus it would be expected that changes in ionic strength would affect the rate of iron sulfide formation. This is important in estuarine environments since there is considerable difference in ionic strength as one proceeds down the estuary to the open ocean.

Another possible study could involve the determination of the rate of the reduction reaction. The initial reduction reaction occurred rapidly, and as a result, few measurements were taken during this time period, so that only qualitative statements could be made with respect to the rate and mechanism of the reduction reaction. Prior

to further studies, new developments in the analytical techniques for the measurement of sulfide oxidation products must be made in order to decrease the time required to make these measurements.

## APPENDIX A

## Data Tables for Reaction Runs

These tables list the time each series of measurements was taken (in minutes), the pH measurement at that time, the concentrations of the various species measured (in mM), and the calculated values for released  $\text{OH}^-$  and reduced iron (electron balance) (also in mM). Initial conditions are given for pH, total sulfide (in mM), total iron (in mM), and the surface area of the reactant iron species (in  $\text{m}^2/\text{l}$ ).



Run 6

$$pH_i = 7.554$$

$$S_{T_i}^{\bar{=}} = 4.50$$

$$Fe_{T_i} = 1.12, 6.52 \text{ m}^2/1$$

Time	pH	$+\Delta OH^-$	$S_4^{\bar{=}}$	$S_5^{\bar{=}}$	$S_2O_3^{\bar{=}}$	$S^\circ$	$S_T^{\bar{=}}$	$S_C^{\bar{=}}$	$S_P^{\bar{=}}$	Reduced Iron
0	7.561						4.27			0.22
27	7.554				0.05	0.13	4.51	4.38		0.68
198	7.524		0.01	0.01	0.05	0.24	4.54	4.07	0.15	1.02
386	7.540	0.06	0.01	0.01	0.06	0.18	4.31	3.80	0.21	0.99
735	7.550	0.11	0.02	0.01	0.07	0.07	4.07	3.84	0.36	0.94
1449	7.563	0.27	0.03	0.02	0.07	0.09	3.64	3.19	0.43	1.09
2907	7.564	0.28	0.04	0.02	0.07	0.09	3.87	3.21	0.57	1.16

Run 7       $\text{pH}_i = 7.974$   
 $\text{S}_{\text{T}_i}^{\bar{\bar{=}}} = 4.65$   
 $\text{Fe}_{\text{T}_i} = 1.12, 6.52 \text{ m}^2/1$

Time	pH	$+\Delta\text{OH}^-$	$\text{S}_4^{\bar{\bar{=}}}$	$\text{S}_5^{\bar{\bar{=}}}$	$\text{S}_2\text{O}_3^{\bar{\bar{=}}}$	$\text{S}^\circ$	$\text{S}_{\text{T}}^{\bar{\bar{=}}}$	$\text{S}_{\text{C}}^{\bar{\bar{=}}}$	$\text{S}_{\text{P}}^{\bar{\bar{=}}}$	Reduced Iron
0	7.953				0.00		4.66			0.04
19	7.974				0.01		4.60	4.40		0.10
198	7.973	0.01	0.01	0.00	0.00	0.08	4.25	4.30		0.27
376	7.959		0.01	0.00	0.01	0.11	4.37	4.31	0.09	0.46
742	7.959	0.01	0.02	0.01	0.02	0.17	4.23	4.09	0.18	0.70
1451	7.960	0.01	0.02	0.01	0.01	0.27	4.46	4.12	0.33	0.88

Run 9       $\text{pH}_i = 7.583$   
 $S_{T_i}^- = 4.00$   
 $\text{Fe}_{T_i} = 5.62, 32.6 \text{ m}^2/1$

Time	pH	$+\Delta \text{OH}^-$	$S_4^-$	$S_5^-$	$S_2O_3^-$	$S^\circ$	$S_T^-$	$S_C^-$	$S_P^-$	Reduced Iron
0	7.506				0.02		4.93			0.18
21	7.583		0.01	0.00	0.02	0.25	4.02	4.16	0.10	0.72
214	7.598	0.32	0.04	0.02		0.13	4.05	3.06	0.79	0.61
370	7.647	1.00	0.04	0.03	0.02	0.35	3.97	2.36	1.36	1.39
725	7.663	1.32	0.07	0.05	0.04	0.27	3.23	1.29	2.24	1.61
1455	7.708	1.98	0.03	0.03	0.03	0.44	3.67	0.55	2.36	1.54

Run 11       $\text{pH}_i = 7.58$

$S_{T_i}^- = 4.30$

$\text{Fe}_{T_i} = 1.19, 14.0 \text{ m}^2/1$

Time	pH	$+\Delta \text{OH}^-$	$S_4^-$	$S_5^-$	$S_2O_3^-$	$S^\circ$	$S_T^-$	$S_C^-$	$S_P^-$	Reduced Iron
0	7.580						4.56			
24	7.689		0.03	0.02	0.03	0.94	3.81	3.11	1.17	2.45
193	7.683		0.03	0.03	0.03	1.05	4.10	3.03	1.40	2.73
383	7.668		0.03	0.03	0.04	1.06	4.21	3.00	1.46	2.86
720	7.656		0.03	0.03	0.02	1.00	3.58	3.02	1.13	2.56
1366	7.702		0.04	0.02	0.03	1.90	3.42	2.88	1.03	2.44



Run 12       $\text{pH}_i = 8.51$

$S_{T_i}^- = 4.73$

$\text{Fe}_{T_i} = 1.19, 14.0 \text{ m}^2/1$

Time	pH	$+\Delta \text{OH}^-$	$S_4^-$	$S_5^-$	$S_2O_3^-$	$S^\circ$	$S_T^-$	$S_C^-$	$S_P^-$	Reduced Iron
0	8.51						5.03			
29	8.55		0.04	0.02	0.04		4.37	3.38	0.96	0.70
197	8.55		0.04	0.02	0.04	1.05	4.10	3.17	1.13	2.81
379	8.57		0.04	0.02	0.05	0.68	4.23	3.09	1.00	2.40
727	8.53		0.04	0.02	0.05	0.38	3.93	3.08	1.00	1.54
1461	8.53		0.04	0.02	0.05	0.44	4.79	3.06	1.51	1.69

Run 17     $\text{pH}_i = 7.605$   
 $S_{T_i}^{\equiv} = 4.16$   
 $\text{Fe}_{T_i} = 5.10, 5.45 \text{ m}^2/1$

Time	pH	$+\Delta\text{OH}^-$	$S_4^{\equiv}$	$S_5^{\equiv}$	$S_2O_3^{\equiv}$	$S^\circ$	$S_T^{\equiv}$	$S_C^{\equiv}$	$S_P^{\equiv}$	Reduced Iron
0	7.467						5.54			
30	7.605	0.30	0.01	0.00			4.20			0.10
190	7.585		0.02	0.01		0.09	4.68		0.08	0.40
363	7.618	0.44	0.04	0.02		0.18	4.36		0.16	0.71
719	7.581		0.06	0.03	0.04	0.18	4.28		0.37	1.28
1444	7.620	0.49	0.07	0.03	0.05	0.49	4.17		0.74	2.11

Run 21      $\text{pH}_i = 7.529$   
 $\text{S}_{\text{T}_i}^= = 4.80$   
 $\text{Fe}_{\text{T}_i} = 2.36, 2.51 \text{ m}^2/1$

Time	pH	+ $\Delta\text{OH}^-$	$\text{S}_4^=$	$\text{S}_5^=$	$\text{S}_2\text{O}_3^=$	$\text{S}^\circ$	$\text{S}_\text{T}^=$	$\text{S}_\text{C}^=$	$\text{S}_\text{P}^=$	Reduced Iron
0	7.486						5.56			
33	7.529		0.01	0.00	0.02	0.15	4.82	4.64		0.54
390	7.527		0.02	0.01			4.55	4.45	0.05	
725	7.515		0.02	0.01			4.80	4.25	0.16	
1351	7.503		0.03	0.02	0.03	0.28	4.94	4.44	0.35	1.09
2168	7.497		0.03	0.02			4.73	4.02	0.56	
2827	7.517		0.04	0.02	0.02		4.60	4.09	0.66	
3612	7.493									
4245	7.552		0.04	0.03	0.04	0.57	4.60	3.60	0.78	1.86

Run 22       $\text{pH}_i = 7.736$   
 $\text{S}_{\text{T}_i}^- = 4.90$   
 $\text{Fe}_{\text{T}_i} = 1.04, 6.34 \text{ m}^2/1$

Time	pH	$+\Delta \text{OH}^-$	$\text{S}_4^-$	$\text{S}_5^-$	$\text{S}_2\text{O}_3^-$	$\text{S}^\circ$	$\text{S}_{\text{T}}^-$	$\text{S}_{\text{C}}^-$	$\text{S}_{\text{P}}^-$	Reduced Iron
0	7.716						4.99			
26	7.736	0.27	0.01	0.00	0.01	0.07	4.89	4.76	0.04	0.30
184	7.726	0.14	0.01	0.00	0.01	0.12	5.34	4.78	0.12	0.44
348	7.759	0.68	0.02	0.01	0.02	0.12	4.17	3.82	0.23	0.61
814	7.753	0.55	0.03	0.02	0.02	0.25	4.86	4.30	0.46	0.97
1503	7.781	0.99	0.03	0.02	0.03	0.54	4.24	3.92	0.82	1.70
3010	7.795	1.20	0.05	0.03	0.03	0.72	4.79	3.91	1.40	2.20



Run 24     $\text{pH}_i = 7.564$   
 $\text{S}_{\text{T}_i}^{\equiv} = 4.70$   
 $\text{Fe}_{\text{T}_i} = 2.62, 15.2 \text{ m}^2/1$

Time	pH	$+\Delta \text{OH}^-$	$\text{S}_4^{\equiv}$	$\text{S}_5^{\equiv}$	$\text{S}_2\text{O}_3^{\equiv}$	$\text{S}^\circ$	$\text{S}_{\text{T}}^{\equiv}$	$\text{S}_{\text{C}}^{\equiv}$	$\text{S}_{\text{P}}^{\equiv}$	Reduced Iron
0	7.554				0.01		5.16			0.08
45	7.564		0.01	0.00	0.01	0.12	4.72	4.52	0.06	0.42
90	7.574									
221	7.545	0.04	0.02	0.01		0.46	4.70	4.44	0.46	1.14
375	7.576	0.23	0.03	0.02	0.03	0.46	4.59	3.91	0.72	1.44
740	7.604	0.61	0.04	0.03	0.02	0.56	4.69	3.54	1.53	1.76
1756	7.634	1.06	0.04	0.04	0.04	1.19	4.66	2.84	1.97	3.28

Run 25       $\text{pH}_i = 7.332$   
 $\text{S}_{\text{T}_i}^{\bar{\bar{=}}} = 4.80$   
 $\text{Fe}_{\text{T}_i} = 1.05, 6.52 \text{ m}^2/1$

Time	pH	$+\Delta \text{OH}^-$	$\text{S}_4^{\bar{\bar{=}}}$	$\text{S}_5^{\bar{\bar{=}}}$	$\text{S}_2\text{O}_3^{\bar{\bar{=}}}$	$\text{S}^\circ$	$\text{S}_{\text{T}}^{\bar{\bar{=}}}$	$\text{S}_{\text{C}}^{\bar{\bar{=}}}$	$\text{S}_{\text{P}}^{\bar{\bar{=}}}$	Reduced Iron
0	7.329						5.26			
19	7.332		0.00	0.00	0.00		4.78	4.53	0.02	0.08
105	7.340	0.10	0.01	0.01				4.36	0.27	0.10
192	7.317		0.02	0.01	0.01	0.12	4.63	4.32		0.54
242	7.344									
280	7.328		0.02	0.01				4.05		0.24
396	7.368	0.49	0.02	0.02	0.02	0.18	4.10	3.69	0.33	0.82
762	7.366	0.55	0.03	0.03	0.02	0.39	3.44	3.26	0.75	1.36
1452	7.388	0.70	0.05	0.04	0.04	0.43	4.26	3.54	1.38	1.72

Run 28       $\text{pH}_i = 7.582$   
 $S_{\text{T}_i}^{\text{--}} = 2.60$   
 $\text{Fe}_{\text{T}_i} = 2.62, 15.2 \text{ m}^2/1$

Time	pH	$+\Delta\text{OH}^-$	$S_4^{\text{--}}$	$S_5^{\text{--}}$	$S_2O_3^{\text{--}}$	$S^\circ$	$S_T^{\text{--}}$	$S_C^{\text{--}}$	$S_P^{\text{--}}$	Reduced Iron
0	7.524						3.10			
35	7.582					0.19	2.56	2.31	0.03	0.38
140	7.563		0.00	0.00		0.26	2.95	2.58	0.15	0.58
255	7.570	0.03	0.02	0.01	0.00	0.23	2.82	2.38	0.32	0.69
425	7.571	0.08	0.02	0.02		0.38	2.75	2.02	0.54	1.02
790	7.588	0.21	0.03	0.03	0.01	0.56	3.11	1.56	1.10	1.62
1527	7.632	0.77	0.04	0.04	0.01	0.68	2.75	1.21	1.43	1.98

Run 29      $\text{pH}_i = 7.540$   
 $S_{T_i}^{\bar{\bar{=}}} = 8.70$   
 $\text{Fe}_{T_i} = 2.60, 15.2 \text{ m}^2/1$

Time	pH	$+\Delta\text{OH}^-$	$S_4^{\bar{\bar{=}}}$	$S_5^{\bar{\bar{=}}}$	$S_2O_3^{\bar{\bar{=}}}$	$S^\circ$	$S_T^{\bar{\bar{=}}}$	$S_C^{\bar{\bar{=}}}$	$S_P^{\bar{\bar{=}}}$	Reduced Iron
0	7.528						9.45			
30	7.540		0.01	0.00		0.30	8.71	8.74	0.05	0.71
160	7.566	0.40	0.03	0.02	0.01	0.36	9.16	8.28	0.55	1.11
323	7.595	0.82	0.05	0.02	0.03	0.35	9.58	7.86	1.58	1.40
476	7.580	0.75	0.06	0.03	0.08	0.39	8.75	6.89	2.08	1.98
755	7.585	0.99	0.07	0.04	0.06	0.36		5.53	1.99	1.94
1375	7.695	2.61	0.06	0.05	0.06	1.28	8.85	3.71	4.55	3.82



Run 30      $\text{pH}_i = 7.555$   
 $\text{S}_{\text{T}i}^{\bar{\bar{=}}} = 1.80$   
 $\text{Fe}_{\text{T}i} = 2.60, 15.2 \text{ m}^2/1$

Time	pH	$+\Delta \text{OH}^-$	$\text{S}_4^{\bar{\bar{=}}}$	$\text{S}_5^{\bar{\bar{=}}}$	$\text{S}_2\text{O}_3^{\bar{\bar{=}}}$	$\text{S}^\circ$	$\text{S}_{\text{T}}^{\bar{\bar{=}}}$	$\text{S}_{\text{C}}^{\bar{\bar{=}}}$	$\text{S}_{\text{P}}^{\bar{\bar{=}}}$	Reduced Iron
0	7.516				0.00		2.11			0.04
39	7.555		0.00	0.00	0.00	0.45	1.77	1.86		0.99
175	7.568	0.02	0.01	0.01	0.00	0.55	1.85	1.75	0.06	1.22
336	7.518	0.03	0.01	0.01	0.01	0.52	1.94	1.51	0.23	1.29
403	7.551									
465	7.551	0.04	0.01	0.01	0.02	0.63	1.80	1.37	0.44	1.59
470	7.545									
760	7.529	0.09	0.02	0.02	0.02	0.56	1.72	1.11	0.49	1.53
1500	7.536	0.14	0.02	0.03	0.03	0.85	1.70	0.78	0.75	2.32

Run 31       $\text{pH}_i = 7.542$

$S_{T_i}^- = 4.76$

$\text{Fe}_{T_i} = 3.17, 18.5 \text{ m}^2/1$

Time	pH	$+\Delta\text{OH}^-$	$S_4^-$	$S_5^-$	$S_2O_3^-$	$S^\circ$	$S_T^-$	$S_C^-$	$S_P^-$	Reduced Iron
0	7.501				0.02		5.40			0.16
27	7.542		0.00	0.00	0.01	0.17	4.77	4.74		0.50
178	7.564	0.37	0.02	0.01	0.01	0.37	4.49	3.89	0.29	1.02
333	7.577	0.51	0.02	0.02	0.02	0.54	4.82	4.01	1.05	1.50
475	7.568	0.48	0.03	0.02	0.04	0.70	4.78	3.46	1.15	2.12
605	7.593	0.82	0.04	0.03	0.03	0.46	4.62	3.15	1.43	1.64
1476	7.620	1.27	0.05	0.06	0.03	1.20	4.44	2.05	2.77	3.42

Run 32      $\text{pH}_i = 7.572$   
 $\text{S}_{\text{T}_i}^- = 4.78$   
 $\text{Fe}_{\text{T}_i} = 1.94, 11.3 \text{ m}^2/1$

Time	pH	$+\Delta\text{OH}^-$	$\text{S}_4^-$	$\text{S}_5^-$	$\text{S}_2\text{O}_3^-$	$\text{S}^\circ$	$\text{S}_\text{T}^-$	$\text{S}_\text{C}^-$	$\text{S}_\text{P}^-$	Reduced Iron
0	7.526		0.00				5.20			0.01
50	7.572	0.37	0.02	0.01	0.01			4.26		0.26
170	7.603	0.76	0.02	0.01	0.01	0.12	4.45	4.14		0.52
316	7.564		0.02	0.01	0.02	0.18	4.38	4.11	0.15	0.73
465	7.620	0.97	0.02	0.01	0.01	0.25	4.82	4.07	0.20	0.82
615	7.609	0.87	0.03	0.02	0.02	0.19	4.18	3.82	0.24	0.80
1465	7.618	1.02	0.05	0.02	0.00	0.10	4.12	3.39	0.65	0.66
1556*	7.650	1.47	0.04	0.03	0.02	0.50	4.22	3.10	0.82	1.62

\*Stirred at 11.5 hrs (690 min)

Run 33       $\text{pH}_i = 7.050$

$\text{S}_{\text{T}_i}^{\equiv} = 4.50$

$\text{Fe}_{\text{T}_i} = 1.06, 6.52 \text{ m}^2/\text{l}$

Time	pH	$+\Delta\text{OH}^-$	$\text{S}_4^{\equiv}$	$\text{S}_5^{\equiv}$	$\text{S}_2\text{O}_3^{\equiv}$	$\text{S}^\circ$	$\text{S}_{\text{T}}^{\equiv}$	$\text{S}_{\text{C}}^{\equiv}$	$\text{S}_{\text{P}}^{\equiv}$	Reduced Iron
0	7.070		0.00	0.00	0.02		4.90			0.16
40	7.050		0.00	0.00	0.02		4.54	4.48		0.21
170	7.074	0.10	0.01	0.01	0.03	0.17	4.31	4.51	0.15	0.72
310	7.095	0.39	0.02	0.01	0.04	0.32	4.21	3.89	0.30	1.17
473	7.097	0.47	0.02	0.02	0.06	0.30	4.50	3.89	0.53	1.40
600	7.114	0.56	0.03	0.02	0.06	0.32	4.25	3.82	0.69	1.49
1450	7.136	0.69	0.04	0.04	0.07	0.71	4.41	3.34	0.91	2.51



Run 34       $\text{pH}_i = 7.173$

$S_{T_i} = 5.17$

$\text{Fe}_{T_i} = 1.06, 6.52 \text{ m}^2/1$

Time	pH	$+\Delta\text{OH}^-$	$S_4^-$	$S_5^-$	$S_2O_3^-$	$S^\circ$	$S_T^-$	$S_C^-$	$S_P^-$	Reduced Iron
0	7.186						5.41			0.00
33	7.173		0.00	0.00	0.00	0.17	4.89	5.12		0.39
161	7.180	0.25	0.01	0.01	0.02	0.25	5.07	4.41	0.18	0.75
312	7.225	0.56	0.02	0.02	0.03	0.28	4.84	4.43	0.38	1.06
455	7.237	0.74	0.02	0.02	0.04	0.30	4.81	4.06	0.49	1.20
610	7.217	0.63	0.03	0.02	0.04	0.45	4.69	3.94	0.75	1.53
1331	7.244	0.91	0.04	0.03	0.05	0.29	4.42	3.56	0.97	1.47

Run 35       $\text{pH}_i = 7.419$   
 $S_{T_i}^{\circ} = 5.50$   
 $\text{Fe}_{T_i} = 1.06, 6.52 \text{ m}^2/1$

Time	pH	$+\Delta \text{OH}^-$	$S_4^{\circ}$	$S_5^{\circ}$	$S_2O_3^{\circ}$	$S^{\circ}$	$S_T^{\circ}$	$S_C^{\circ}$	$S_P^{\circ}$	Reduced Iron
0	7.410				0.02		5.72			0.16
30	7.419				0.03	0.22	5.52	5.40		0.69
166	7.433	0.20	0.00	0.00	0.04	0.20	5.45	5.05	0.03	0.83
316	7.452	0.40	0.01	0.00	0.05		5.29	4.98	0.10	
460	7.434		0.01	0.01	0.05	0.35	5.32	5.01	0.23	1.34
481	7.472		0.02	0.01						
605	7.447	0.42	0.02	0.01	0.06	0.36	5.28	4.94	0.45	1.45
1450	7.498	1.02	0.05	0.03	0.09	0.23	4.77	4.24	0.76	1.67

Run 36     $\text{pH}_i = 7.400$   
 $S_{T_i}^{\bar{}} = 5.40$   
 $\text{Fe}_{T_i} = 1.06, 6.52 \text{ m}^2/1$

Time	pH	$+\Delta\text{OH}^-$	$S_4^{\bar{}}$	$S_5^{\bar{}}$	$S_2O_3^{\bar{}}$	$S^{\circ}$	$S_T^{\bar{}}$	$S_C^{\bar{}}$	$S_P^{\bar{}}$	Reduced Iron
0	7.400				0.01		5.75			
35	7.400		0.01	0.00	0.02		5.38	4.96		
171	7.411	0.12	0.01	0.01	0.03		5.10	5.31	0.05	
315	7.418	0.22	0.02	0.01	0.04		5.23	5.14	0.13	
465	7.425	0.38	0.02	0.01	0.04		4.90	4.67	0.30	
602	7.465	0.81	0.03	0.02	0.06		5.16	4.56	0.43	
1225	7.479	1.00	0.05	0.03	0.06		4.66	4.33	0.78	

## APPENDIX B

## Initial Rate Method

The kinetics for the reaction of aqueous bisulfide ion and goethite was studied by the initial rate method. The rate law for this reaction can be considered to be:

$$R_i = d(\text{FeS})/dt = k (\text{H}^+)^x [\text{HS}^-]^y A_{\text{FeOOH}}^z$$

where  $R_i$  is the rate of formation of iron sulfide,  $(\text{H}^+)$  is the hydrogen ion activity,  $[\text{HS}^-]$  is the bisulfide ion concentration,  $A_{\text{FeOOH}}$  is the surface area of the reactant goethite, and  $k$  is the rate constant. The coefficients  $x$ ,  $y$ , and  $z$  are the reaction orders for the respective species.

The initial rate method or differential method is based on the fact that:

$$\ln R_i = \ln k + x \ln (\text{H}^+) + y \ln [\text{HS}^-] + z \ln A_{\text{FeOOH}}$$

The equation is rather complex for a reaction dependent on several reactants, but it is possible to simplify the expression by maintaining all but one of the reactants constant. This results in

$$\ln R_i = \ln k^* + x \ln (\text{H}^+)$$

where

$$\ln k^* = \ln k + y \ln [\text{HS}^-] + z \ln A_{\text{FeOOH}}$$



A plot of the log of the initial rate vs. the log of the particular variable, ( $H^+$ ) in this case, will yield a straight line with a slope  $x$ . This process is repeated until the reaction orders for the reactants are determined.

The initial rate in this study was determined from plots of the acid extractable iron sulfide ( $>.2\mu$ ) concentrations vs. time. Then a smooth curve or straight line was fitted to the curve by a least squares regression method. The initial rate was determined from this equation by taking the first derivative of the curve's equation and setting the value of  $x$  equal to zero. For example:

$$y = a + bx + cx^2$$

$$dy/dt = b + 2 cx$$

$$dy/dt = b \quad \text{at } x = 0$$

For the several experimental runs in which one reactant was varied, a log-log plot of  $b$  vs. the concentration of the species varied was made. A straight line was drawn through the points by a least squares regression. All but three of the curves were fit by a parabolic function. The remaining three were fit by a linear regression. The "goodness of fit" of these curves was determined by one of two methods. The linear equations were tested by an equal tails test of the correlation coefficient at the 95% confidence level. The quadratic curves were tested by the F-test method (Kreyszig, 1970) at the 95% confidence level. All of the curves fit the data at the above confidence limits.

The rate constant ,  $k$ , for the reaction could then be determined from the knowledge of the reaction order and concentrations of the various reactants in the rate expression and the initial rate,  $R_i$ .

$$k = \frac{R_i}{(H^+)^x [HS^-]^y A_{FeOOH}^z}$$

All calculations, curve fitting, significance testing and regression analyses were performed on a Hewlett-Packard HP-65 calculator. All programs were found in their Stat Pac 1. Significance of linear correlation coefficients were determined from tables in Crow et al. (1960). F-testing of parabolic curves was performed from tables in Kreyszig (1970).

## BIBLIOGRAPHY

- Atkinson R.J., Posner A.M. and Quirk J.P. (1968) Crystal nucleation in Fe(III) solutions and hydroxide gels. *J. Inorg. Nucl Chem.* 30, 2371-2381.
- Baas Becking L.G.M. (1956) Biological processes in the estuarine environment. VI. The state of iron in the estuarine mud iron sulfides. *Koninkl. Nederl. Akad. Wetenschappen* 59B, 181-189.
- Baes C.F. and Mesmer R.E. (1976) The Hydrolysis of Cations. Wiley.
- Barnes H.L. and Czamanski G.K. (1967) Solubilities and transport of ore minerals. Geochemistry of Hydrothermal Ore Deposits (editor H. L. Barnes), Holt, Rinehart, and Wilson, 334-381.
- Bartlett J.K. and Skoog D.A. (1954) Colorimetric determination of elemental sulfur in hydrocarbons. *Anal. Chem.* 26, 1008-1011.
- Ben-Yaakov S. (1973) pH buffering of pore water of recent anoxic sediments. *Limn. and Oceanog.* 18, 86-94.
- Berner R.A. (1964a) Iron sulfides formed from aqueous solution at low temperatures and atmospheric pressure. *J. Geol.* 72, 293-306.
- Berner R.A. (1964b) Stability fields of iron minerals in anaerobic marine sediments. *J. Geol.* 72, 826-834.
- Berner R.A. (1964c) Distribution and diagenesis of sulfur in some sediments from the Gulf of California. *Mar. Geol.* 6, 117-140.
- Berner R.A. (1967) Thermodynamic stability of sedimentary iron sulfides. *Am. J. Sci.* 265, 773-785.
- Berner R.A. (1969) The synthesis of framboidal pyrite. *Econ. Geol.* 64, 383-384.
- Berner R.A. (1970) Sedimentary pyrite formation. *Am. J. Sci.* 268, 1-23.
- Berner R.A. (1971) Principles of Chemical Sedimentology. McGraw-Hill.



- Berner R.A. (1972) Sulfate reduction, pyrite formation and the oceanic sulfur budget. The Changing Chemistry of the Oceans (editors D. Dryssen and D. Jagner) Wiley, 347-361.
- Bertine K.K. (1972) The deposition of molybdenum in anoxic waters. Mar. Chem. 1, 43-54.
- Blyholden G. and Richardson E.A. (1962) Infrared and volumetric data on the adsorption of ammonia, water, and other gases on activated iron (III) oxide. J. Phys. Chem. 66, 2597-2602.
- Bray J.T., Bricker O.P. and Troup B.N. (1973) Phosphate in interstitial waters of anoxic sediments: oxidation effects during sampling procedures. Science 180, 1362-1363.
- Brewer P.G. and Spencer D.W. (1974) Distribution of some trace elements in Black Sea and their flux between dissolved and particulate phases. Am. Assoc. Petrol. Geol. Mem. 20, 137-143.
- Brooks R.R., Presley B.J. and Kaplan I.R. (1968) Trace elements in the interstitial waters of marine sediments. Geochim. Cosmochim. Acta 32, 397-414.
- Brongersma-Sanders M. (1957) Mass mortality in the sea. Treatise on Marine Ecology and Paleoecology (editor J. W. Hedgpeth) Geol. Soc. Am. 1, 941
- Budd M.S. and Bewick H.A. (1952) Photometric determination of sulfides and reducible sulfur in alkalies. Anal. Chem. 24, 1536-1540.
- Carrol D. (1958) Role of clay minerals in the transportation of iron. Geochim. Cosmochim. Acta 14, 1-27.
- Caspers H. (1957) In Treatise on Marine Ecology and Paleoecology (editor J. W. Hedgpeth) Geol. Soc. Am. 1, 801
- Charlot G. (1964) Colorimetric Determination of Elements. Elsevere.
- Chen K.Y. and Morris J.C. (1972) Kinetics of oxidation of aqueous sulfide by O<sub>2</sub>. Environ. Sci. Tech. 6, 529-537.
- Cheng M. (1972) Effect of ferrous iron on the oxygenation of reduced sulfur species. M.S. thesis, U. Md.
- Christensen H.E. and Luginbyhl T.T. (1974) The Toxic Substances List 1974 Edition. USDHEW.
- Chiu J.D. and Richards F.A. (1969) Oxygenation of hydrogen sulfide in seawater at constant salinity, temperature, and pH. Environ Sci. Tech. 3, 838-843.



- Crow E.L., Davis F. A. and Maxfield M.W. (1960) Statistics Manual. Dover.
- Deer W.A., Howie R.A. and Zussman J. (1966) An Introduction to the Rock Forming Minerals. Wiley.
- Doyle R.W. (1968) Identification and solubility of iron sulfide in anaerobic lake sediment. Am. J. Sci. 266, 980-994.
- Drever J.I. (1971) Magnesium-iron replacement in clay minerals in anoxic marine sediments. Science 172, 1334-1336.
- Edwards J.O., Greene E.F. and Ross J. (1968) From stoichiometry and rate law to mechanism. J. Chem. Ed. 45, 381-385.
- Erd R.C., Evans H.T. and Richter D.H. (1957) Smythite, a new iron sulfide and associated pyrrhotite from Indiana. Am. Mineral. 42, 309-333.
- Garrells R.M. and Christ C.L. (1965) Solutions, Minerals and Equilibria. Harper and Row.
- Gast R.G., Landa E.R. and Meyer G.W. (1974) The interaction of water with goethite ( $\alpha$ -FeOOH) and amorphous hydrated ferric oxide surfaces. Clays and Clay Min. 22, 31-39.
- Gibbs R.J. (1973) Mechanism of trace metal transport in rivers. Science 180, 71-73.
- Giggenbach W. (1972) Optical spectra and equilibrium distribution of polysulfide ions in aqueous solution at 20°. Inorg. Chem. 11, 1201-1207.
- Goldhaber M.B. and Kaplan I.R. (1975) Apparent dissociation constants of hydrogen sulfide in chloride solutions. Mar. Chem. 3, 83-104.
- Harvey H.W. (1955) The Chemistry and Fertility of Sea Water. Cambridge Univ. Press.
- Hem J.D. (1960) Some chemical relationships among sulfur species and dissolved ferrous iron. USGS Water Supply Paper 1459-C, 57-73.
- Hem J.D. and Cropper W.H. (1954) Survey of ferrous-ferric chemical equilibria and redox potentials. USGS Water Supply Paper 1459-A, 1-31.
- Jefferson D.A., Tricker M.J. and Winterbottom A.P. (1975) Electron-microscopic and mössbauer spectroscopic studies of iron stained kaolinite minerals. Clays and Clay Min. 23, 355-360.

- Jenne E.A. (1968) Controls on Mn, Fe, Co, Ni, Cu and Zn concentrations in soils and water: the significant role of hydrous Mn and Fe oxides. Trace Inorganics in Water (editor R. F. Gould) Am. Chem. Soc. Adv. in Chem. Ser. 73, 337-387.
- Kaplan I.R., Emery K.O. and Rittenberg S.C. (1963) The distribution and isotopic abundance of sulfur in recent marine sediment off southern California. *Geochim. Cosmochim. Acta* 27, 297-332.
- Kennedy V.C., Zellweger G.W. and Jones B.F. (1974) Filter pore-size effects on the analysis of Al, Fe, Mn, and Ti in water. *Water Resources Research* 10, 785-790.
- Kester D.R., Byrne R.H.Jr. and Liang Yu-Jean. (1975) Redox reactions and solution complexes of iron in marine systems. Marine Chemistry in the Coastal Environment (editor T. M. Church). Am. Chem. Soc., 56-79.
- Krauskopf K.B. (1956) Factors controlling the concentrations of thirteen rare metals in sea water. *Geochim. Cosmochim. Acta* 19, 1-32.
- Krauskopf K.B. (1967) Introduction to Geochemistry. McGraw-Hill.
- Kreyszig E. (1970) Introductory Mathematical Statistics. Wiley.
- Landa E.R. and Gast R.G. (1973) Evaluation of crystallinity in hydrated ferric oxides. *Clays and Clay Min.* 21, 121-130.
- Laurence G.S. and Ellis K.S. (1972) Oxidation of iodide ion by iron (III) in aqueous solution. *J. Chem. Soc. London Dalton*, 2229-2233.
- Moelwyn-Hughes E.A. (1933) The Kinetics of Reactions in Solutions. Oxford at the Clarendon Press.
- Murakami E. (1952) Sulfate-producing bacteria. *Int. Symp. Enzyme Chem.* (Tokyo) 7, 53-54.
- Nissenbaum A., Presley B.J. and Kaplan I.R. (1972) Early diagenesis in a reducing fjord, Saanich Inlet, British Columbia. I. Chemical and isotopic changes in major components of interstitial water. *Geochim. Cosmochim. Acta* 36, 1007-1027.
- O'Brien D.J. (1974) Kinetics of the oxidation of reduced sulfur species in aqueous solution. Ph.D. thesis, U. Md.



- Ozretich R.J. (1975) Mechanism for deep water renewal in Lake Nitinat, a permanently anoxic fjord. *Est. Coast. Mar. Sci.* 3, 189-200.
- Parks G.A. and De Bruyn P.L. (1962) The zero point of charge of oxides. *J. Phys. Chem.* 66, 967-973.
- Parks G.A. (1965) The isoelectric points of solid oxides, solid hydroxides, and aqueous hydroxo complex systems. *Chem. Reviews* 165, 177-198.
- Parks G.A. (1968) Aqueous surface chemistry of oxides and complex oxide minerals, isoelectric point and zero point of charge. *Equilibrium Concepts in Natural Water Systems* (editor W. Stumm). *Am. Chem. Soc. Adv. Chem. Ser.* 67, 121-161.
- Perrin D.D. and Dempsey B. (1974) Buffers for pH and Metal Ion Control. Wiley.
- Pilling M.J. (1975) Reaction Kinetics. Clarendon Press.
- Pohl H.A. (1954) The formation and dissolution of metal sulfides. *J. Am. Chem. Soc.* 76, 2182-2184.
- Presley B.J., Kolodny Y., Nissenbaum A. and Kaplan I.R. (1972) Early diagenesis in a reducing fjord, Saanich Inlet, British Columbia. II. Trace element distribution in interstitial water and sediment. *Geochim. Cosmochim. Acta* 36, 1073-1090.
- Reynolds W.L. and Lumry R.W. (1966) Mechanism of Electron Transfer. Ronald Press Co.
- Richards F.A. and Vaccaro R.F. (1956) The Cariaco Trench, an anaerobic basin in the Caribbean Sea. *Deep Sea Res.* 3, 214-228.
- Richards F.A. (1965) Anoxic basins and fjords. Chemical Oceanography (editors J. P. Riley and G. Skirrow). Academic Press 1, 611-645.
- Rickard D.T. (1969a) The chemistry of iron sulfide formation at low temperatures. *Stockholm Contr. Geol.* 20, 67-95.
- Rickard D.T. (1969b) The microbial formation of iron sulfides. *Stockholm Contr. Geol.* 20, 49-66.
- Rickard D.T. (1974) Kinetics and mechanism of the sulfidation of goethite. *Am. J. Sci.* 274, 941-952.
- Rickard D.T. (1975) Kinetics and mechanism of pyrite formation at low temperatures. *Am. J. Sci.* 275, 636-652.

- Roberts W.M., Walker A.L. and Buchanan A.S. (1969) The chemistry of pyrite formation in aqueous solution and its relation to the depositional environment. *Mineralium Deposits* 4, 18-29.
- Rozanov A.G., Volkov I.I., Zhabina N.N. and Yagodinskiy T.A. (1971) Hydrogen sulfide in the sediments of the continental slope, northwest Pacific ocean. *Geokhimiya* 5, 543-550.
- Schwarzenbach G. and Fischer A. (1960) Die Acidität der Sulfane und die Zusammensetzung wässriger Polysulfidlösungen. *Helv. Chim. Acta* 43, 1365-1390.
- Siegbahn K. (1967) ESCA: atomic, molecular and solid state structure studied by means of electron spectroscopy. *Nova. Acta R. Soc. Sci. Upsal. Ser. IV*, 20.
- Skinner B.J., Erd R.C. and Grimaldi F.S. (1964) Greigite, the thiospinel of iron: a new mineral. *Am. Min.* 49, 543-555.
- Stumm W. and Lee G.F. (1961) Oxygenation of ferrous iron. *Ind. Eng. Chem.* 53, 143-146.
- Stumm W. and Morgan J.J. (1970) Aquatic Chemistry. Wiley-Interscience.
- Sweeney R.E. and Kaplan I.R. (1973) Pyrite framboid formation: laboratory synthesis and marine sediments. *Econ. Geol.* 68, 618-634.
- Teder A. (1971) The equilibrium between elementary sulfur and aqueous polysulfide solutions. *Acta Chem. Scand.* 25, 1722-1728.
- Thode H.G. and Kemp A.L.W. (1968) The mechanism of bacterial reduction of sulfate and of sulfite from isotopic fractionation studies. *Geochim. Cosmochim. Acta* 32, 71-91.
- Trudinger P.A., Lambert I.B. and Skyring G.W. (1972) Biogenic sulfide ores: a feasibility study. *Econ. Geol.* 67, 1114-1127.
- Troup B.N., Bricker O.P. and Bray J.T. (1974) Oxidation effects on the analysis of iron in the interstitial waters of recent sediments. *Nature* 249, 237.
- Urban P.J. (1961) Colorimetry of sulfur anions. *Z. Anal. Chem.* 179, 415-422.
- Van Straaten L.M.J.V. (1954) Composition and structure of recent sediments of the Netherlands. *Leidse Geol. Mededel* 19, 1-110.



- Walton A.G. (1967) The Formation and Properties of Precipitates. Interscience.
- West P.W. and Gaeke G.C. (1956) Fixation of sulfur dioxide as disulfitomercurate (II) and subsequent colorimetric estimation. Anal. Chem. 28, 1816-1819.
- Wilkins R.G. (1974) The Study of Kinetics and Mechanism of Reaction of Transition Metal Complexes. Allyn and Bacon.
- Zajic J.E. (1969) Microbial Biogeochemistry. Academic Press.